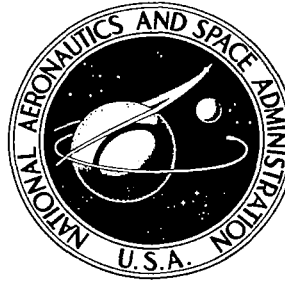


NASA CONTRACTOR REPORT

NASA CR-2027



NASA CF

C.1



LOAN COPY: RETURN TO
AFWL (DOUL)
KIRTLAND AFB, N. M.

DEVELOPMENT OF A SORBER TRACE CONTAMINANT CONTROL SYSTEM INCLUDING PRE- AND POST-SORBERS FOR A CATALYTIC OXIDIZER

by Thomas M. Olcott

Prepared by
LOCKHEED MISSILES & SPACE COMPANY
Sunnyvale, Calif.
for Langley Research Center

NATIONAL AERONAUTICS AND SPACE ADMINISTRATION • WASHINGTON, D. C. • MAY



0061333

1. Report No. NASA CR-2027	2. Government Accession No.	3. Recipient's Catalog No.	
4. Title and Subtitle DEVELOPMENT OF A SORBBER TRACE CONTAMINANT CONTROL SYSTEM INCLUDING PRE- AND POST-SORBERS FOR A CATALYTIC OXIDIZER		5. Report Date May 1972	6. Performing Organization Code
		8. Performing Organization Report No.	
7. Author(s) Thomas M. Olcott		10. Work Unit No.	
9. Performing Organization Name and Address Lockheed Missiles and Space Company Biotechnology Organization Sunnyvale, Calif.		11. Contract or Grant No. NAS 1-9242	
		13. Type of Report and Period Covered Contractor Report	
12. Sponsoring Agency Name and Address National Aeronautics & Space Administration Washington, DC 20546		14. Sponsoring Agency Code	
		15. Supplementary Notes	
16. Abstract A general methodology was developed for spacecraft trace contaminant control system design. Elements considered for contaminant control were catalytic oxidation with isotope or electrical heat and pre- and post-sorbbers, charcoal with regeneration and non-regeneration, and reactive constituents. A technique is described for sizing a charcoal bed for a multiple contaminant load. The system design methodology is based primarily on information reported in CR-1582, CR-66346, CR-66347, and CR-66739 (as well as this contract) and verified in a closed loop test of 240 days.			
17. Key Words (Suggested by Author(s)) contaminant control, trace contaminant, life support system		18. Distribution Statement Unclassified - Unlimited	
19. Security Classif. (of this report) Unclassified	20. Security Classif. (of this page) Unclassified	21. No. of Pages 188	22. Price* \$3.00



LIST OF CONTRIBUTORS

<u>Name</u>	<u>Area of Contribution</u>
T. Olcott	Project Direction
M. Ballestrasse	System Design
R. Lamparter	Analysis and Optimization
E. Kawasaki	Model System Test Analysis
O. Leong	Model System Test Analysis
R. Tuttle	Model System Test Analysis
R. Joy	Model System Test Design
D. Komm	Computer Programming
Subcontract - MSAR	
A. Juhola	Project Direction
J. Moustellar	MSAR-Director of Research

NASA TECHNICAL MONITOR

Rex Martin
Space Systems Division
Component and Processes Section
NASA-Langley Research Center

CONTENTS

	<u>Page</u>
LIST OF CONTRIBUTORS	iii
LIST OF FIGURES	vii
LIST OF TABLES	xi
SUMMARY	1
INTRODUCTION	4
REVISED CONTAMINANT MODEL	6
Biological Contaminants	6
Non-Biological Contaminants	9
CARBON BED PERFORMANCE	13
Saturation Capacity of Charcoal	21
Sorbent Selection	21
Effects of Moisture and Impregnation	23
Saturation Capacity for Multiple Contaminants	25
Determination of the Adsorption Zone	27
Charcoal Desorption	39
Regeneration of Carbons Exposed to Contaminants with $V_m > 80$	40
Regeneration of Carbons Exposed to Contaminants with $V_m < 80$	40
SYSTEM SELECTION AND ANALYSIS	49
System Optimization	51
Charcoal Bed Performance Analysis	63
Fixed Sorbent Bed	64
Regenerative Sorbent Bed	67
System Performance Summary	72

CONTENTS (Con't.)

	<u>Page</u>
MODEL SYSTEM TEST	76
Objective	76
Apparatus	76
Procedure	80
Selection of Contaminants to be Used in the Model Test	81
Fixed Sorbent Bed	81
Regenerative Bed	84
Catalytic Oxidizer	84
Chemical Analysis Techniques	85
Results	87
Discussion	87
Catalytic Oxidizer	87
Regenerative Bed	108
Fixed Bed	109
MODIFICATIONS TO THE DESIGN PROCEDURE	111
SYSTEM DESIGN	115
Catalytic Oxidizer	115
Pre- and Post-Sorbent Canisters	118
Fixed Bed	118
Regenerative Bed	122
CONCLUSIONS	124
REFERENCES	125
APPENDIX A - ADSORPTIVE CAPACITIES	A-1
APPENDIX B - EXPERIMENTAL PROCEDURE FOR THE CARBON BED PERFORMANCE STUDIES	B-1
APPENDIX C - DERIVATION OF METHANE REMOVAL EFFICIENCY CORRECTION FACTOR	C-1
APPENDIX D - CHARCOAL BED ADSORPTION PROGRAM	D-1

LIST OF FIGURES

<u>FIGURE</u>		<u>PAGE</u>
1	Average Contaminant Off-Gassing Rate for Twenty Typical Spacecraft Nonmetallic Materials	10
2	Adsorption Zone, Fast Adsorption Rate, $t \approx 0$	14
3	Adsorption Zone, Slow Adsorption Rate, $t \approx 0$	15
4	Typical Adsorbate Distribution	16
5	Effluent Concentration Curve	18
6	Adsorption Zone Length	20
7	Potential Plot for Various Carbons	22
8	Potential Plot for Barnebey Cheney G1 Carbon	24
9	Potential Plot for Barnebey Cheney BD Carbon	26
10	Blockage Effects with Multiple Contaminants	28
11	Sensitivity of Required Charcoal to $\Delta A_{\text{critical}}$	29
12	Adsorption Zone Lengths for Various Contaminants	31
13	Adsorption Zone Length for Acetone on BC-G1 Carbon	32
14	Adsorption Zone Length for Freon II on BC-G1	33
15	Adsorption Zone Length for Acetone on BC-G1, Acetone-Freon II Mixture	35
16	Adsorption Zone Length for Acetone on BC-G1, Acetone, Freon II-Methylcyclohexane Mixture	36
17	Adsorption Zone Length for Freon II on BC-G1, Freon II-Acetone Mixture	37
18	Adsorption Zone Length for Freon II on BC-G1, Freon II, Acetone and Methylcyclohexane Mixture	38
19	Effluent Concentration Curves for Acetone Adsorbed on Regenerated S154, 2.70 g Carbon Regeneration at 100°C and 10^{-4} mm of Hg Pressure	45

LIST OF FIGURES (Con't.)

<u>FIGURE</u>		<u>PAGE</u>
20	Effluent Concentration Curves for Acetone Adsorbed on Regenerated 5154, 2.70 g Carbon Regeneration at Ambient Temperature and 10^{-4} mm of Hg Pressure	47
21	Candidate System with a High Flow Regenerative Bed	52
22	Candidate System with a Fixed Bed and Regenerative Bed in Series	52
23	Candidate System with Fixed Bed and Regenerative Beds in Parallel	52
24	Performance of a Group I Regenerative Bed	54
25	Performance of a Group I Fixed Bed	56
26	Effect of Cycle Time on Total Equivalent Weight of the Regenerative Bed, Ref. Fig. 22	58
27	Effects of Cycle Time on Total Equivalent Weight of the Regenerative Bed, Ref. Fig. 23	59
28	Effect of Cycle Time on Total Equivalent Weight of the Regenerative Bed, Including the Effects on the Catalytic Oxidizer System	60
29	Power Requirements for the Regenerative Bed	62
30	Required Size of the Regenerative Bed	69
31	Model System Test Apparatus Schematic	77
32	Model System Test Apparatus	78
33	Dew Point and Oxygen Partial Pressure Monitoring Equipment	79
34	Model System Test Cont. Introduction	83
35	System Dew Point Temperature	88
36	Methane Performance	89
37	Carbon Monoxide Performance	90
38	Acetylene Performance	91

LIST OF FIGURES (Con't.)

<u>FIGURE</u>		<u>PAGE</u>
39	Ethylene Performance	92
40	Ethane Performance	93
41	Acetone Performance	94
42	Freon 11 Performance	95
43	Freon 12 Performance	96
44	Vinyl Chloride Performance	97
45	Ammonia Performance	98
46	Sulfur Dioxide Performance	99
47	N-Propyl Alcohol Performance	100
48	Freon 114 Performance	101
49	Halogenated Hydrocarbon Inlet Concentration to the Catalytic Oxidizer	102
50	Nitrous Oxide Effluent Concentration from the Catalytic Oxidizer	103
51	Freon 12 Effluent Concentration from the Regenerative Bed on Test Day 141	104
52	Sulfur Dioxide Inlet Concentration to the Catalytic Oxidizer	105
53	Isotope Heated Catalytic Oxidizer System	116
54	Pre-Sorbent Canister	119
55	Post-Sorbent Canister	120
56	Fixed Charcoal Sorbent Bed	121
57	Regenerative Charcoal Sorbent Bed	123

<u>FIGURE</u>	<u>PAGE</u>
A-1	Effluent Concentration Curves for Runs 25 and 27, Acetone on G1 Carbon A-3
A-2	Effluent Concentration Curve for Run 29 A-4
A-3	Effluent Concentration Curves for Freon 11 on Barnebey Cheney G1 Carbon A-5
A-4	Effluent Concentration Curves for Freon 11 on H ₃ PO ₄ Treated Barnebey Cheney Carbon A-6
A-5	Effluent Concentration Curves for Freon 11 on Barnebey Cheney G1 Carbon, Run 67. A-7
A-6	Effluent Concentration Curves for Freon 11 and Acetone Mixture on Barnebey Cheney G1, 0.350 g of Carbon, Run 48 . . . A-17
A-7	Effluent Concentration Curves for Adsorption of Mixture of Methylcyclohexane, Freon 11 and Acetone on BC-G1, 0.352 g Carbon, Run 50 A-18
B-1	Adsorption Line Apparatus B-2
B-2	Adsorption Tube B-5
B-3	Sample Concentration and Injection System B-7
C-1	Location of Catalytic Oxidizer Effluent Sampling Point. C-1
D-1	System Card Sequence D-3
D-2	Potential Plot for Barnebey Cheney. D-6

LIST OF TABLES

<u>TABLE</u>		<u>PAGE</u>
1	Revised Contaminant Model.	7
2	Results on Carbons Exposed to High Molar Volume Contaminants and Regenerated at 200°C and 10 ⁻⁴ mm Hg Pressure	41
3	Vacuum Regeneration of Superactivated Carbon (138% CCl ₄ Act.) Exposed to Acrolein	42
4	Regeneration at 100°C and 10 ⁻⁴ mm Hg Pressure of Superactivated Carbon Exposed to Acetone.	44
5	Regeneration of Ambient Temperature and 10 ⁻⁴ mm Hg Pressure of Superactivated Carbon (154% CCl ₄ Act.) Exposed to Acetone.	46
6	Fixed Sorbent Bed Computer Analysis Results.	65
7	Regenerative Sorbent Bed Computer Analysis Results	68
8	Potential Sources of Contaminants Requiring Excessive Charcoal for Control	70
9	System Performance Summary	73
10	Contaminants Used in the Model System Test	82
11	Zone Lengths for the Regenerative Bed Based on Freon 12 Performance	112
12	Zone Lengths for the Fixed Bed Based on N-Propyl Alcohol Performance.	112
A-1	Adsorptive Capacities Single Contaminants.	A-2
A-2	Adsorptive Capacity of S154 for Acetone, 34% RH, Run 25. .	A-8
A-3	Adsorptive Capacity of S154 for Acetone, with Dry Carrier Gas, Run 27.	A-9
A-4	Adsorptive Capacity of Barnebey Cheney G1 for Acetone, 50% RH Carrier Gas, Run 29	A-10
A-5	Adsorptive Capacity of Barnebey Cheney G1 for Freon 11, 50% RH Carrier Gas, Run 46	A-11

LIST OF TABLES (Cont.)

<u>TABLE</u>		<u>PAGE</u>
A-6	Adsorptive Capacity of Barnebey Cheney GI for Freon 11, 50% RH Carrier Gas, Runs 47 and 49	A-12
A-7	Adsorptive Capacity of Phosphoric Acid Treated Barnebey Cheney GI for Freon 11, 50% RH, Run 66	A-13
A-8	Adsorptive Capacity of Phosphoric Acid Treated Barnebey Cheney GI for Freon 11, 50% RH, Run 71	A-14
A-9	Adsorptive Capacity of Phosphoric Acid Treated Barnebey Cheney GI for Freon 11, 50% RH, Run 67	A-15
A-10	Acetone and Freon 11 Mixture.	A-19
A-11	Acetone, Freon 11, Methylcyclohexane Mixture.	A-20
B-1	Contaminant Mixtures	B-3

DEVELOPMENT OF A SORBER TRACE CONTAMINANT CONTROL SYSTEM
INCLUDING PRE- AND POST-SORBERS FOR A CATALYTIC OXIDIZER

BY THOMAS M. OLCOTT

BIOTECHNOLOGY
LOCKHEED MISSILES & SPACE CO.

SUMMARY

A program was conducted which resulted in the development and preliminary design of regenerative and non-regenerative charcoal sorbent beds. These elements of a trace contaminant control system were integrated with an isotope heated catalytic oxidizer system, with pre- and post-sorbent beds, that had been developed under previous NASA contracts. These previous efforts were accomplished under NAS 1-6256 and NAS 1-7433, and are reported in NASA CR 66346, CR 66347 and CR 66739.

The contaminant load generation rates developed during these previous studies were reviewed and refined. The original equipment production rate data were based on Apollo off-gassing data for a 14-day mission. These rates were modified in this study to account for the decrease in off-gassing that will occur with extended mission time.

The allowable contaminant levels were also modified to be consistent with the recommendations of the National Academy of Sciences Panel on Air Standards for Manned Space Flight.

The adsorption process in a carbon bed was defined for system design purposes and experiment data were taken to provide design information on carbon beds. The approach used in this phase of the effort was to treat the carbon bed as two elements defined as the saturated layer and the adsorption zone. The performance of the saturated layer portion of the carbon bed can be predicted by use of the potential plot which defines the equilibrium capacity of various adsorbates for single contaminants. Tests were conducted to develop potential plots for candidate adsorbates to select the carbon with the highest capacity for the contaminants of interest. Additional data were

then taken on the selected carbon to establish the effects of moisture and phosphoric acid impregnation on the carbon bed capacity.

Based on experimental data with multiple contaminants, a technique was then developed to predict carbon bed capacity in the saturated layer for multiple contaminants. The performance of the adsorption zone portion of carbon beds was established experimentally by making plots of the time to break through or service time of various contaminants as a function of the bed length. An extrapolation of these data to a service time of zero determines the adsorption zone length for a given contaminant, adsorbate and velocity. These data were obtained for a variety of contaminants singly and in groups. It was concluded from these data that the adsorption zone length could be related to the potential parameter and that complete co-existence between contaminants occurred in the adsorption zone. The final experimental investigation required to develop the regenerable sorbent bed design was the determination of the desorption characteristics of the carbon. A number of tests were run on various contaminants which were exposed to multiple adsorption/desorption cycles to determine what conditions are required to achieve no build up in residue contaminant at the end of the desorption cycle.

The conclusions of these tests are that for contaminants with a molar volume greater than 185, thermal and vacuum desorption is inadequate. For contaminants in the molar volume region between 80 and 185, adequate desorption can be achieved at desorption conditions of 2 hours at 10^{-4} mm Hg vacuum and 200°C temperature. For molar volumes less than 80, adequate desorption can be achieved at desorption conditions of 2 hours at 10^{-4} mm Hg vacuum and 100°C temperature.

The program also developed a design methodology for sizing carbon beds utilizing the results of the experimental data. A computer program was developed to perform the calculations required for carbon bed sizing. With the aid of the computer program, several candidate systems were evaluated. An optimization study was then conducted comparing total equivalent weight to determine the best system concept. The selected system consisted of a

high flow (76 CFM) fixed bed containing charcoal impregnated with phosphoric acid for control of ammonia and high molar volume contaminants. A low flow (3 CFM) loop was provided in parallel with the fixed bed containing a regenerative bed, and a catalytic oxidizer with pre- and post-sorbent beds.

A 1/10 scale model of the system was then fabricated and evaluated for over 180 days of continuous operation. The results of this test indicated that the system performed satisfactorily; however, certain modifications were required in the design procedure. The test results indicated that the velocity correlation factor utilized to determine adsorption zone length needed to be modified from velocity to the 0.5 power to velocity to the 1.0 power.

Utilizing the modified design procedure, the design of a full-scale system, sized for a 12-man crew with a 180-day resupply, was determined. Layout drawings of these system components were then developed.

INTRODUCTION

The development of an isotope-heated catalytic oxidizer for control of trace contaminants was initiated in 1966 under Contract NAS 1-6256. This contract between the Lockheed Missiles & Space Company (LMSC) with TRW Systems as a major subcontractor, and the NASA-Langley Research Center resulted in engineering layout drawings of the selected approach and long term testing of a model system. The results of this effort are described in NASA CR 66346, NASA CR 66347 and NASA CR 66497. The tasks accomplished under NAS 1-6256 included the following:

- o Mission Definition
- o Contaminant Load Definition
- o Isotope Selection
- o Catalyst Selection
- o Catalyst Performance Tests
- o Analysis and Optimization
- o Design Layout Drawings
- o Development Plan

Following the conclusion of this program, the NASA-Langley Research Center directed LMSC to continue this development program under Contract NAS 1-7433. This effort was initiated in 1968. TRW Systems was also a major subcontractor in this additional effort. The program conducted under NAS 1-7433 is reported in NASA CR 66739 and dealt with additional development of the isotope-heated catalytic oxidizer system including detailed design of a unit utilizing a resistively heated simulated isotope and development and detailed design of pre- and post-sorbent beds. The tasks involved in this program are shown below:

- o Contaminant load definition for a pre- and post-sorbent bed
- o Design and fabrication of a model pre-sorbent bed
- o Long term sorbent bed evaluation
- o Design and fabrication of a model post-sorbent bed
- o Detailed design of full scale pre- and post-sorbent beds

- o Specifications for the isotope heat source materials of construction
- o Joining and fabrication tests on the isotope heat source materials of construction
- o Fabrication and evaluation of the test heater to be used in the simulated isotope heat source
- o Compatibility tests to determine the extent of interdiffusion between the graphite reentry aid and the noble metal cladding
- o Fabrication and evaluation of the thermal insulation to be used in the isotope-heated catalytic oxidizer
- o Detailed design of the isotope-heated catalytic oxidizer including the resistively heated simulated isotope heat source.

The objective of the effort described in this report was to expand the development of the catalytic oxidizer trace contaminant control system developed under these previous NASA contracts to include the remaining elements of a complete spacecraft contaminant control system which include regenerable and non-regenerable charcoal sorbent beds.

This effort was continued under NAS 1-9242 for the NASA-Langley Research Center by LMSC in 1969, with MSAR as a major subcontractor. The tasks involved in this phase of the program are shown below and are described in detail in this report:

- o Contaminant Load Review and Refinement
- o Establishing Carbon Bed Performance Characteristics
- o System Analysis and Optimization
- o Long-Term Model System Testing
- o Full-Scale System Preliminary Design

REVISED CONTAMINANT MODEL

The original contaminant load developed in Contract NAS 1-6256 was reviewed during this program and revised to reflect a change in the nominal crew size from 9 to 12 men, and to take into account the fact that the original estimates made no allowance for the reduction in equipment contaminant off-gassing as a function of time. The allowable contaminant levels were also modified to reflect the latest data of the panel on Air Standards for Manned Space Flight of the Space Science Board, National Academy of Sciences⁽¹⁾. The revised contaminant model is shown in Table 1; also included in this table are the original equipment contaminant production rates generated during NAS 1-6256.

Biological Contaminants

The biologically produced contaminant production rates were based on a 12-man crew size. The production rates for pyruvic acid, ethyl alcohol, methyl alcohol, nu-butyl alcohol, acetone, and acetaldehyde were based on the experimental measurements of R. A. Dora, et al⁽²⁾. In these tests, a number of subjects were enclosed in bags, and the contaminant build-up rates were noted. The average rates observed were used in Table 1. The presence of these contaminants in the effluents of man has been observed by other investigations⁽³⁾. The ammonia production rate was based primarily on data in the NASA Life Sciences Data Book on the concentration of ammonia in sweat with some allowance for ammonia production from urine. Carbon monoxide and methane production rates were based on experimental buildup data from closed system tests and data in the NASA Life Sciences Data Book. Hydrogen production was based on literature values for the quantity of hydrogen in human flatus. The indole production was based on a fraction of the indole content of human feces.

For those contaminants cited in the literature as known biological contaminants, such as caprylic acid, ethyl mercaptan, methyl mercaptan, propyl mercaptan, valeraldehyde, and valeric acid, for which no rate data are available, a rate consistent with Dora's production rates for similar compounds was established.

Table 1
REVISED CONTAMINANT MODEL

Contaminant	12-Man Biological Production Rate gms/day	Initial or Maximum (1) Equipment Production Rate gms/day	Average or Nominal (1) Equipment Production Rate gms/day	Maximum Allowable Concn. Mg/M ³
Acetone	.0015	10.2	1.02	700
Acetaldehyde	.001	F	F	35
Acetic Acid		S	S	2.5
Acetylene		P	P	6400
Acetonitrile		S	S	7
Acrolein		S	S	0.25
Allyl Alcohol		S	S	0.50
Ammonia	3.0	P	P	17.5
Amyl Acetate		S	S	53
Amyl Alcohol		S	S	36
Benzene		S	S	3.2
n-Butane		P	P	180
iso-Butane		S	S	180
Butane-1		F	P	180
cis-Butene-2		S	S	180
trans-Butene-2		F	P	3.2
1,3 Butadiene		P	P	220
iso-Butylene		S	S	180
n-Butyl Alcohol	.016	P	P	30
iso-Butyl Alcohol		S	S	30
sec-Butyl Alcohol		S	S	30
tert-Butyl Alcohol		S	S	30
Butyl Acetate		S	S	71
Butraldehyde		S	S	70
Butyric Acid		S	S	14
Carbon Disulphide		S	S	6
Carbon Monoxide	0.400	P	P	17
Carbon Tetrachloride		S	S	6.5
Carbonyl Sulphide		S	S	25
Chlorine		S	S	033
Chloroacetone		S	S	100
Chlorobenzene		S	S	35
Chlorofluoromethane		S	S	24
Chloroform		P	P	24
Chloropropane		S	S	84
Caprylic Acid	0.110			155
Cumene		S	S	25
Cyclohexane		P	P	100
Cyclohexene		S	S	100
Cyclohexanol		S	S	20
Cyclopentane		S	S	100
Cyclopropane		S	S	100
Cyanamid		S	S	45
Decalin		S	S	5.0
1, 1 Dimethyl Cyclohexane		S	S	120
trans 1, 2, Dimethyl Cyclohexane		S	S	120
2,2 Dimethyl Butane		S	S	93
Dimethyl Sulphide		S	S	15
1,1 Dichloroethane		P	P	40
Di-iso-Butyl Ketone		S	S	29
1,4 Dioxane		P	P	36
Dimethyl Furan		S	S	3.0
Dimethyl Hydrazine		S	S	0.1
Ethane		P	P	180
Ethyl Alcohol	0.048	P	P	190
Ethyl Acetate		P	P	140
Ethyl Acetylene		S	S	180
Ethyl Dichloride (1,2 Dichloro ethene)		S	S	44
Ethyl Ether		P	P	120
Ethyl Butyl Ether		P	P	200
Ethyl Formate		P	P	30
Ethylene		P	P	180
Ethylene Glycol		P	P	114
trans 1, Methyl 3, Ethyl Cyclohexane		S	S	117
Ethyl Sulfide		S	S	97
Ethyl Mercaptan	0.010			2.5
Freon 11		S	S	5600
Freon 12		P	P	4000
Freon 21		S	S	420
Freon 22		S	S	350
Freon 23		S	S	12
Freon 113		S	S	142
Freon 114		P	P	7000
Freon 114 unsym		S	S	7000
Freon 125		S	S	25
Formaldehyde		S	S	25
Furan		S	S	3
Furfural		S	S	2
Hydrogen	0.600	P	P	215
Hydrogen Chloride		S	S	0.15

Table 1 (Continued)

Contaminant	12-Man Biological Production Rate gm/day	Initial or Maximim Equipment Production Rate gm/day	Average or Nominal Equipment Production Rate gm/day	Maximum Allowable Conc. mg/M ³
Hydrogen Fluoride		S	S'	0.08
Hydrogen Sulfide	0.0009			1.5
Heptane		S	S'	200
Hexene-1		S	S'	180
n-Hexene		P	P'	180
Hexamethylcyclotrisiloxane		S	S'	240
Indole	.300			126
Isoprene		S	S'	140
Methylene Chloride		P	P'	21
Methyl Acetate		P	P'	61
Methyl Butyrate		S	S'	30
Methyl Chloride		S	S'	21
Methyl-1 Butene		S	S'	1430
Methyl Chloroform		P	P'	190
Methyl Furan		S	S'	3
Methyl Ethyl Ketone		P	P'	59
Methyl Isobutyl Ketone		S	S'	41
Methyl Isopropyl Ketone		P	P'	70
Methyl Cyclohexane		S	S'	200
Methyl Acetylene		P	P'	165
Methyl Alcohol	0.017			26
3-Methyl Pentane		S	S'	295
Methyl Methacrylate		S	S'	41
Methane	7.20	29.50	2.95	1720
Mesitylene		S	S'	2.5
mono-Methyl Hydrazine		S	S'	0.035
Methyl Mercaptan	0.010			2
Naphthalene		S	S'	5
Nitric Oxide		S	S'	32
Nitrogen Peroxide		S	S'	1.4
Nitrogen Dioxide		S	S'	0.9
Nitrous Oxide		S	S'	235
Propylene		P	P'	180
iso-Pentane		P	P'	295
n-Pentane		P	P'	295
Pentene-1		S	S'	180
Pentene-2		S	S'	180
Propane		P	P'	180
n-Propyl Acetate		S	S'	84
n-Propyl Alcohol		P	P'	75
iso-Propyl Alcohol		P	P'	98
n-Propyl Benzene		S	S'	44
iso-Propyl Chloride		S	S'	260
iso-Propyl Ether		S	S'	120
Propionaldehyde		S	S'	30
Propionic Acid		S	S'	15
Propyl Mercaptan	0.010			82
Propylene Aldehyde		S	S'	10
Pyruvic Acid	2.51			0.9
Phenol		S	S'	1.9
Skatol	0.300			141
Sulfur Dioxide		S	S'	0.8
Styrene		S	S'	42
Tetrachloroethylene		S	S'	67
Tetrafluoroethylene		S	S'	205
Tetrahydrofuran		S	S'	59
Toluene		S	S'	75
Trichloroethylene		P	P'	52
1,2,4 Trimethyl Benzene		S	S'	49
1,1,3 Trimethyl Cyclohexane		S	S'	140
Valeraldehyde	0.010			70
Valeric Acid	0.010			110
Vinyl Chloride		P	P'	130
Vinyl Methyl Ether		S	S'	60
Vinylene Chloride		S	S'	20
O-xylene		P	P'	44
M-xylene		P	P'	44
P-xylene		P	P'	44

(1) Where arbitrary equipment production rates have been assigned, based on a percentage of the total, symbols have been utilized to designate these rates. Contaminants with the symbol P are considered primary equipment off-gassing contaminants, and those with the symbol S are considered secondary contaminants. The prime indicates the reduced rates. The rates utilized in the design studies are P = 2.5 gms/day, S = 0.25 gms/day, P' = 0.25 gms/day, S' = 0.025 gms/day.

Non-Biological Contaminants

In the original IHCOS study, the total production rate of non-biological contaminants was based on an extrapolation of experimental data from out-gassing of Apollo equipment. These data were extrapolated to a typical space station; however, no allowance was made in the original IHCOS study for the fact that the Apollo outgassing rates were based on a fourteen day mission and that the space station mission would be considerably longer. Due to this longer total exposure, it is anticipated that the average total daily contaminant production rate would be reduced. A review of available material on off-gassing studies was made to determine if any pertinent data existed. The most appropriate data from which an estimate of this effect can be made were taken by Cox and Smith. In their studies, 22 samples of representative space cabin organic materials were investigated. These materials were placed in a bell jar, and the contaminant off-gassing rate was monitored as a function of time. The average off-gassing rate as a function of time for the 20 materials is presented in Figure 1. The experimental data were obtained for a time period of 45 days and extrapolated to 180 days.

Based on these data, an average off-gassing rate was established for the first 14 days, and an average rate was determined for 180 days. The ratio of these two rates was approximately 4.9. Thus, the average production rate developed utilizing Apollo data could be as much as 4.9 times the average rate anticipated for 180 days.

The original IHCOS contaminant load assumed for a space station included a total estimated equipment load of 50 grams/day. The individual maximum contaminant equipment production rates were assumed as an arbitrary percent of this total; however, the sum of these individual maximum rates was in excess of 50 grams/day (i.e., 168 grams/day). In order to size a sorbent bed system for the total design contaminant load, it is necessary to have a model of the contaminant load utilizing nominal individual rates. The individual maximum rates could still be utilized to establish the sorbent bed flow rate requirements. The variation in these maximum rates to bring the total in line with a 50 grams/day total production rate would be a reduction by a factor of 3.37. Combining this factor with the reduction related to the change in production rate with time, yields a potential reduction factor of 16.5.

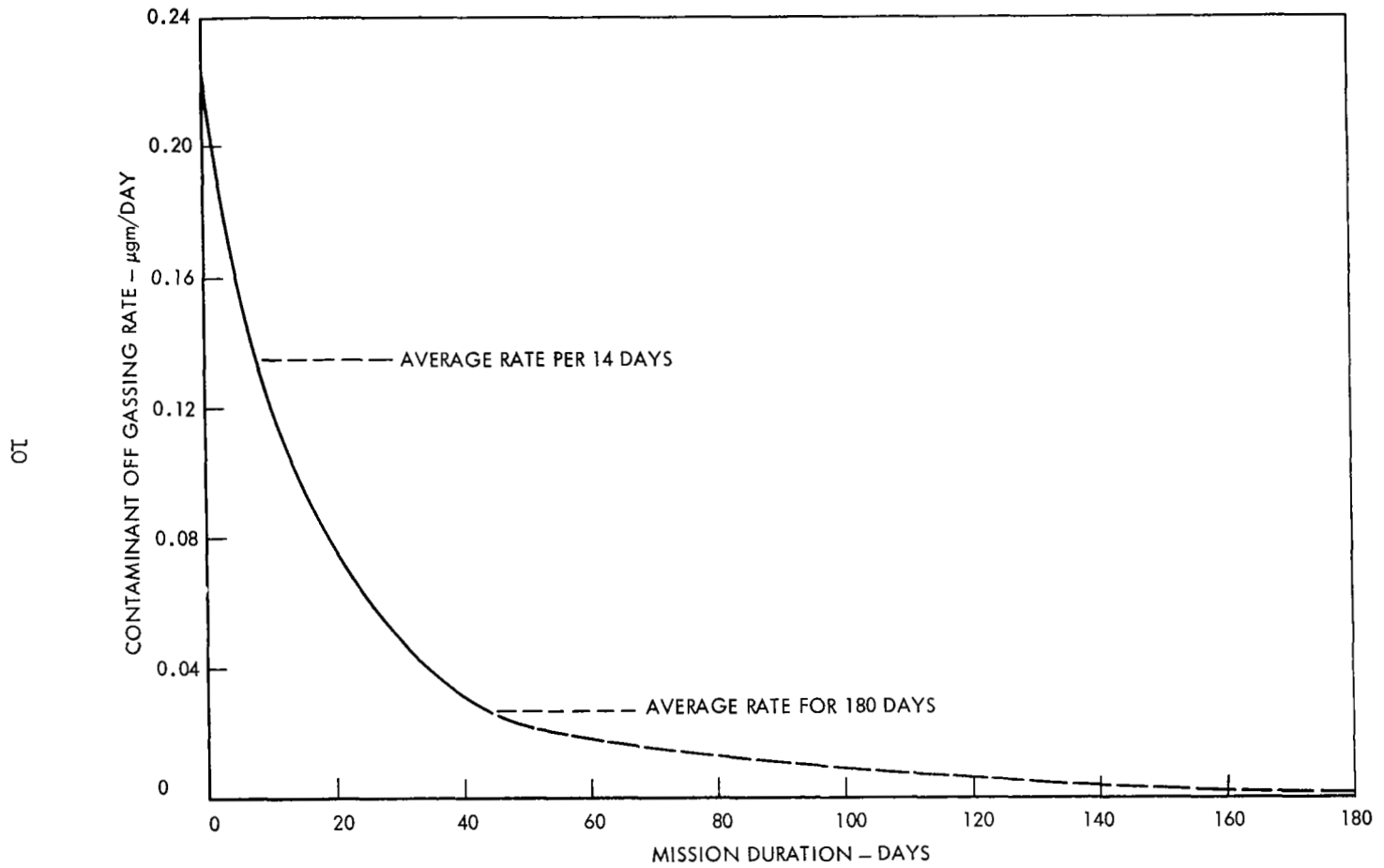


Figure 1 Non-Metallic Average Contaminant Off-Gassing Rates for Twenty Typical Spacecraft Non-Metallic Materials

The IHCOS contaminant load was compared with the contaminant model used in the AILSS study. The total number of contaminants used in the AILSS model was quite small and probably unrealistic for a space station. The individual equipment production rates of those contaminants were compared with the individual IHCOS rates for the same contaminants. The total IHCOS rate for these 10 contaminants is 16.5 times the total AILSS rate. This, however, is heavily influenced by methane which is over one-half of the total IHCOS rate for these 10 contaminants. Not considering methane, the IHCOS rate for the remaining 9 contaminants is 7.4 times the AILSS rate. Based on the above considerations, it appears that justification exists for reducing the maximum individual IHCOS equipment production rates by a factor of between 7 and 16 to obtain nominal rates to be used for the sorbent bed design. It was, therefore, decided to reduce the IHCOS equipment rates by a factor of 10. These data are shown in Table 1. It should be recognized that this reduction is primarily based on the fact that the contaminant off-gassing rate will decrease with time. This means that the nominal production rates presented in Table 1 actually represent average rates throughout the mission. In reality, production rates will be higher initially and lower at the end of the mission. Therefore, average or nominal rates are suitable for sizing expendable sorbent beds but system flow rates should be based on the initial or maximum production rates. Also, the quantity of sorbent required for regenerative sorbent beds should be based on initial or maximum production rates. Thus, the nominal rates presented in Table 1 were used for sizing the expendable beds, and the nominal equipment, production rates, plus the metabolic production rates, were used to establish system flow rates and the quantity of regenerative sorbent.

Arbitrary equipment production rates have been assigned, based on a percentage of the total equipment rate and symbols have been utilized in Table 1 to designate these rates. For those contaminants considered to be primary candidates for equipment off-gassing, the symbol P is utilized. For those contaminants considered to be secondary candidates for equipment off-gassing, the symbol S is used. The prime is used to designate the nominal equipment production rate, which is one-tenth the maximum equipment rate. For the design studies, the primary individual maximum equipment rates were

taken to be 5% of the total or 2.5 grams/day, and the secondary rates were taken to be 0.5% of the total or 0.25 grams/day. The nominal design rates were then assumed to be one-tenth of these. The contaminants considered to be primary were those contaminants that have been detected in several manned systems such as spacecrafts, submarines or simulator tests. The contaminants considered to be secondary were those detected in only a few manned systems or only in material off-gassing studies.

CARBON BED PERFORMANCE

During the adsorption process, the adsorbate vapor distribution through a carbon bed can take several forms, depending on the adsorbability and rate of adsorption relative to the space velocity and bed length. Figures 2, 3, and 4 illustrate the three common vapor distribution curves. L designates the bed length in each case and C the vapor concentration in the bed. In Figure 2, the vapor has just started to flow through the bed, hence, time t is essentially zero. This type of curve is obtained when the rate of adsorption is very fast relative to space velocity and bed length. Figure 3 illustrates the other extreme, where the adsorption rate is slow. In this case, the gas could penetrate the bed immediately.

In each case, the length of the curve along the L axis measures the length of the adsorption zone. If the vapor input is continued, the adsorption zone of Figure 2 increases and in time, a steady state is attained in a segment of the bed. Figure 4 illustrates the steady state curve at time t , when a steady state is first attained, and at time t_b , when the vapor has just started to penetrate the bed. The service time is then t_b , when penetration concentration is C_b .

For the type curve in Figure 4, the length of the adsorption zone may be designated as I , and $L-I$ then represents the saturated layer length. The amount adsorbed in $L-I$ can be calculated by use of the potential theory equation to obtain A , the potential parameter, and then determine q , the charcoal capacity, from the potential theory plot of q vs. A .⁽⁴⁾ In the equation,

$$A = \frac{T^0}{V_m} \log \frac{C_s}{C_i} ,$$

C_i is the influent concentration, as in Figures 2 to 4, C_s is the saturation concentration at temperature T , and V_m is the molar volume of the contaminant vapor being adsorbed. q is an equilibrium value; hence, is only dependent on the contaminants adsorbability at temperature T on the particular carbon and the relative vapor concentration C_i/C_s .

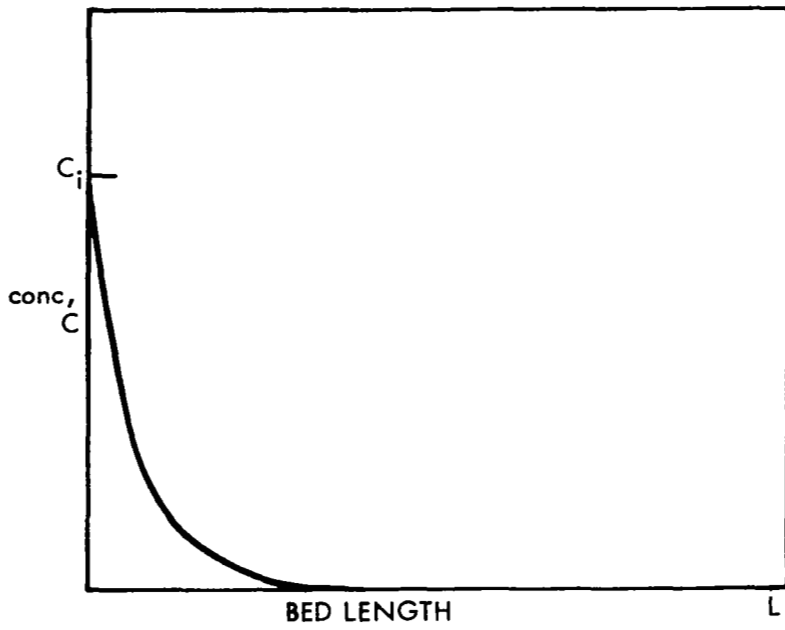


Figure 2 Adsorption Zone, Fast Adsorption Rate $t \cong 0$

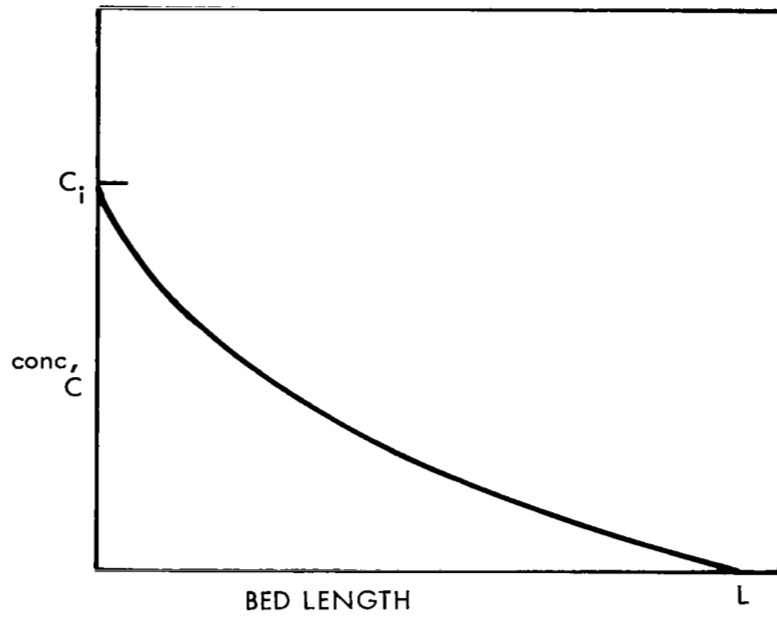
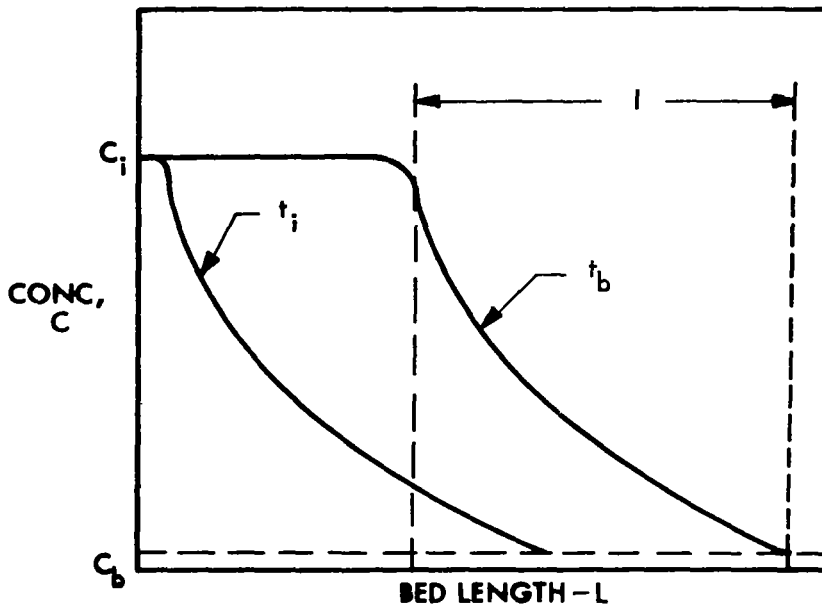


Figure 3 Adsorption Zone, Slow Adsorption Rate $t \cong 0$



NOTES:

- t_i = LOAD PROFILE AT TIME WHEN A
BED SEGMENT FIRST REACHES
STEADY STATE FIRST OBTAINED
- t_b = BED PROFILE AT SERVICE TIME
WHEN BED OUTLET CONCEN-
TRATION EQUALS C_b
- L = ACTIVE ADSORPTION ZONE
LENGTH

Figure 4 Typical Adsorbate Distribution

The adsorption zone length I may be a function of many parameters, i.e., space velocity, carbon particle diameter, temperature, diffusion in the pores, chemical reactions on the carbon surface and C_i/C_b . I. M. Klotz (5) did theoretical studies to relate these parameters to the adsorption zone length and derived the following equation,

$$I = I_t + I_r$$

I_t is a function of diffusion rate of adsorbate molecules from the gas stream to the carbon surface, and I_r is a function of processes occurring within the pores of the carbon. The latter could be diffusion of molecules through the pore structure and adsorption or chemical reaction on the carbon surface.

$$I_t = \frac{2.30}{a} \left[\frac{D_p U_m}{\mu} \right]^{0.41} \left[\frac{\mu}{\rho D_v} \right]^{0.67} \log \frac{C_i}{C_b}$$

and

$$I_r = k U_m \log \frac{C_i}{C_b}$$

In these equations

a = superficial area of particles per unit bulk volume, cm^2/cm^3

D_p = mean particle diameter, cm

U_m = linear velocity of gas between particles, cm/sec

ρ = density of gas mixture, g/cc

μ = viscosity of gas mixture, poise

D_v = diffusion coefficient of adsorbate vapor, cm^2/sec

C_i = influent concentration

C_b = penetration concentration

k = a constant

when the carrier gas is 31% O_2 - 69% N_2 at 298°C and 517 mm of Hg pressure.

$$I = \left\{ 1.55 \left[\frac{1}{a} D_p^{0.41} U_m^{0.41} \left(\frac{1}{D_v} \right)^{0.67} \log \frac{C_i}{C_b} \right] + k U_m \right\} \log \frac{C_i}{C_b}$$

For high molecular weight vapors, (i.e., $V_m \approx 100$), $I = I_t$ with very little contribution from I_r .

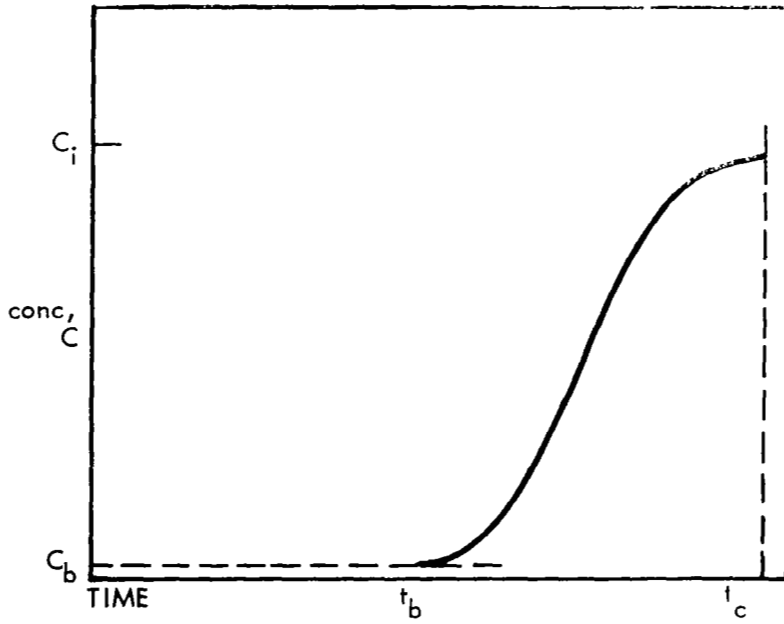


Figure 5 Effluent Concentration Curve

For lighter molecules, I_t decreases relatively while I_r increases. Since I_r cannot be determined analytically, adsorption zone length must be determined experimentally.

There are two ways to experimentally determine the adsorption zone length: (1) by determining the effluent concentration curve, and (2) by determining the adsorption zone length. The effluent concentration curve is illustrated in Figure 5 and can be used for this purpose if the adsorption zone has attained a steady state before it penetrates the bed. Then

$$\left[\frac{t_c - t_b}{t_c} \right] L = I$$

Figure 6 illustrates an adsorption zone length curve. To obtain this curve, service times (t_b) are determined for progressively longer bed depths (L). The intercept of the straight portion of the curve with the L axis determines I . This is the technique that was used in this program.

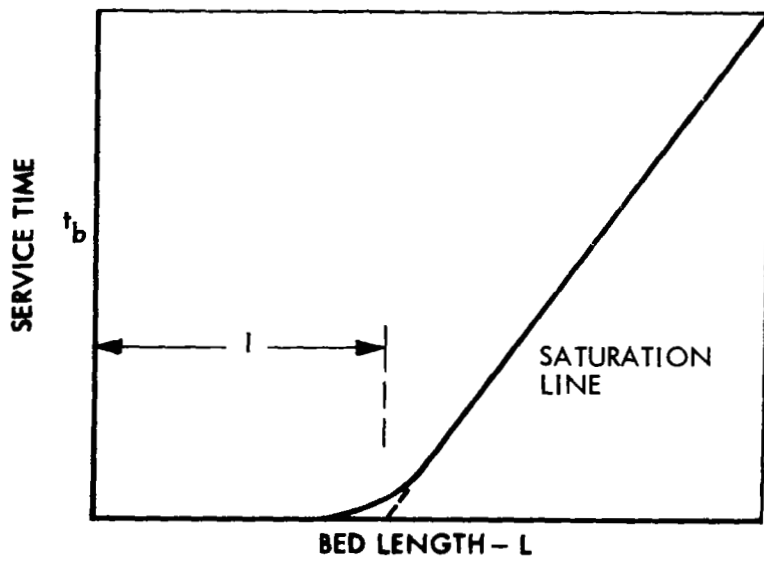


Figure 6 Adsorption Zone Length

Saturation Capacity of Charcoal

The following sections describe the techniques used to determine the saturation capacity of the charcoal.

Sorbent Selection

The major portion of a contaminant adsorbed by a charcoal bed is retained in the saturated layer. This was demonstrated experimentally and is described in the discussion of adsorption zone length. For this reason, the equilibrium capacity of carbon in the saturated layer is the primary guide for selecting the charcoal most suited for a given application. It was initially assumed in this program that super-activated charcoal would yield the highest overall capacity since experiments with CCl_4 had indicated capacity increases over other carbons of up to 150%.

Thus, the first carbon investigated was a super-activated coconut charcoal. A potential plot for this carbon was developed and is shown in Figure 7. The supporting experimental data are presented in Appendix A, and the apparatus and procedures for obtaining the data are described in Appendix B. When the complete potential plot was obtained for the super-activated charcoal, it was observed that the super-activated carbon had higher capacity for well-adsorbed contaminants than for poorly adsorbed contaminants when compared with Barnebey-Cheney BD. The super-activated carbon is treated in a manner which opens the pore structure resulting in increased capacity for large molecules (i.e., low A value). For typical spacecraft requirements, only small amounts of charcoal would be required for the removal of contaminants with small A values. The major portion of the bed would be required for poorly adsorbed contaminants with larger A values. The distribution of pore sizes in the super-activated charcoal is such that the BD charcoal yields better performance in the region of interest for spacecraft contaminants.

When it was discovered that the BD charcoal was superior to the super-activated, it was decided to investigate Pittsburgh BPL and Barnebey Cheney G1, which were both considered as good candidates. No additional capacity data were obtained on BD since its capacity was extremely well documented. The potential plots for the Pittsburgh BPL and Barnebey Cheney G1 are also shown

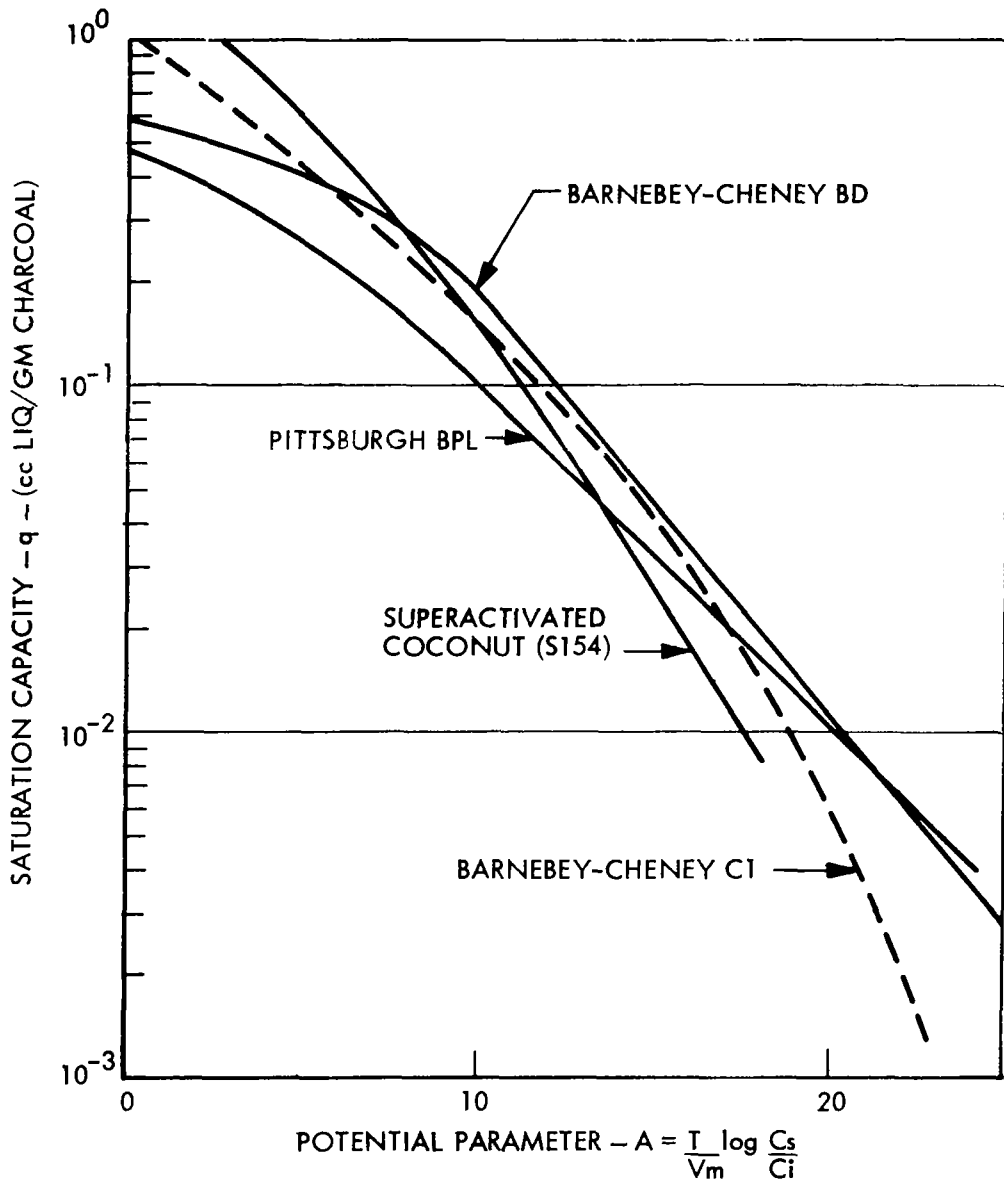


Figure 7 Potential Plot for Various Carbons

in Figure 7, and the supporting experimental data is presented in Appendix A. Neither the G1 or the BPL charcoal appeared to be superior to the BD in the region of interest. For this reason, BD was selected for use on the final system design.

Since, however, a great deal of the experimental data had been taken on the G1 carbon, it was decided to use this carbon for the comparative tests to establish the effects of humidity and phosphoric acid impregnation. These data were then extrapolated to the BD charcoal.

Effects of Moisture and Impregnation

Data presented for activated charcoal are generally taken for single contaminants and a dry gas feed. When spacecraft requirements are considered, the desirability of selecting a 50% inlet RH is evident. Also, the use of a phosphoric acid treatment of the charcoal is proposed as a candidate for the removal of ammonia gas. Impregnating charcoal with phosphoric acid can be accomplished with no additional weight and with only a slight reduction in overall charcoal performance.

The trade-off studies presented in a subsequent section have indicated that this removal technique for ammonia is superior to providing a separate ammonia sorbent.

Data were taken by MSAR on G1 charcoal with both humid and dry inlet streams and with G1 charcoal treated with phosphoric acid in a humid stream to determine the effect upon the potential plot. These data are presented in Figure 8, and in detail in Appendix A.

Tests were conducted with both acetone and F-11 in a dry inlet feed gas. These tests confirmed the potential plot for the charcoal. Subsequent tests with a 50% RH inlet gas showed a negligible reduction for acetone, a soluble material, and a 30% reduction in adsorption of F-11, an insoluble material. Data taken with F-11 in a 50% RH carrier gas on charcoal treated with phosphoric acid showed a further 40 percent reduction in capacity for the insoluble F-11. These test results are presented in Figure 8.

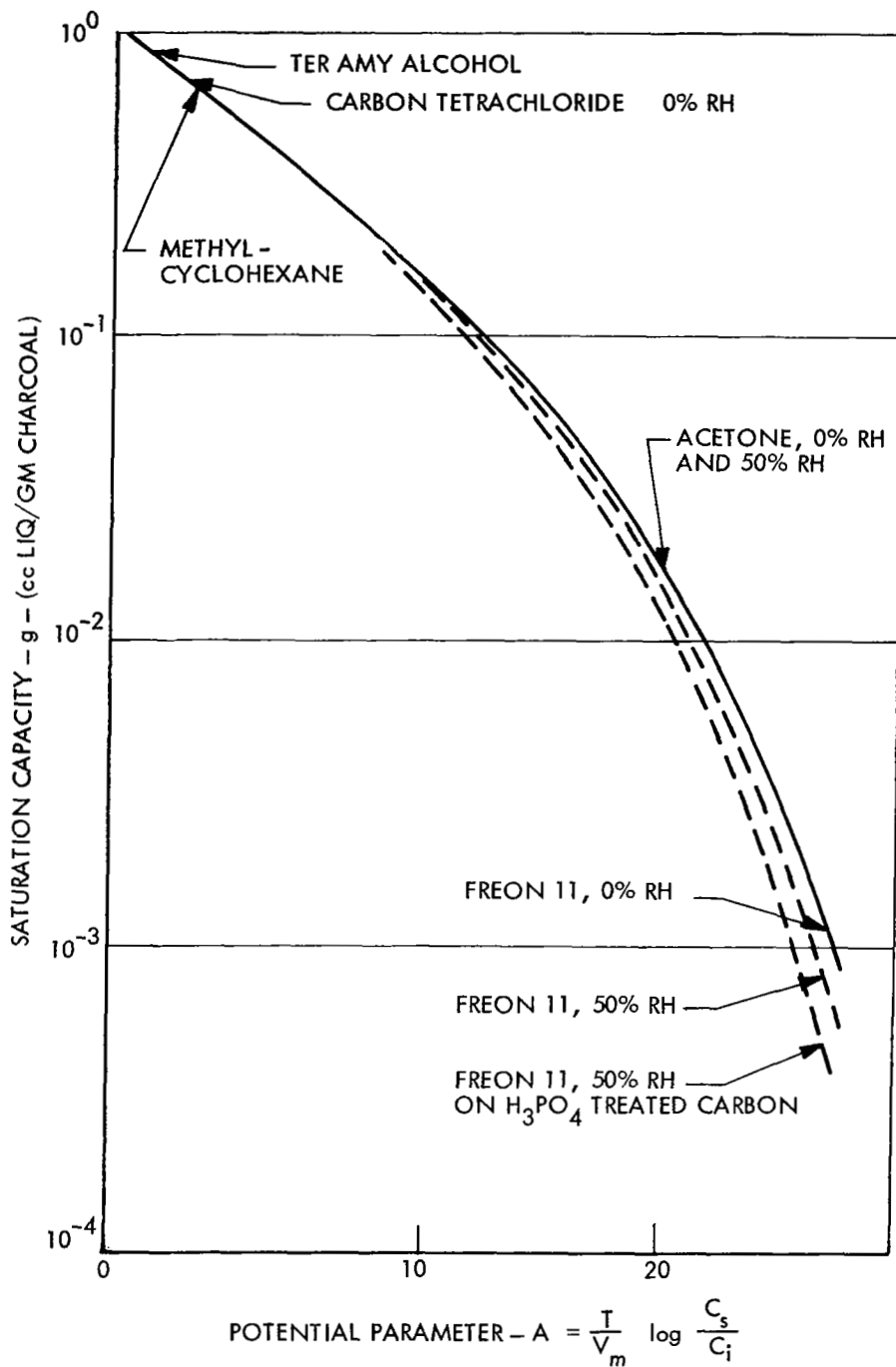


Figure 8 Potential Plot for Barnebey Cheney G-1 Carbon

The proposed mechanism behind these results lies in the adsorption of water by charcoal, resulting in a displacement of contaminants. In the case of acetone, which is water soluble, the acetone dissolves in the water, migrates to an adsorption site and is adsorbed in the charcoal, easily displacing the water which has a much higher A value. In the case of F-11, which is water insoluble, the water effectively blocks the adsorption sites reducing the capacity. Therefore, two adsorption lines are proposed for the potential plots, one for soluble constituent and one for insoluble ones. The postulated effect of phosphoric acid is that this delequent material increases the blockage effects of water. For materials having a very large molar volume and a low A value, the heat of adsorption should be sufficient to drive water progressively from adsorption sites resulting in no decrease in capacity for these materials. Thus, the presence of phosphoric acid would only offset the insoluble contaminants.

Using these mechanisms and results, the potential plot for Barneby-Cheney BD charcoal has been modified, as shown in Figure 9, to allow for the effect of humidity and phosphoric acid for insoluble contaminants. The basic line is assumed valid for soluble contaminants such as acetone.

Saturation Capacity for Multiple Contaminants

The potential plot presented in Figure 9 presents the equilibrium capacity in the saturated layer as a function of the potential parameter A. These data were obtained with single contaminants, and the correlation can be used to establish the capacity of a carbon sorbate for single contaminants. A theory is needed, however, to allow prediction of equilibrium capacity for multiple contaminants. The most conservative interpretation for multiple contaminant situations would take the sum of the charcoal required by all of the contaminants individually, assuming no co-existence between contaminants. The other limit or optimistic view would take just the quantity of charcoal required for the most poorly adsorbed (or the single contaminant that required the greatest quantity of charcoal) and assume that all other contaminants would also be adsorbed on this quantity of charcoal. This latter approach implies complete co-existence. In reality, the situation lies somewhere between these two limits.

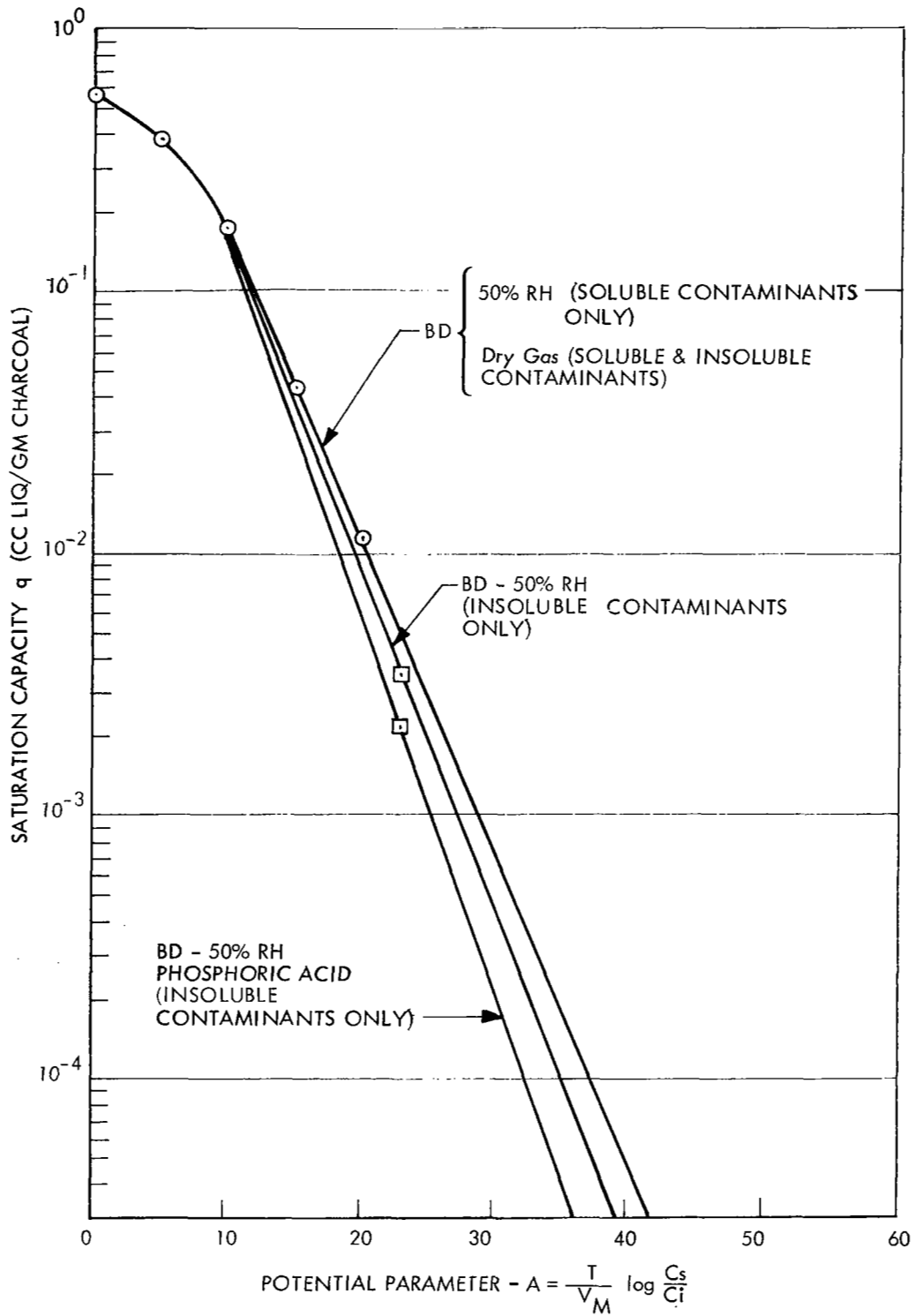


Figure 9 Potential Plot for Barnebey Cheney BD Carbon

Several theories have been proposed for multiple contaminant adsorption; however, the theory that best fits the experimental data obtained in this and other programs is based on the assumption that the blockage of one contaminant by another is a function of the difference in adsorption potential between the two contaminants. Such a correlation is shown in Figure 10. The data presented in Figure 10 were taken from mixed contaminant adsorption experiments conducted under NAS 1-5847 and by MSAR during this effort. The data show the percentage blockage of one contaminant as a function of the difference in adsorption potential between the two contaminants. It appears from these data that a linear relation exists and that complete blockage occurs for differences in adsorption potential greater than 16. Two dotted lines are shown on the curve, one indicating complete blockage at a potential difference of 11 and the other indicating complete blockage at a potential difference of 20. These lines represent what might be considered reasonable uncertainty in the data.

A computer program that defines the required quantity of charcoal for a given application was developed and is described in the optimization study. Utilizing this program, it was possible to determine the sensitivity of the quantity of charcoal required to the assumed difference in adsorption potential that results in a 100% blockage. The results of the study are shown in Figure 11 for both the fixed carbon bed and regenerative beds that were selected as a result of the optimization study.

The results of this sensitivity analysis indicated that in the region of uncertainty in $\Delta A_{\text{critical}}$ (i.e., ΔA at 100% blockage), the effect on the required quantity of charcoal is less than 10%. A high $\Delta A_{\text{critical}}$ represents a high degree of co-existence and hence the minimum amount of charcoal required, whereas an $\Delta A_{\text{critical}}$ of zero represents no co-existence and hence the maximum quantity of charcoal required. It appears from Figure 11 that if $\Delta A_{\text{critical}}$ is greater than 10, it has little effect on the required quantity of charcoal.

Determination of the Adsorption Zone

In the determination of activated charcoal required for the removal of trace contaminants, two areas of adsorption are of interest. These are the saturated layer of the bed, which is discussed in the previous sections, and

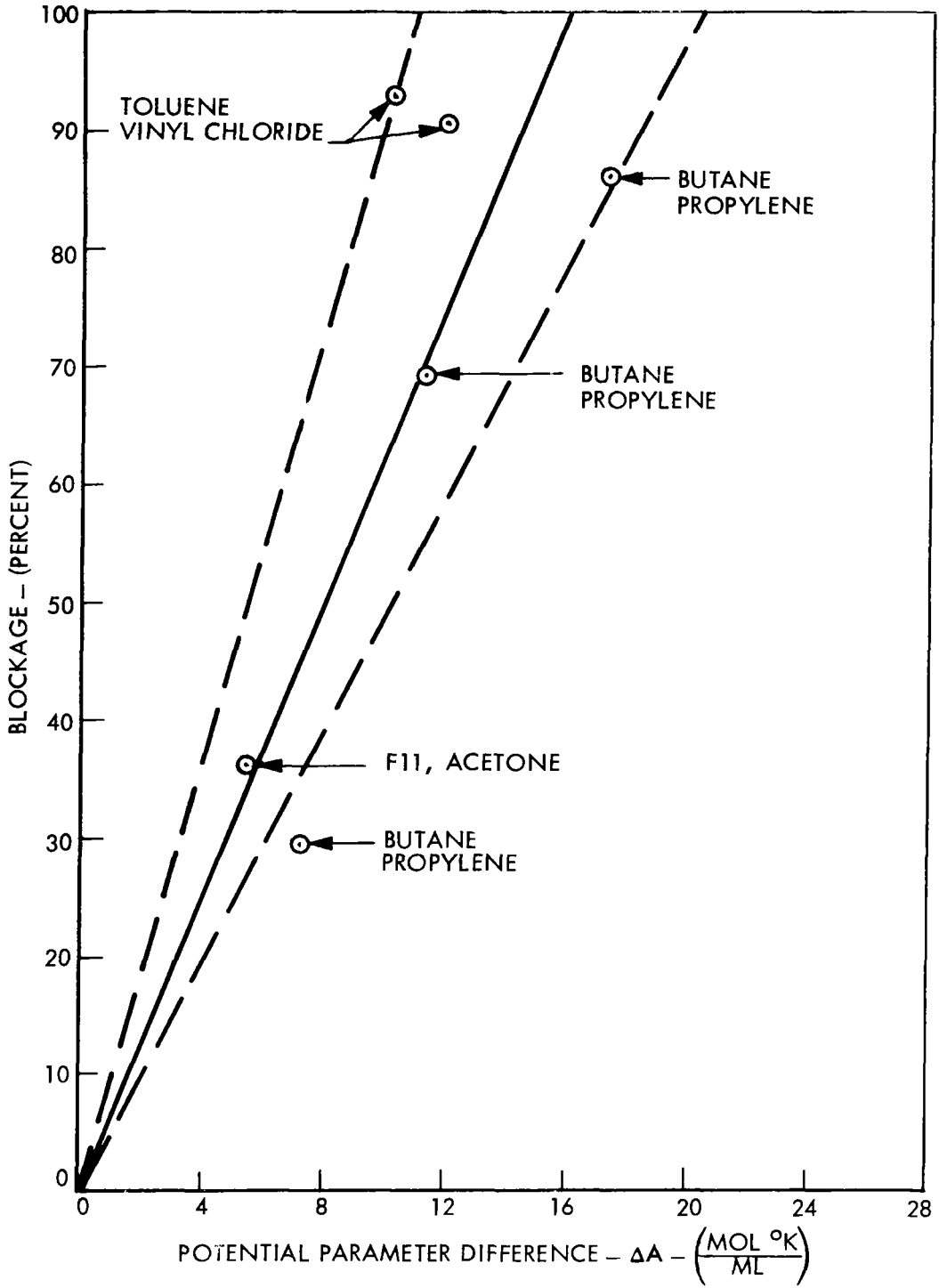


Figure 10 Blockage Effects with Multiple Contaminants

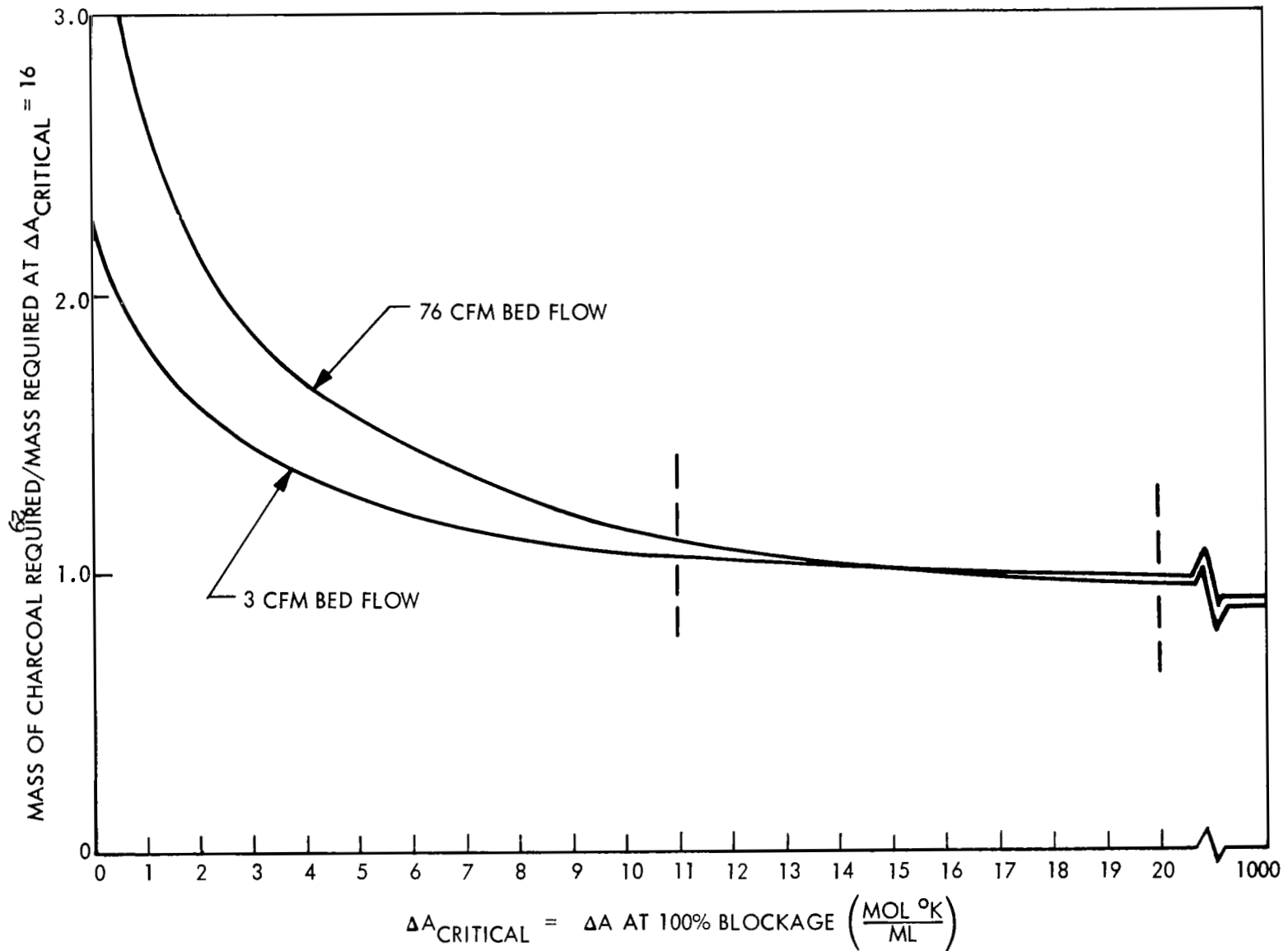


Figure 11 Sensitivity of Required Charcoal to $\Delta A_{\text{critical}}$

the adsorption zone. The thickness of the adsorption zone was previously defined by the following equation:

$$I = 1.55 \left[\frac{1}{a} D_p^{.41} U_m^{.41} \left(\frac{1}{D_v} \right)^{.67} + kU_m \right] \log \frac{C_i}{C_b}$$

This equation shows that the critical parameters in the definition of the adsorption zone are:

- a = superficial particle area
- D_p = particle diameter
- U_m = gas velocity
- D_v = vapor diffusivity
- C_b = penetration concentration
- k = a constant

Since all of the variables are not known in the above equation, it is necessary to obtain experimental data to establish the length or quantity of charcoal required in the adsorption zone. For a given charcoal and linear velocity, all of the variables relating to the adsorption zone length are constant with the exception of the vapor diffusivity (D_v) and the penetration concentration (C_b). The vapor diffusivity (D_v) is strongly related to the molar volume, and, therefore, it was decided to attempt to correlate the adsorption length for various contaminants as a function of the potential parameter A. This parameter was chosen since it involved both concentration and molar volume.

Adsorption zone length data were taken for both Freon 11 and Acetone and are presented in Figure 12 as a function of A value. The adsorption zone length life curves for Freon 11 and acetone from which the adsorption zone data were derived are presented in Figures 13 and 14. The adsorption zone length is established by the intercept between an extension of the linear portion of the curve and the carbon bed length. This is because the linear portion of the curve represents the saturated layer and, thus, the remainder of the bed is the adsorption zone. The slopes of the linear curves were determined from the capacity data. These slopes were then matched with the experimentally obtained adsorption zone length curves.

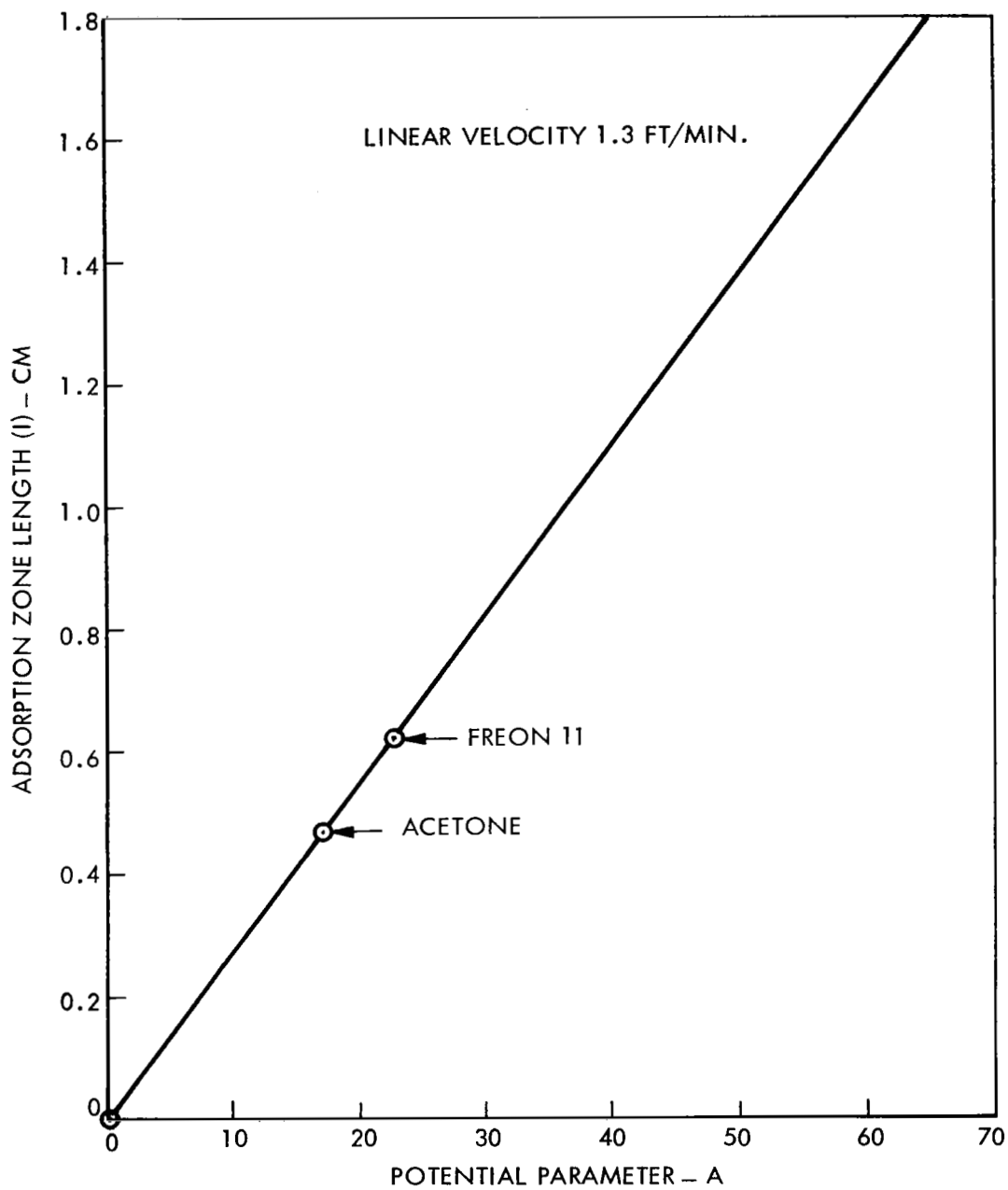


Figure 12 Adsorption Zone Lengths for Various Contaminants

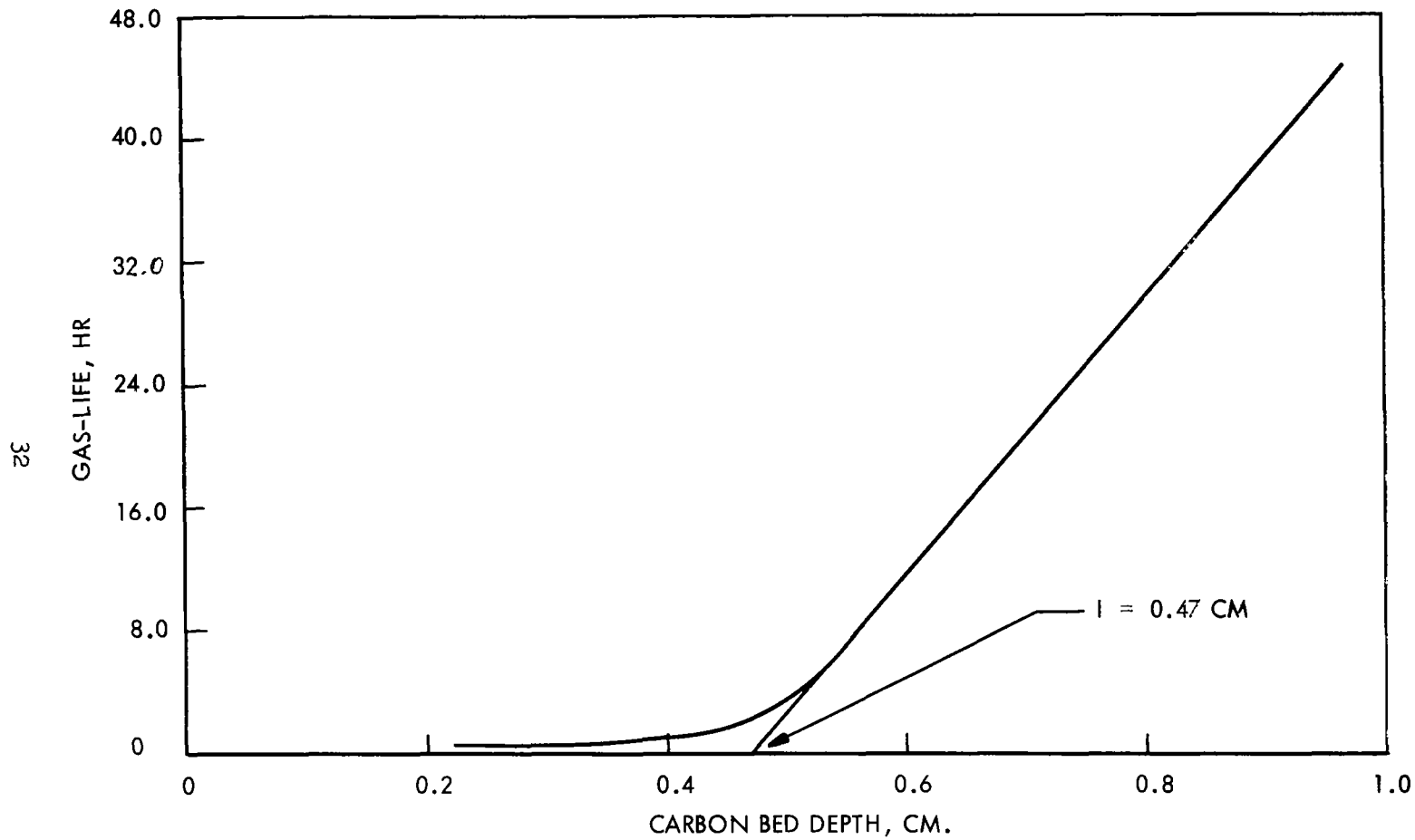


Figure 13 Adsorption Zone Length for Acetone on BC-G1 Carbon

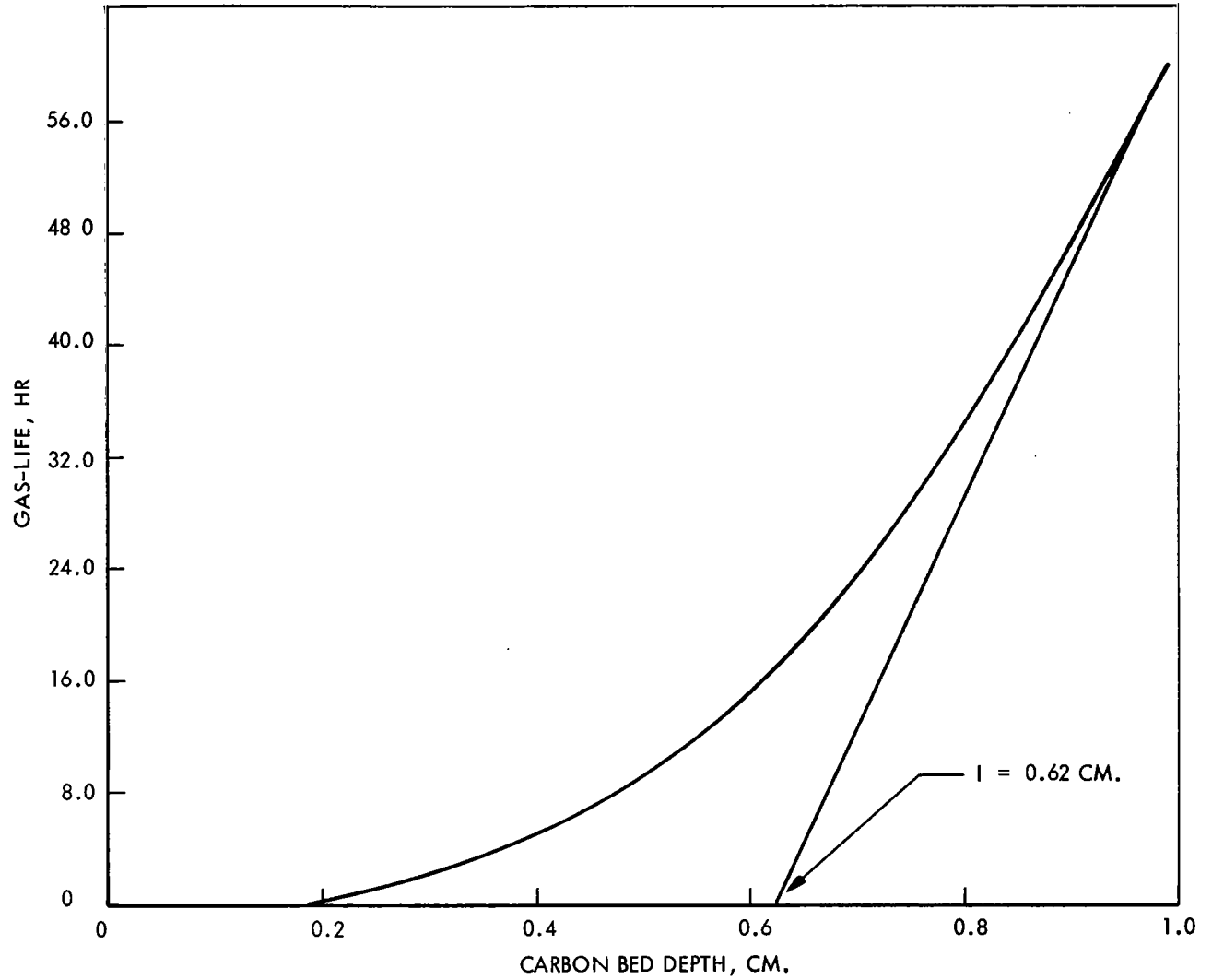


Figure 14 Adsorption Zone Length for Freon 11 on BC-G1

The data presented in Figure 12 are for a linear velocity of 1.3 ft/min. Klotz's equation indicates that the adsorption zone length varies somewhere between $U_m^{0.4}$ and $U_m^{1.0}$. Experimental evidence at this point indicates that $U_m^{0.5}$ yields the best correlation.

To accomplish a sorbent bed design, it is necessary to know what the adsorption zone length is for multiple contaminants. To establish this, adsorption zone length curves were obtained for a mixture of contaminants. A mixture of Freon 11, acetone and methylcyclohexane were used for this study, and adsorption zone curves were established for (1) F11 with acetone, (2) F11 with acetone and methylcyclohexane, (3) Acetone with F11 and (4) Acetone with F11 and methylcyclohexane. These data are presented in Figures 15 through 18.

It was anticipated that the effect of increasing the number of contaminants would tend to increase the adsorption zone length. The adsorption zone data for acetone bore this out. Acetone singly had an adsorption zone length of 0.47 cm while the adsorption zone for acetone increased slightly to 0.62 cm with the addition of Freon 11. The adsorption zone for acetone increased a little further to 0.65 cm when methylcyclohexane was added to the mixture. The experimental results with Freon 11, however, were contrary to what was anticipated. The adsorption zone length for Freon 11 singly was 0.62 cm; however, the adsorption zone decreased to 0.49 cm with acetone and remained at 0.49 cm with the addition of methylcyclohexane. While acetone and Freon 11 did not behave as anticipated, it appears as if one can draw the conclusion that going to multiple contaminants produces no significant effect on the adsorption zone length and that probably nearly complete co-existence occurs in the adsorption zone. The reason for the shift in experimental results from acetone to Freon 11 can probably be attributed to data scatter. It is also evident from these data that the adsorption zone length required is less than 1 inch and is, therefore, a very small portion of the total bed length. Thus, for this particular application, uncertainties in the adsorption zone length are not of great concern.

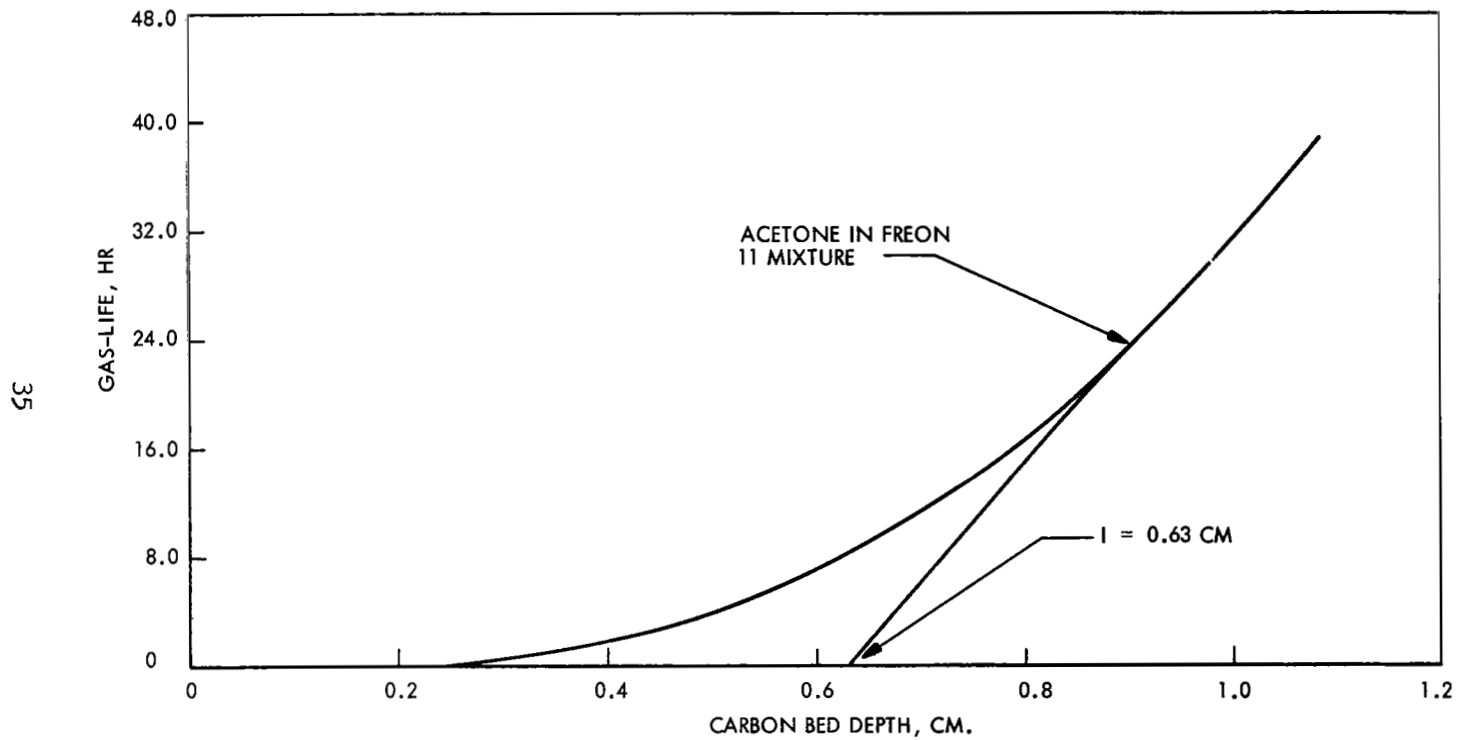


Figure 15 Adsorption Zone Length for Acetone on BC-G1, Acetone-Freon 11 Mixture

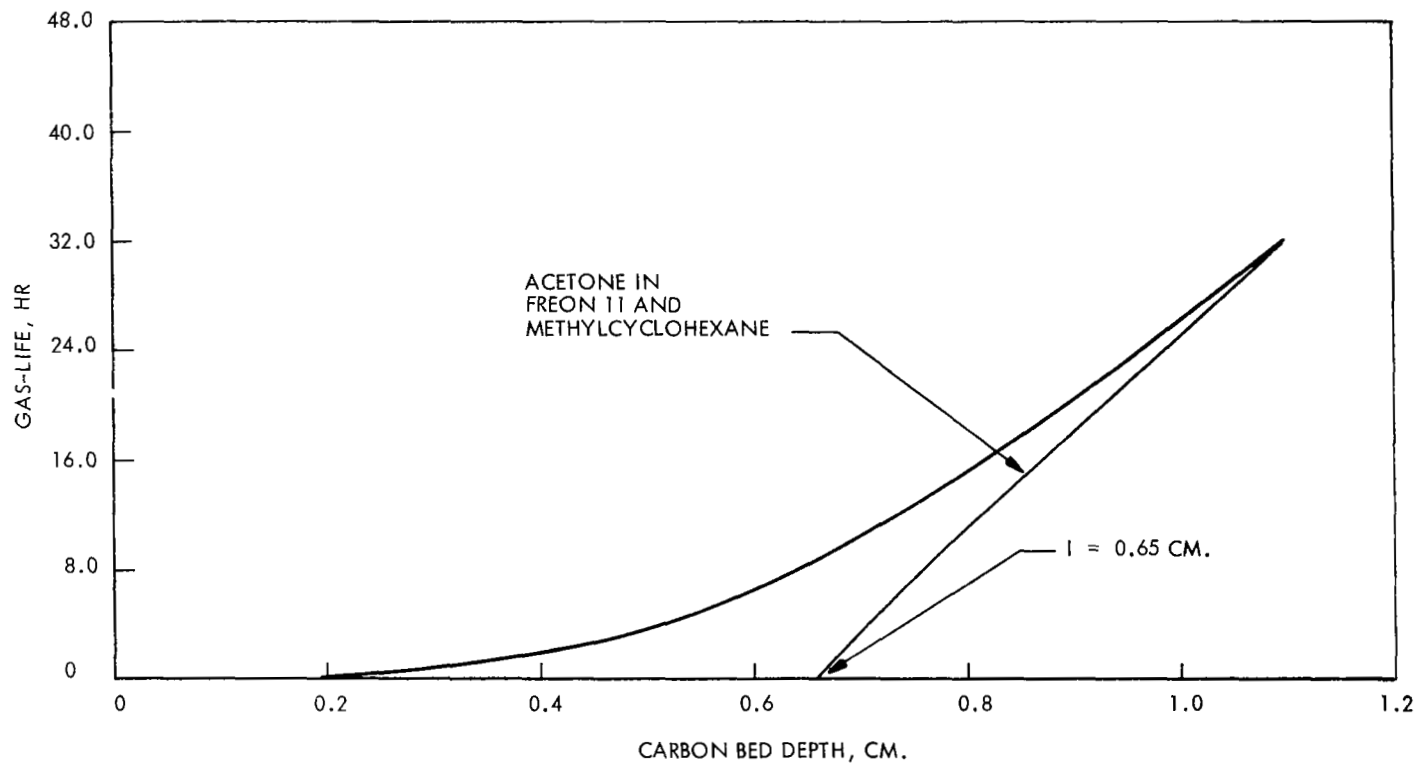


Figure 16 Adsorption Zone Length for Acetone on BC-G1, Acetone, Freon 11, Methylcyclohexane Mixture

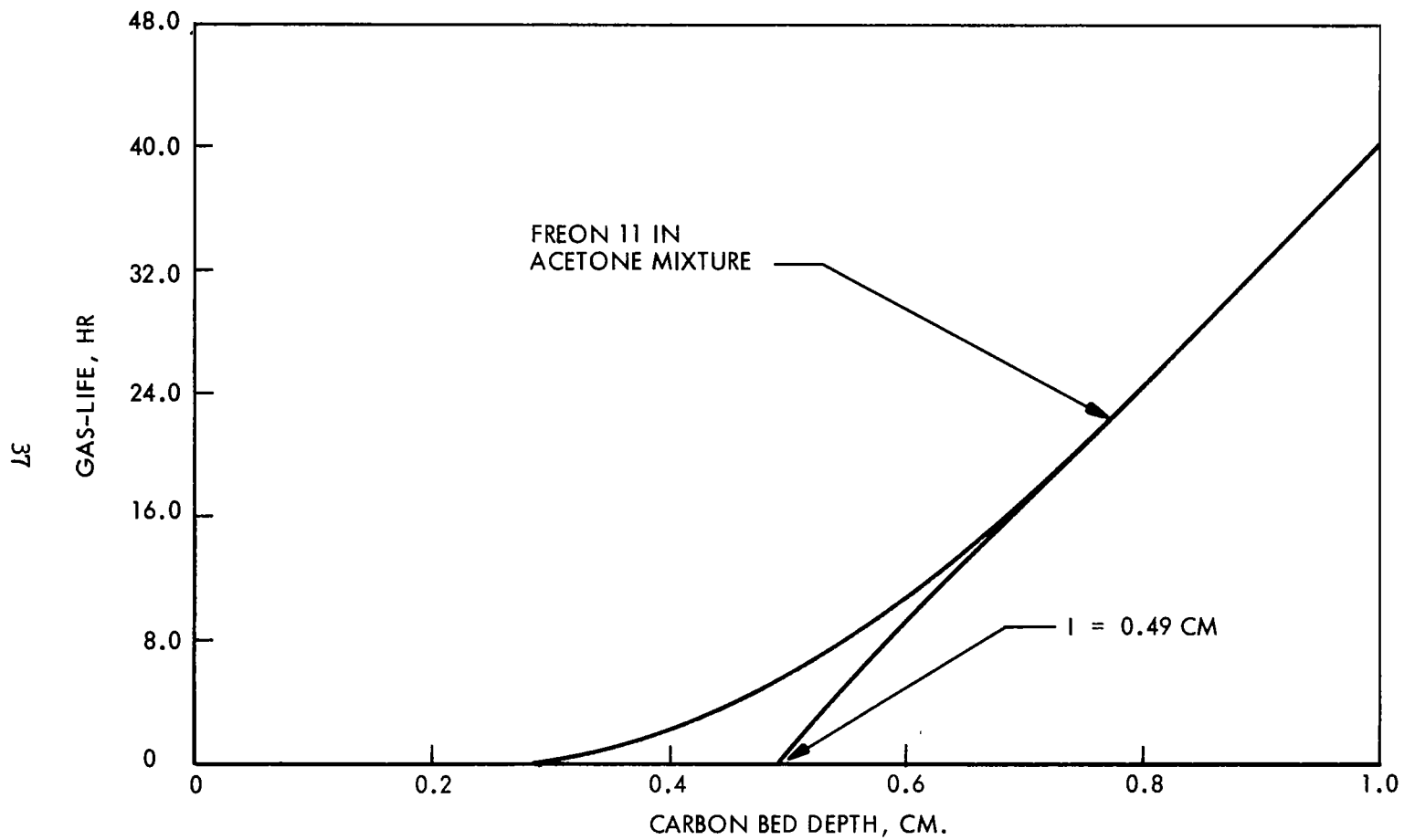


Figure 17 Adsorption Zone Length for Freon 11 on BC-G1, Freon 11 Acetone Mixture

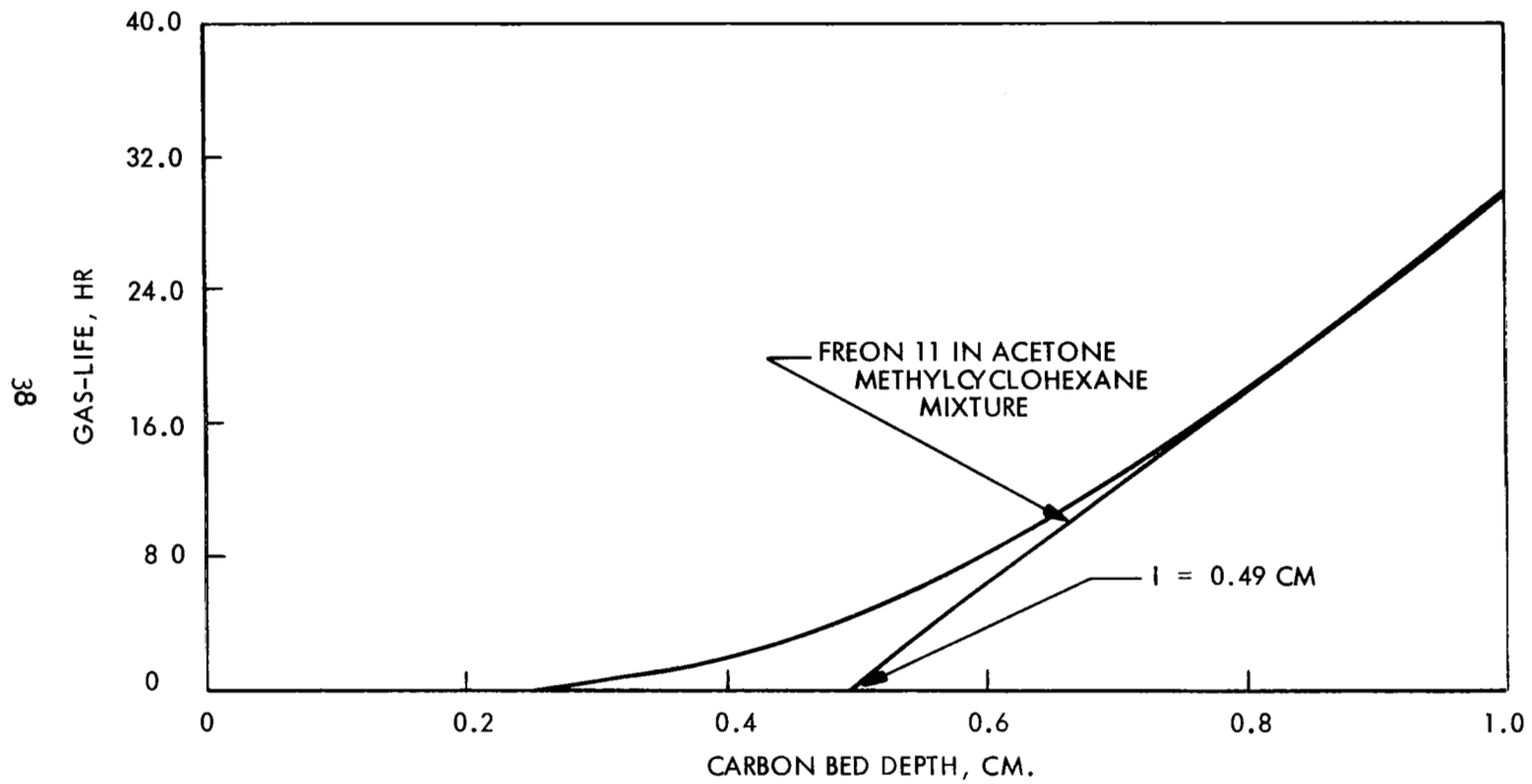


Figure 18 Adsorption Zone Length for Freon 11 on BC G1, Freon 11, Acetone, and Methylcyclohexane

Charcoal Desorption

The regeneration of charcoal is an important factor in reducing the weight of a trace contaminant removal system. An experimental investigation was conducted to establish the conditions under which contaminants could be successfully regenerated under vacuum and heating conditions.

The test results have shown that materials which are very strongly adsorbed cannot be completely desorbed from activated carbon using a heat and vacuum cycle. Attempts to desorb diisobutyl ketone showed a residual loading after several hours of desorption at 200°C and vacuum. Runs made with caprylic acid also show this residual loading. As these runs were performed at high sorbent loadings and as spacecraft conditions will result in low loadings, it is felt that the residual in these desorption experiments will be in the same order as the actual operating conditions in a spacecraft. Thus, it is expected that materials with a high molar volume ($V_m > 185$) may not be desorbed by heating and vacuum.

Data taken on n-octane ($V_m = 180$) and below indicate that desorption of these materials is possible. Desorption time of 1 to 2 hours seem adequate to completely remove the adsorbed materials.

In order to assess the desorption of weakly adsorbed material, cyclic desorption tests were run on acetone. These runs showed that capacity is not decreased measurably over several cycles at a desorption temperature of 100°C. However, reducing the temperature to 25°C resulted in very poor desorption, even with desorption periods as high as 8 hours. Tests with acrolein showed a tendency of this material to polymerize. No tests were conducted with this material at low concentrations which should eliminate this problem.

In summary, desorption tests have shown that contaminants in the V_m range of 180 to 80 are satisfactorily desorbed at 200°C over a 2-hour period and that 100°C and 2 hours is adequate for those contaminants with a molar volume of less than 80.

The following sections describe these experimental investigations.

Regeneration of Carbons Exposed to Contaminants with $V_m > 80$.- The regeneration of the carbons exposed to contaminants with high molar volumes was conducted at 200°C under vacuum between 10^{-4} and 10^{-5} mm of Hg pressure. One or more hours of heat treatment was applied during each regeneration. The adsorption phase was carried out at atmospheric pressure with dry nitrogen as carrier gas for the contaminant. To obtain the gas mixture, nitrogen was metered through the liquid contaminant in a bubbler and the mixture diluted further with metered nitrogen. The gas flows were varied between 1.93 and 2.3 l/min for carbon bed of 2.83 cm² area.

At the concentrations employed, the amount of contaminant adsorbed varied between 30% to 75% by weight as compared to the 1% expected adsorption during actual application. For this reason, the regeneration was not considered successful unless the contaminant was completely desorbed, i.e., to less than 0.1 mg/g.

To prepare the carbons for the regeneration experiment, they were given a prior treatment identical to the one received during the regeneration. In this way, a reliable initial weight of the carbon and adsorption tube was obtained.

Table 2 presents results, and also conditions, of a number of regeneration runs. It is certain that n-octane ($V_m = 180$) and contaminants lower than $V_m = 180$ can be completely desorbed in a reasonable length of time. Complete desorption of caprylic acid ($V_m = 197$) is doubtful, while diisobutyl ketone cannot be completely desorbed.

Regeneration of Carbons Exposed to Contaminants with $V_m < 80$.- Regeneration experiments were conducted on carbons exposed to acrolein ($\text{CH}_2 = \text{CHCHO}$) and acetone. The adsorption phase of the acrolein experiment was conducted at a high influent concentration, on the order used in the previous experiments. The results and conditions are presented in Table 3. Attempts were first made to desorb the acrolein at ambient temperature. This was not very effective, whereupon the regeneration was resumed at 100°C.

TABLE 2
RESULTS ON CARBONS EXPOSED TO HIGH MOLOR VOLUME CONTAMINANTS
AND REGENERATED AT 200°C AND 10⁻⁴ mm Hg PRESSURE

<u>Contaminant</u>	<u>Type Carbon</u>	<u>Weight carbon, g</u>	<u>Ads influent conc, mg/l</u>	<u>Amt cont ads</u>		<u>Regeneration time, hr</u>	<u>Weight residue on carbon, g/g</u>
				<u>g</u>	<u>g/g</u>		
Diisobutyl Ketone	super- actv. 138% CCl ₄	5.25	---	2.443	0.466	3.25	0.0063
						7.0	0.0048
						23.0	0.0051
Caprylic acid	super- actv. 154% CCl ₄	5.68	---	0.106	0.0187	2.0	0.0012
n-Octane	super- actv. 154% CCl ₄	5.74	9.9	4.300	0.749	1.75	0.0003
Methyl cyclohexane	super- actv. 154% CCl ₄	5.76	39.3	3.417	0.593	1.0	0.0042
						3.5	0.0000
Methyl cyclohexane	Pgh. BPL	9.45	15.8	3.020	0.319	2.0	0.0003
ter-Amyl alcohol	BC GI	2.23	29.5	1.331	0.596	2.0	0.0000
Cyclohexane	Super- actv. 154% CCl ₄	5.68	--	1.731	0.305	1.0	0.0000

TABLE 3
 VACUUM REGENERATION OF SUPERACTIVATED CARBON
 (138% CCl₄ ACT.) EXPOSED TO ACROLEIN

Weight Carbon:	22.70g
Carrier gas :	dry N ₂
Gas flow :	2.3 l/min
Pressure :	atmospheric
Acrolein conc:	1.1 mg/l (est)
Amt ads :	0.682 g: 0.030 g/g

<u>Time, hr</u>	<u>Temp, °C</u>	<u>Wt ads on carbon, g/g</u>
0	25	0.0300
1	25	0.0233
18	25	0.0175

Regeneration continued at elevated temperature

0	25	0.0175
2	100	0.0152

Regeneration temperature increased

0	100	0.0152
1.5	200	0.0144
4.5	200	0.0021

Regeneration was still slow, and so the temperature was increased to 200°C. The residue remaining after the 200°C regeneration was still sizable, considering the extended time of regeneration. Although acrolein ($V_m = 66$) was not strongly adsorbed initially, its retentivity was good. This was believed to be due to a possible polymerization which, however, could not occur at the very low concentration levels in the spacecraft.

The acetone regenerations were conducted on superactivated carbons exposed to acetone at low influent concentration, i.e., 0.021 mg/l. The carrier gas was 30% O₂ - 70% N₂ at 34% relative humidity and 10 lb/in² (abs) pressure. Because of the moisture content in the carrier gas, the weighing method could not be used as reliably as when dry gas was used. Also, the weight of contaminant is very small, on the order of 0.007 g/g maximum, hence weighing errors would be large. To determine regenerability, the gas-life was determined after each regeneration and the gain or loss in gas-life used to determine the effectiveness of the regeneration.

Regenerations were conducted at 100°C and at ambient temperatures, under vacuum. The conditions and results for the 100°C regenerations are presented in Table 4 and Figure 19. The conditions and results for the ambient temperature regenerations are given in Table 5 and Figure 20.

If the gas-life is designated as the adsorption time to the time when the effluent concentration reaches 1% of the influent concentration, the effluent concentration curves of Figure 19 indicate the following changes in carbon activity over four regenerations.

<u>Regeneration</u>	<u>Regeneration Time, hr</u>	<u>Gas-life, min</u>
initial carbon	--	100
1st	1	90
2nd	1	60
3rd	1	60
4th	2	90

TABLE 4
 REGENERATION AT 100°C AND $<10^{-4}$ mm Hg
 PRESSURE OF SUPERACTIVATED CARBON EXPOSED TO ACETONE

Carbon weight: 2.711 g
 Carrier gas : 30% O₂ - 70% N₂
 Pressure : 10 lb/ in² (abs)
 Gas flow : 2.83 l/min
 Acetone conc.: 0.021 mg/l
 Rel. hum. : 34%

Effluent conc data on successive runs

<u>time, min</u>	<u>conc., % of influent</u>				
	<u>Initial</u> <u>Run 20</u>	<u>1st reg</u> <u>Run 21</u>	<u>2nd reg</u> <u>Run 22</u>	<u>3rd reg</u> <u>Run 23</u>	<u>4th reg</u> <u>Run 25</u>
40	0.0	0.2	0.4	0.7	0.0
90	0.8	1.2	2.3	1.5	1.2
120	2.1	---	5.8	4.3	3.1
140	3.2	3.6	7.2	5.0	---
160	5.9	6.2	12.1	8.5	6.8
180	7.9	8.6	13.5	12.7	---
200	13.8	13.5	20.5	16.0	---
240	18.9	20.1	29.0	28.0	26.4
300					58.8
360					82.5
420					80.3
480					96.0

Adsorptive capacity, g, for Run 25 : 0.0069 g/g
 0.0087 cc liq/g

A = 17.6

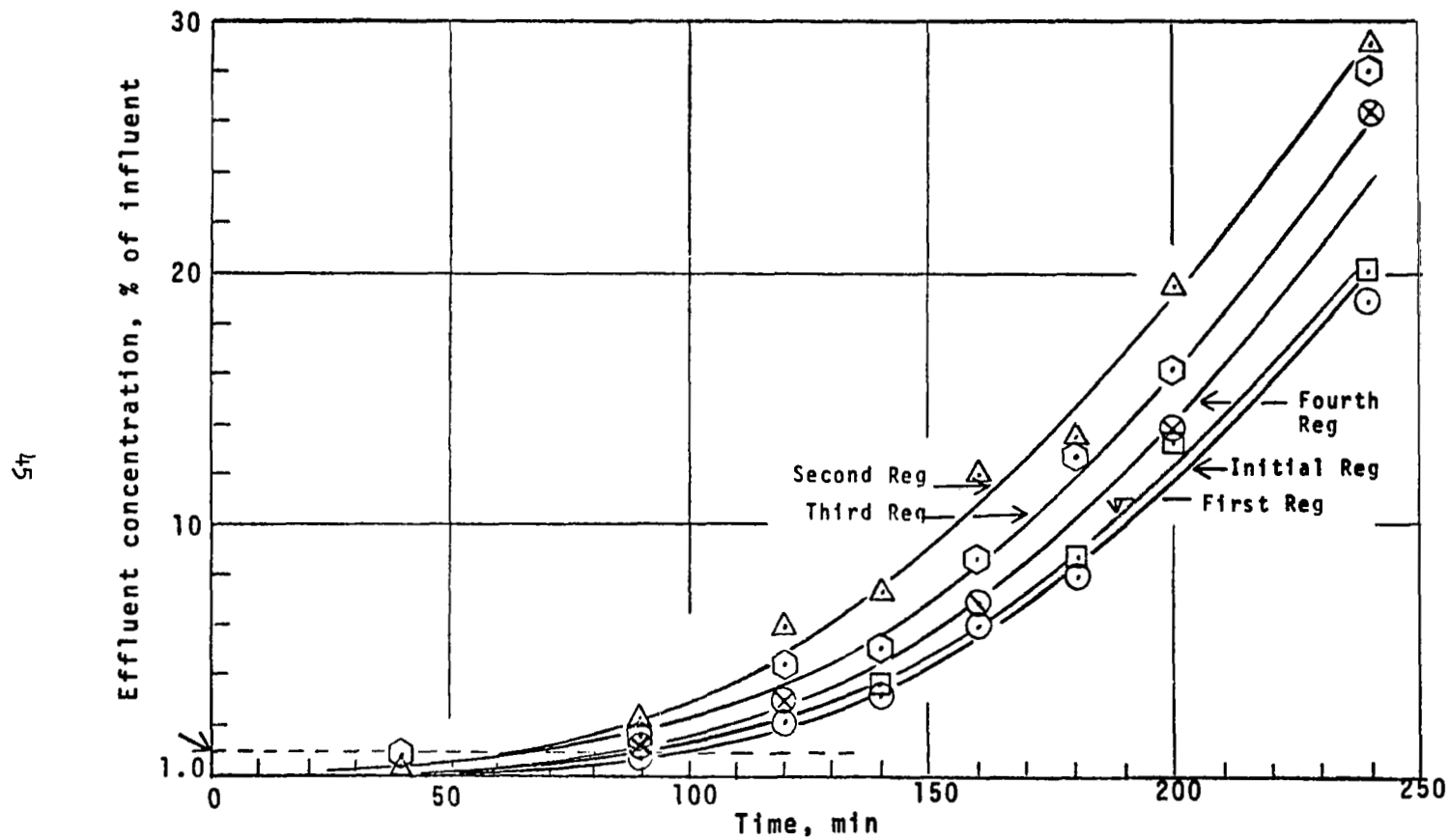


Figure 19 Effluent Concentration Curves for Acetone Adsorbed on Regenerated S154,
2.70 g Carbon, Regeneration at 100°C and 10^{-4} mm of Hg Pressure

TABLE 5
 REGENERATION AT AMBIENT TEMPERATURE AND $< 10^{-4}$ mm Hg PRESSURE
 OF SUPER-ACTIVATED CARBON (154% CCl_4 Act.) EXPOSED TO ACETONE

Carbon weight:	2.703 g
Carrier gas :	30% O_2 - 70% N_2
Rel. hum. :	34%
Gas flow :	2.83 l/min
Acetone conc.:	0.021 mg/l
Pressure :	10 lb/in ² (abs)

Effluent conc. data on successive runs

<u>Time, min</u>	<u>Conc., % of influent</u>		
	<u>Initial Run 19</u>	<u>1st Reg. Run 24</u>	<u>2nd Reg. Run 26</u>
40	0.1	0.0	2.7
90	1.3	0.5	5.0
120	3.3	1.8	7.4
140	4.6	2.8	8.6
160	7.6	5.2	13.0
180	10.6	6.6	15.4
200	12.6	11.5	19.0
240	15.6	22.2	31.2
Regenerated		26 hr	8 hr

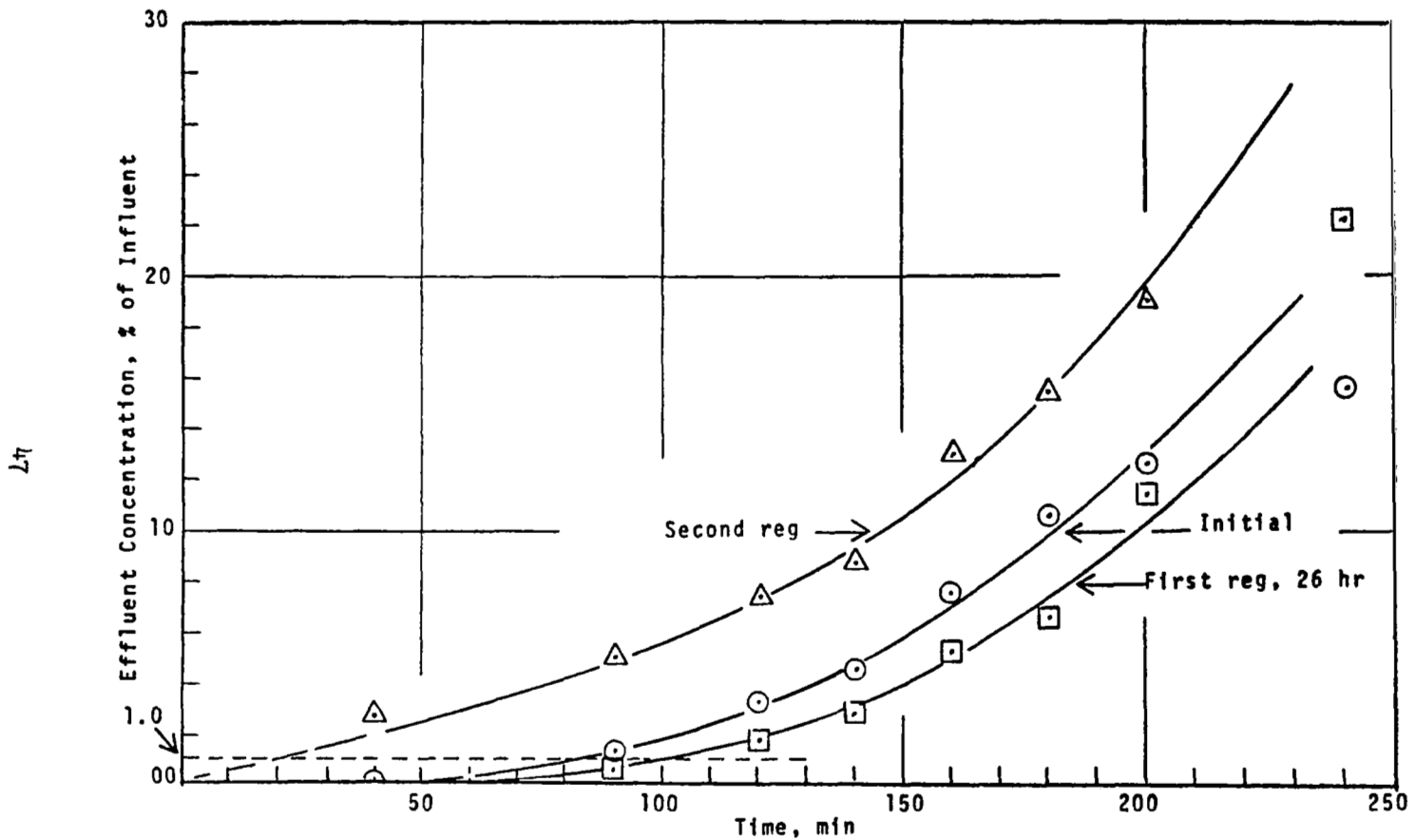


Figure 20 Effluent Concentration Curves for Acetone Adsorbed on Regenerated S154, 2.70 g Carbon, Regeneration at Ambient Temperature and 10^{-4} mm of Hg Pressure

Regenerations 1, 2, and 3 were of 1-hour duration, and the carbon lost activity between the first and second regeneration but stabilized on the third regeneration. On the fourth regeneration, the regeneration time was increased to 2 hr, and the activity increased again to bring the gas-life to 90 min, which was the life at the end of the first regeneration. It is believed that a 2-hr regeneration time at 100°C will regenerate the carbon exposed to any of the contaminants with a $V_m < 80$.

The effluent concentration curves of Figure 20, for ambient temperature regenerations, indicate the following changes in carbon activity.

<u>Regeneration</u>	<u>Regeneration time, hr</u>	<u>Gas-life, min.</u>
initial carbon	--	85
1st	26	97
2nd	8	20

These results indicate that ambient temperature regeneration must be considerably longer than 8 hr to recover the initial carbon activity and that complete regeneration at ambient temperature may not be feasible.

SYSTEM SELECTION AND ANALYSIS

A contaminant removal system capable of controlling the wide variety of potential spacecraft contaminants must involve many elements, including catalytic oxidation, charcoal adsorbents and chemical pre- and post-sorbents. To develop a complete system design, the size and arrangement of these individual elements, as well as their required flow rates, must be considered. The catalytic oxidizer size and flow rate, along with its attendant pre- and post-sorbent beds, was developed during NASA contracts NAS 1-6256 and NAS 1-7433. The design of the charcoal sorbent beds and their integration with the catalytic oxidizer and pre- and post-sorbent beds was the purpose of this effort.

The design approach utilized to develop the complete system was to assess several candidate approaches to integrating the various potential elements of the system. In conducting these trade-off studies, the constraints imposed were (1) that individual contaminants would not be allowed to exceed the maximum allowable concentration and (2) that potential catalyst poisons would not be allowed to enter the catalytic oxidizer at concentrations greater than 20% of the maximum allowable concentration. Further, as many contaminants as possible would be removed by oxidation.

Of the contaminants listed in the contaminant model, 18 require a flow rate greater than 3 CFM for removal. This means that these contaminants could not be controlled by a device utilizing the flow rate of the catalytic oxidizer. These contaminants, however, are either adsorbed on charcoal, combine with the moisture present in the charcoal, or are removed by an acid impregnation that can be dispersed on the charcoal. In examining these contaminants, it was found that the gas flow rate and quantity of charcoal sufficient for control of pyruvic acid, which has a substantiated production rate, provided adequate removal for the remaining 17 flow limited contaminants. A review of the remaining contaminants with a requirement for less than 3 CFM flow for removal indicated that a number of these would be controlled by the charcoal quantity required for control of pyruvic acid; however, a large number of these contaminants require considerably more charcoal for control. Thus, the options that

evolved were (1) consideration of a single charcoal bed that would control all of the contaminants requiring charcoal removal, or (2) a high flow charcoal bed for removal of all contaminants adsorbed as well as pyruvic acid and a low flow charcoal bed for control of the more poorly adsorbed contaminants. It became evident that the quantity of charcoal required for control of contaminants adsorbed as well as pyruvic acid was not excessive; however, control of the poorly adsorbed contaminants required a very large quantity of charcoal if it were not regenerated.

Therefore, charcoal regeneration had to be considered for these contaminants. In the trade-off study, consideration was given to systems utilizing a single high flow regenerative bed, or a combination of a high flow fixed bed and a low flow regenerative bed. The results of the optimization study indicated that the latter approach is superior. The following discussion presents the results of the system selection and optimization study, as well as the performance analyses of the regenerative and fixed charcoal beds.

System Optimization

In selecting a concept for a contaminant control system, three arrangements of components were considered. These are shown in Figures 21, 22, and 23. In these schematics, the major differences lie in the carbon beds. In Figure 21, a single carbon bed that is regenerable is used with a separate ammonia sorbent. Downstream of this are the catalytic oxidizer and pre- and post-sorbent beds. The system presented in Figure 22 utilizes a fixed high flow carbon bed impregnated with phosphoric acid for ammonia removal followed by a smaller low flow regenerative carbon bed and the catalytic oxidizer with pre- and post-sorbents. The system shown in Figure 23 differs from that shown in Figure 22 in that the low flow and high flow components are in parallel instead of series. This has the added advantage of increased flexibility in system arrangement; however, it increases the required size of the regenerable bed slightly.

In general, contaminants can be divided into three groups which are contaminants strongly adsorbed (Group I), weakly adsorbed (Group III), and strongly adsorbed in carbon which has been treated with phosphoric acid or a separate sorbent (Group II). As described in the following section, adsorption data have been generalized and a computer program used to predict the required bed sizes. Further, data were taken which demonstrated re-regeneration of the carbon beds using a heat and vacuum cycle. Using these data, the schematics were compared to determine the optimum system.

In these evaluations, the charcoal weight was calculated and fixed percentage increases attributable to hardware weight added. Further, a 400 lb/KW power penalty was assessed for increases in peak power consumption.

The schematic presented in Figure 22 had the lowest penalty of those evaluated. This system takes advantage of a non-regenerable Group I bed. The computer printouts of bed weight as a function of contaminants removed indicated a natural break at Methyl ethyl ketone (MEK) for the Group I bed. This resulted in the removal of all contaminants having an A value of less than 23 in the Group I bed. In this bed, pyruvic acid has a required flow of 76 CFM if the

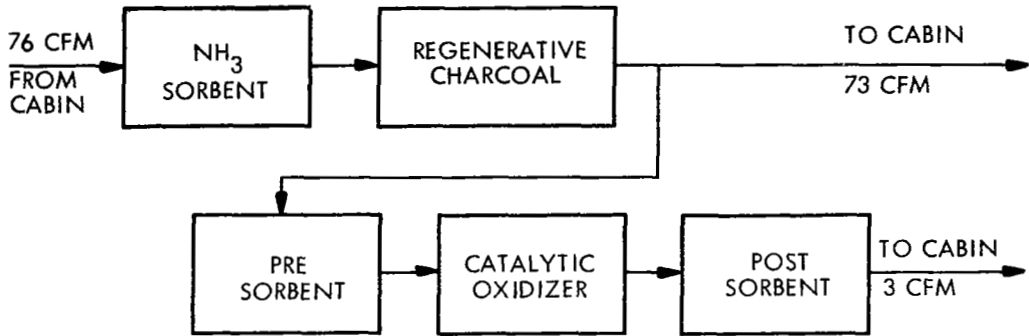


Figure 21 Candidate System With High Flow Regenerative Bed

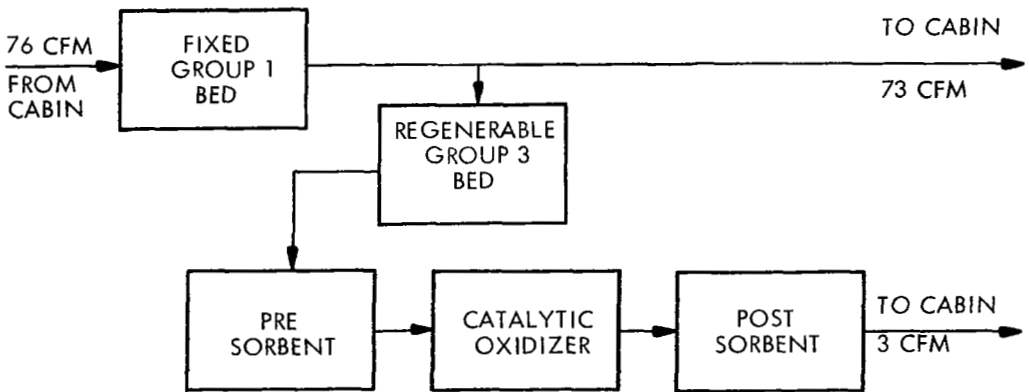


Figure 22 Candidate System With a Fixed Bed and Regenerative Bed in Series

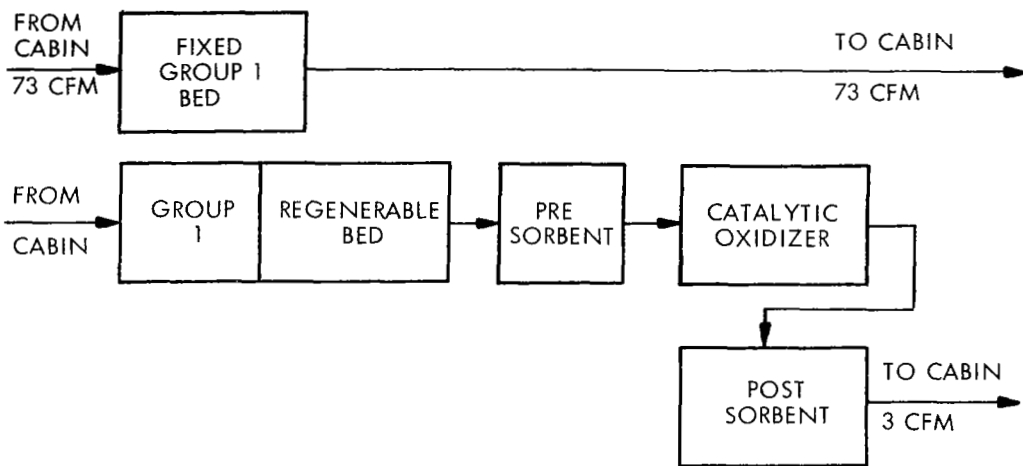


Figure 23 Candidate System With Fixed Bed and Regenerative Bed in Parallel

removal efficiency is 0.9 at breakthrough. This requirement sets the flow of the Group I bed. The flow through the Group III bed is established by the 3 CFM catalytic oxidizer requirement.

In considering the schematic shown in Figure 21, the quantity of sorbent required to remove ammonia must be determined. At the design generation rate for ammonia, 1.29 lb of ammonia must be removed over a 180-day mission. Review of materials for removal of ammonia showed that sorbents and phosphoric acid treated charcoal are equally effective. Maximum ammonia capacity for these materials is in the range of 7 lb of sorbent per pound of ammonia, resulting in a requirement for 9.1 lb of sorbent material which results in a total equivalent weight of 16 lb. The regenerable charcoal bed was then optimized for weight and pressure loss penalty, not including desorption power. The results of the optimization, shown in Figure 24, show a penalty of 57 lb with a 90-day cycle time. This results in a combined penalty for ammonia removal and single regenerable bed in excess of 73 lb, not including the desorptive power penalty. The power required for desorption of a single regenerative bed is 450 watt-hours, and assuming natural losses are negligible for a 6-hour desorption time, a power penalty of 22 lb results. This yields a total equivalent weight of 95 lb for a single regenerative bed. This concept was rejected because of its excessive penalty over those concepts presented in Figures 22 and 23.

The selection of the contaminants to be included in the Group I bed shown in Figures 22 and 23 was established by a review of flow requirements and quantities of charcoal required. Pyruvic acid requires the greatest flow for removal, and thus sets the flow requirement for the Group I bed; it also must be removed in its entirety by this bed. As can be seen below, MEK requires little additional charcoal over Pyruvic Acid. Thus, it was decided to also include this contaminant in the Group I bed for removal in an effort to minimize potential desorption problems in the Group III bed.

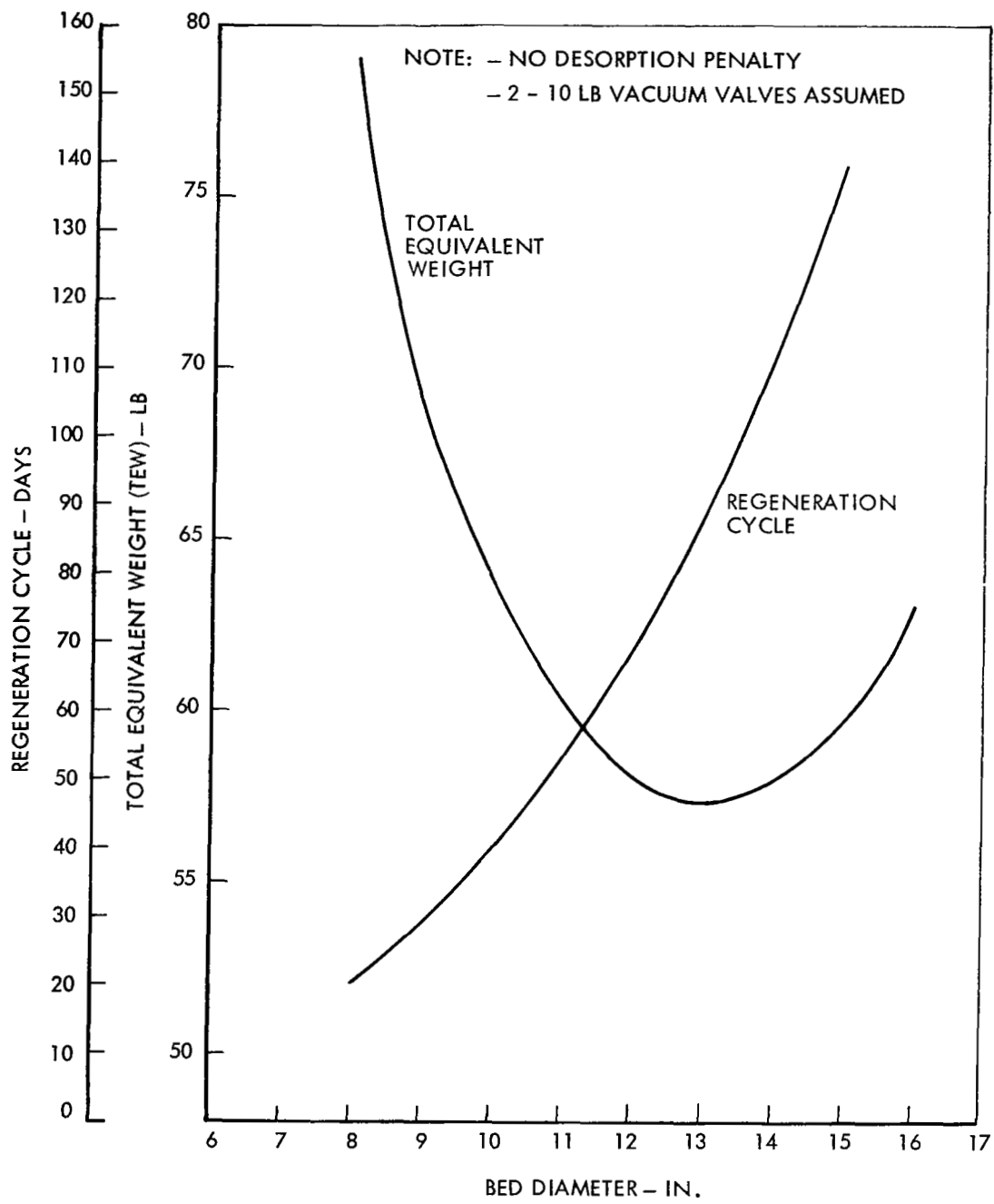


Figure 24 Performance of a Group I Regenerative Bed

<u>Contaminant</u>	<u>Charcoal Required (lb)</u>
Pyruvic Acid	26
MEK	29.5
Dichloroethane	57
N Butane	96

Further inspection of the above data shows a rapid increase in the required Group I bed weight as additional contaminants are included. As a result, the final selection cut-off for the Group I bed was MEK. This quantity of phosphoric acid treated charcoal is also capable of removing the ammonia.

Preliminary calculations showed that pressure loss penalty is a major factor in the design of the Group I bed with the high flow of 76 CFM. Thus, a 4 x 6 mesh charcoal was selected for this bed to minimize this penalty. Figure 24 shows that results of a pressure loss and fixed weight study made for the 32-pound 180-day Group I bed. The curve is based on a saturated charcoal zone of 30 pounds and includes 1.0 inch for the adsorption zone. The adsorption zone is based on a canister bulk velocity of 49 ft/min. The combined motor fan efficiency was assumed to be 0.35 for the purpose of fan power calculations. Canister weight was based on a minimum weight design which results in a 25% packing weight. The curve in Figure 25 shows a decrease in penalty as L/D is reduced. Experience has shown that bed performance becomes unreliable if L/D is less than 0.5. Thus, the design selected has an L/D of 0.5.

The Group I bed has a total equivalent weight of 56 lb and a diameter of 17 inches. Bed length is 8.0 inches. The bed contains 32 lb of BD 4 x 6 mesh activated charcoal in a canister which weighs 8 lb. The pressure loss is 1.6 in H₂O at 76 CFM, requiring a 40-watt fan. The charcoal is impregnated with 2 millimoles of phosphoric acid per gram of charcoal.

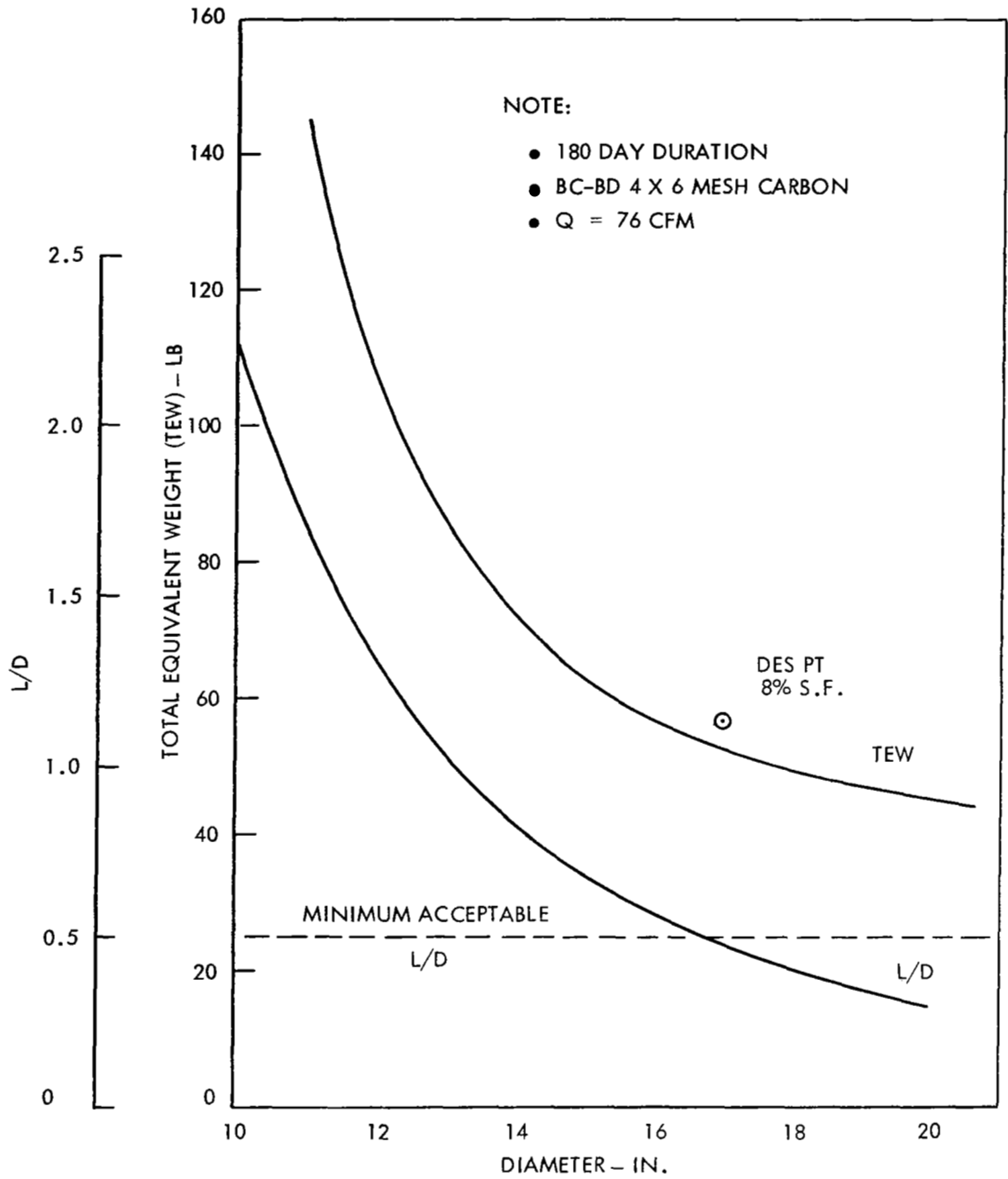


Figure 25 Performance of a Group I Fixed Bed

The regenerable Group III bed was then optimized. In the optimization of the Group III bed, a 6 x 12 mesh BD activated charcoal was selected to minimize channelling problems. For this bed, an adsorption zone length of 1.5 inches was determined based on a velocity of 18 ft/min. A fan efficiency of 23% was assumed. This smaller bed has a canister weight of 0.33 lbs per lb of charcoal held. Figure 26 shows the penalty of regenerable beds having differing cycle times. This curve is based on the above assumptions. The results show that short cycle times are desirable.

In an attempt to assess the penalty of maintaining independence of the 3 CFM catalytic oxidizer loop from the Group I bed, the schematic shown in Figure 23 was generated. This schematic uses the same Group I bed as discussed previously.

The regenerable bed has been increased in size to allow for removal of Group I contaminants that would enter the bed during the 180-day mission. The design philosophy for the Group III contaminants and penalty factors were unchanged for those in the schematic shown in Figure 22. Figure 27 shows the penalty factors for the regenerable bed for the schematic shown in Figure 23. Comparison of Figures 26 and 27 shows only a 2 - lb penalty for independence of the two contaminant control circuits. This was deemed desirable, and the schematic shown in Figure 23 was selected.

A review of Figure 27 indicates that the shortest cycle times are most desirable. However, during the desorptive period, the catalytic oxidizer must be shut down, requiring higher flow rates during times of operation to yield the same contaminant removal capability. The total equivalent weight for each of the regenerable beds were then adjusted for the effect of cycle time on the catalytic oxidizer power and weight. Figure 28 presents these results which shows the optimum cycle time to be 2 days.

An optimization occurred due to the fact that as the cycle time decreased, the weight penalty associated with the regenerative bed increased. However, the weight penalty associated with the catalytic oxidizer increased, which resulted in a minimum combined equivalent weight at a cycle time of 2 days. The selected Group III bed, based on the above results, is 6 inches in diameter and 10 inches long, containing 4.9 lb of 6 x 12 mesh charcoal. The canister weight is 1.7 lb.

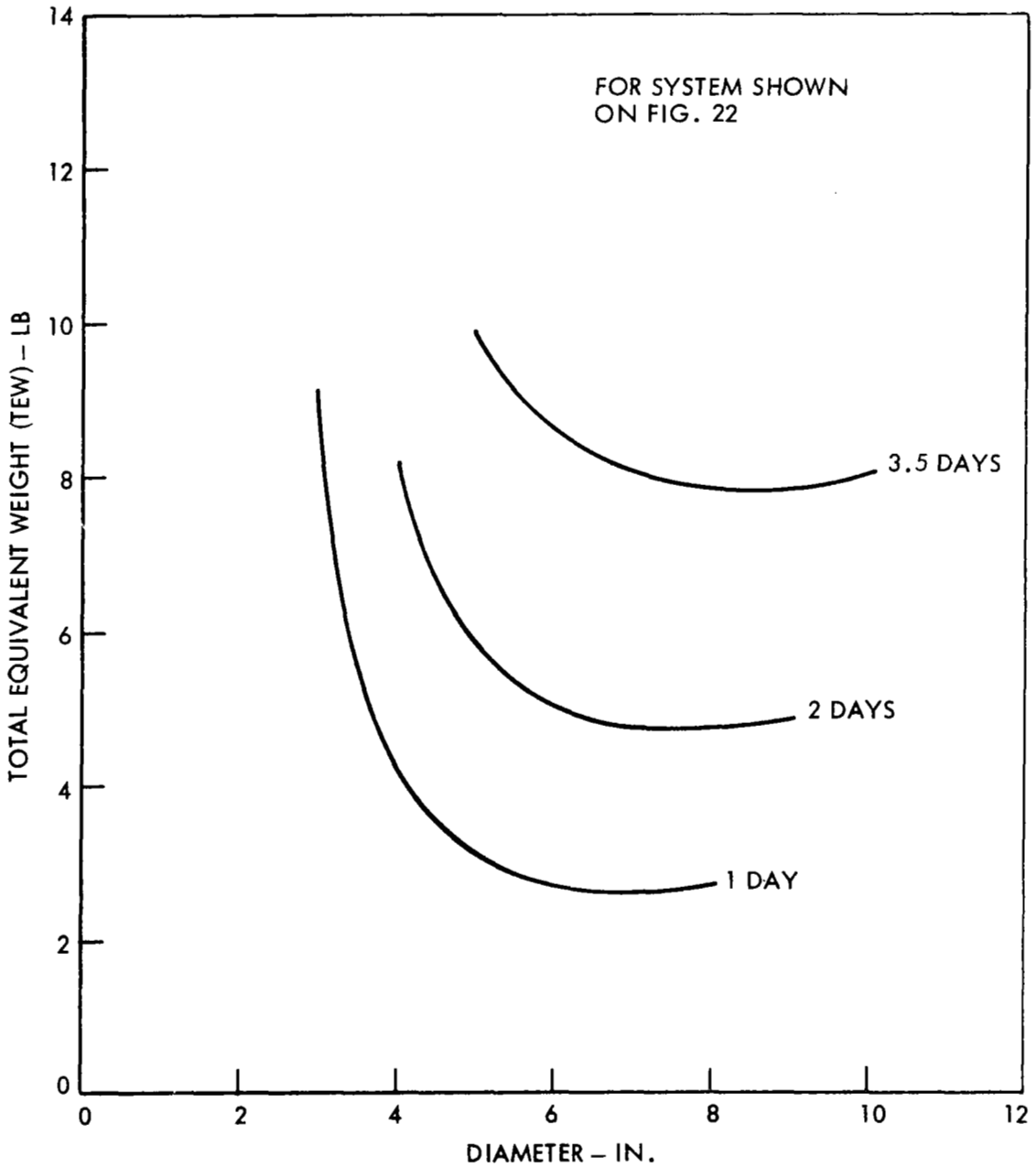


Figure 26 Effect of Cycle Time on Total Equivalent Weight for the Regenerative Bed

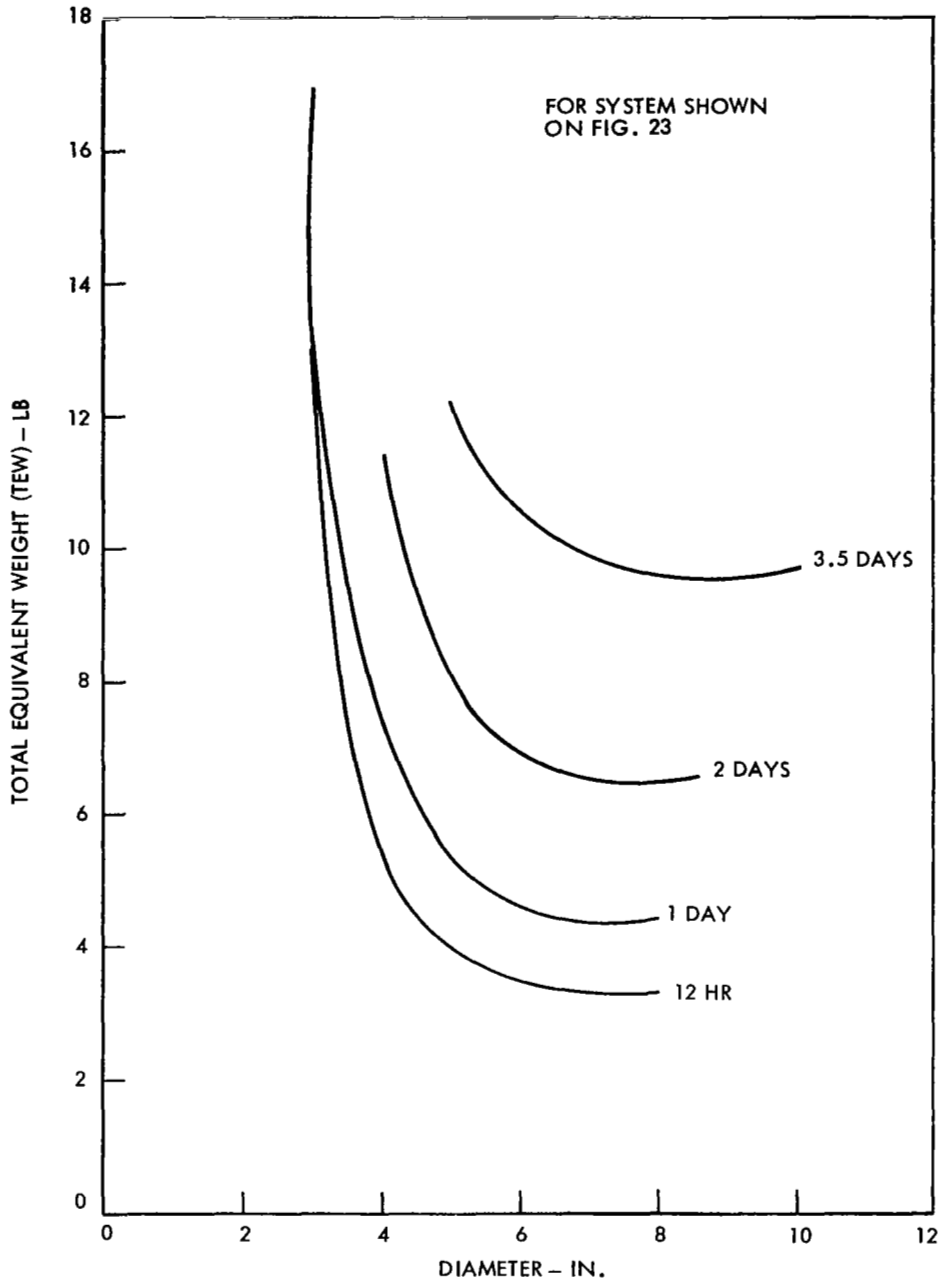


Figure 27 Effect of Cycle Time on Total Weight for the Regenerative Bed

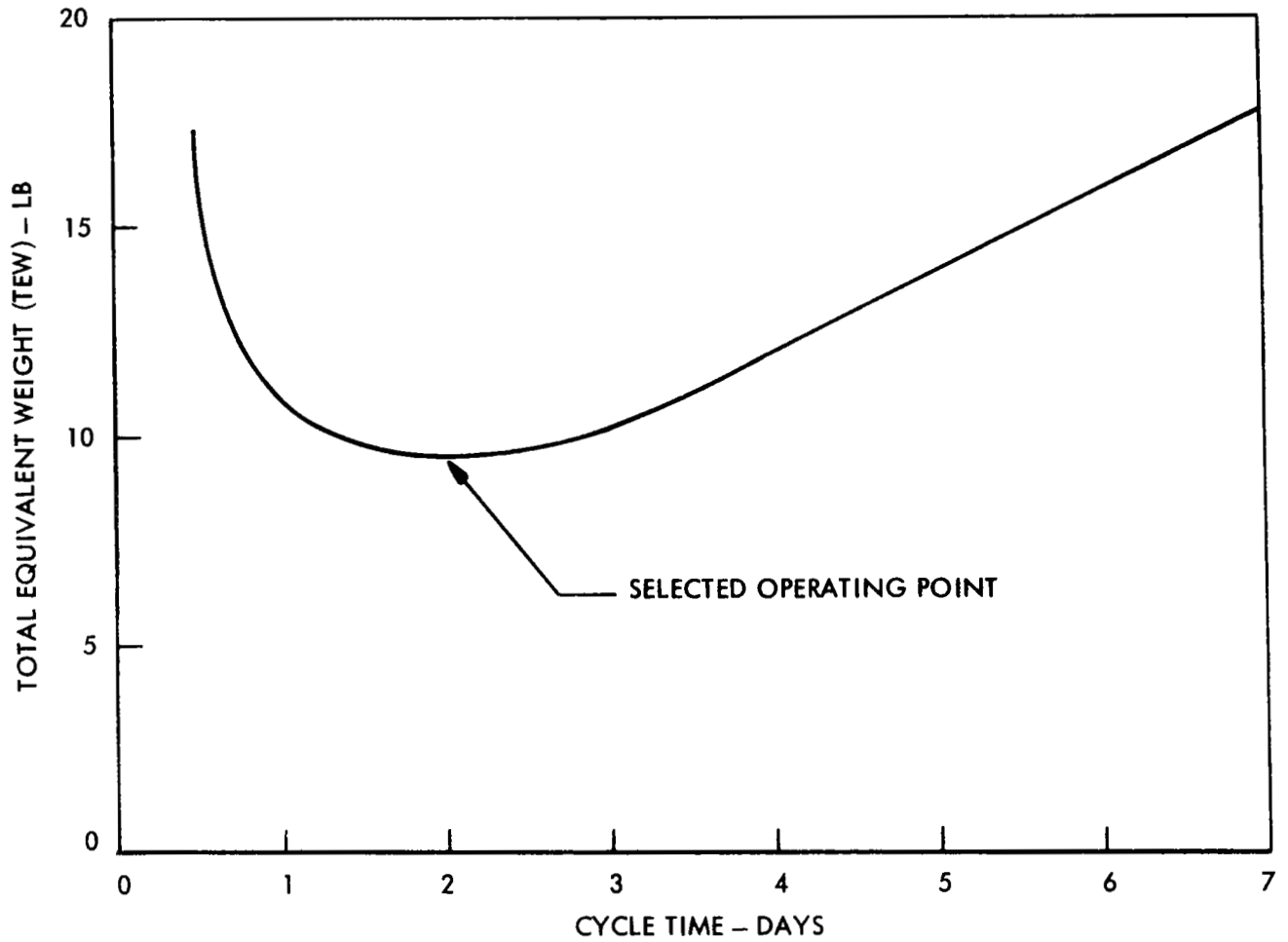


Figure 28 Effect of Cycle Time on Total Equivalent Weight for the Regenerative Bed Including the Effect on the Catalytic Oxidizer System

In the operation of a contaminant control system, the catalytic oxidizer is the largest power consuming device. The catalytic oxidizer developed for this system will consume about 120 watts, of which 71 watts are lost to the flow stream. During the charcoal regeneration cycle, no flow will pass through the oxidizer, making this power available for charcoal bed heating at no penalty of peak power. Thermal calculations on the Group III regenerable bed indicate that this quantity of power is sufficient to raise the temperature of the bed to the required 100°C temperature in 1 hour, allowing an additional hour for desorption above this level. This will be satisfactory for desorption. These results are presented in Figure 29.

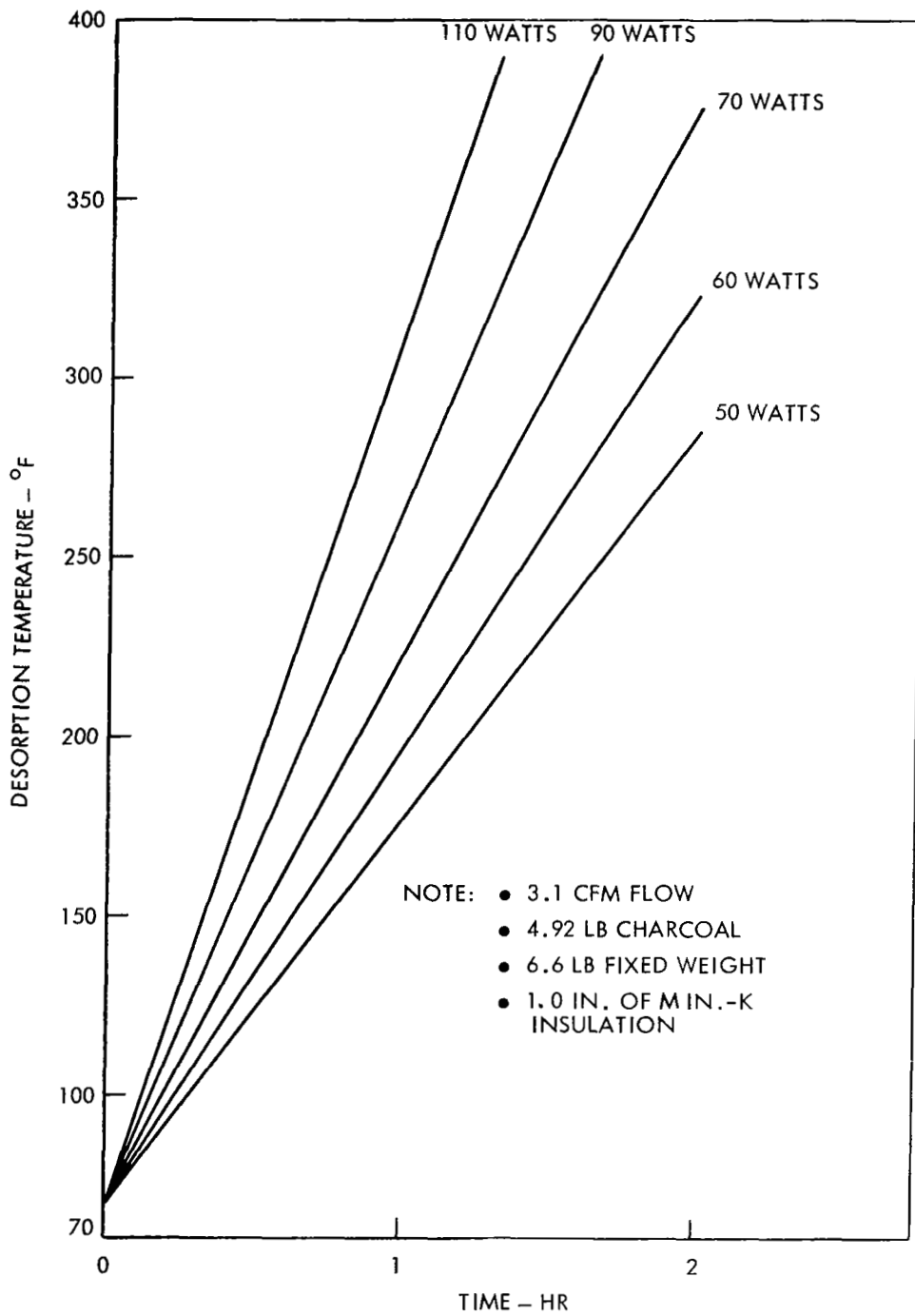


Figure 29 Power Requirements for the Regenerative Bed

Charcoal Bed Performance Analysis

To accomplish the analyses conducted in the system optimization, a computer program was developed to estimate the quantity of charcoal required for control of the various contaminants. A description of this program is presented in Appendix D.

The saturation capacity of activated charcoal for any singly adsorbed material can be estimated from potential adsorption theory. When tests have been conducted with multiple contaminants at spacecraft concentration levels, a displacement effect has been observed in which materials having a low A value will displace those having a higher A value from adsorption sites. If the difference in A values exceeds some critical value, total displacement is observed. Based upon these observations, a computer program was generated to estimate the required quantity of activated charcoal for control of multiple contaminants.

The program scans all contaminants by A value and then orders them from the lowest to highest value. It then calculates the quantity of sorbent required to remove the most strongly adsorbed substance. Using experimental potential plot data, the capacity of this sorbent section for additional substances is then estimated on the assumption that their capacity is less than saturation and is linear with A value difference up to the critical A value. The program then proceeds to the next contaminant, which is not yet completely removed and repeats the calculation. This process is continued until all of the listed contaminants have been completely adsorbed.

In these calculations three potential plots are used: (1) for water insoluble contaminants on phosphoric acid, impregnated charcoal, (2) for water insoluble contaminants on charcoal without phosphoric acid, and (3) for water soluble contaminants on charcoal, either with or without phosphoric acid. The rationale for these selections, as described in previous sections, is as follows: soluble contaminants are not blocked by water since the contaminant dissolves in the water and then migrates to an adsorption site. Insoluble contaminants, however, are blocked by water. The effect of phosphoric acid is to increase the quantity of moisture present in the charcoal, and hence, to increase the blockage rate for insoluble contaminants.

In order to assess the sensitivity of the critical sizing parameters, Δ A critical, flow rate, time, and contaminant loadings were made inputs to the program. The program was used to generate the various designs that were considered during the optimization study. The program results are presented in the following sections for two examples in which a fixed sorbent bed and regenerative sorbent bed are used with flow rates of 76 CFM and 3 CFM respectively.

Fixed Sorbent Bed

The fixed sorbent bent flow rate was established by the production rate and maximum allowable concentration for pyruvic acid, and the bed size was determined by the highest A value contaminant to be removed by the bed, methyl ethyl ketone, and the resupply period of 180 days. The selection of methyl ethyl ketone for sizing was based on the requirements that pyruvic acid required removal by a high flow fixed bed and that the additional quantity of charcoal required to remove methyl ethyl ketone ($\sim 14\%$) was small. This small increase in the size of the fixed bed traded favorably against the potential increase in the desorption temperature of the regenerative bed required, if removal of methyl ethyl ketone were planned for the regenerative bed. Thus, the sizing of the fixed bed was predominantly determined by pyruvid acid which has a substantiated production rate. Benzene and allyl alcohol are also removed in the portion of the bed provided for methyl ethyl ketone. The computer program was utilized to size the saturated layer for this bed and to establish what other contaminants it would control. The program inputs included a flow rate of 76 CFM, a bed temperature of 70^oF, and a required removal efficiency of 90%. Assuming a high required removal efficiency implies a low inlet concentration and, hence, is conservative in establishing bed size since the charcoal adsorption capacity is a function of inlet concentration, the program establishes the contaminant inlet concentration based upon the removal efficiency and flow rate. These inlet concentrations are valid as long as the charcoal capacity has not been exceeded. The modified equipment production rates were utilized in the analysis; however, the impact of the higher equipment rate is discussed in a later section. The results of the computer analyses for the fixed bed are presented in Table 6.

TABLE 6
FIXED SORBENT BED
COMPUTER ANALYSIS RESULTS

<u>Slice 1</u>	<u>Mass of Slice</u> <u>gms/day</u>	<u>Cumulative Mass</u> <u>of Slices</u> <u>gms/day</u>	<u>Slice 9</u>	<u>Mass of Slice</u> <u>gms/day</u>	<u>Cumul. Mass</u> <u>of Slices</u> <u>gms/day</u>
Caprylic Acid Indole* Skatol*	0.0399	0.03988	Hexene-1 Isoprene Valeraldehyde	3.0447	15.6139
<u>Slice 2</u>			<u>Slice 10</u>		
Decalin	0.0759	0.1158	n-pentane Methyl Isopropyl Ketone	0.9950	16.6089
<u>Slice 3</u>			<u>Slice 11</u>		
Hexomethylcyclotrisihexane Valeric Acid	0.0664	0.1822	Pyruvic Acid Cyclohexane Ethyl Acetate Ethyl Isobutyl Ether Methyl Chloroform 1,4 Dioxane Carbon Tetrachloride n-Propyl Alcohol Freon 114 Pentene-2 Pentene -1 iso Butane 2 Methyl 1 Butane Chloropropane Cyclopentane Dimethyl Furane Freon 114 Unsymmetrical Butyric Acid Dimethyl Hydrazine	49.2854	65.8943
<u>Slice 4</u>			<u>Slice 12</u>		
Octane 1,1,3 Trimethyl Cyclohexane Napthalene	0.1896	0.3718	Methyl Ethyl Ketone Benzene Allyl Alcohol	8.2321	74.1214
<u>Slice 5</u>					
O-xylene DI-Isobutyl-Ketone 2,2 Dimethyl Butane Mesitylene Ethyl Benzene 3 Methyl Pentane Cyclohexanol n-Propyl Acetate Amyl Alcohol 1,2,4 Trimethyl Benzene Trans 1 Methyl 3 Ethyl Cyclohexane Methyl Cyclohexane Chlorobenzene n-Propyl Benzene Cumene Iso-Amyl Acetate Methyl Butyrate Methyl Isobutyl Ketone Phenol Methyl Methacrylate Furfural Tetrachloroethylene Ethyl Sulphide	2.8474	3.2192			
<u>Slice 6</u>					
Xylene Ethylene Glycol	0.3850	3.6042			
<u>Slice 7</u>					
n-Hexane Trans 1,2 Dimethyl Cyclohexane 1,1 Dimethyl Cyclohexane iso-Butyl Alcohol	0.9132	4.5174			
<u>Slice 8</u>					
Toluene n-Butyl Alcohol Heptane Methyl Furane Styrene Propionic Acid Propyl Mercatan sec-Butyl Alcohol	8.0518	12.5692			

* Not entered into program, however removed by first slice.

The approach used with the program, as discussed before, was to establish the quantity of charcoal required to remove the contaminant with the lowest A value. The program then calculates the quantity of each of the remaining contaminants that is removed in that section. In doing this, the program considers blockage effects with the production rate of each contaminant and the mission duration given during the program then establishes the quantity of each contaminant yet to be removed. Table 6 lists the lead contaminant that establishes the size of each section and then all of the contaminants fully removed in that section and finally those contaminants that are partially removed in the section. The program must calculate the quantity of charcoal required to remove the remaining amount of the next contaminant with the lowest A value repeating this process until all contaminants have been removed. The reason that more than one contaminant is removed by some sections is due to differing production rates between contaminants and the fact that some contaminants are soluble and some contaminants are insoluble and hence, have different adsorption potential characteristics. Also shown on Table 6 are the cumulative masses of the individual sections. Thus, the quantity of charcoal required in the saturated layer to remove all contaminants through methyl ethyl ketone is 74.12 grams/day, or 29.5 lb for 180 days. To this 29.5 lb of charcoal required for the saturated layer must be added the portion required for the adsorption zone which is 3 lb.

Regenerative Sorbent Bed

The design technique utilized for establishing the quantity of charcoal needed for the saturated layer portion of the regenerative charcoal bed was identical to that used for the fixed bed. The program inputs were: a gas flow rate of 3 CFM, an adsorption temperature of 70^oF, and a removal efficiency of 80%. The results of the computer analysis for the regenerative sorbent bed are presented in Table 7. The contaminants removed by the fixed bed throughout the 180-day period (caprylic acid through methyl ethyl ketone) were not removed from the regenerative bed program. However, this produced no significant effect since the quantity of charcoal required for these contaminants is only about 2% of the total charcoal requirements. A steady state condition is assumed for both the fixed and regenerative charcoal beds. Thus, some contaminants that are initially removed by the fixed bed at a flow rate of 76 CFM will be displaced in a few days, and then their removal rates will be solely determined by the flow rate through the regenerative bed. Table 7 presents cumulative sums of all of the charcoal required to remove all contaminants through cyclopropane. Contaminants removed by other techniques, such as catalytic oxidation and that require extremely large quantities of charcoal were not included in the program. As can be seen from the table and Figure 30, the required weight of charcoal begins to increase quite rapidly after slice 15. It is also clear that the weight of charcoal required to remove all contaminants through cyclopropane would be prohibitive. A study was then made to establish the feasibility of providing a regenerative charcoal bed for all or any of these contaminants. Consideration was given to the source of those contaminants requiring charcoal for removal. Contaminants controlled by other techniques did not need to be considered. Table 8 presents a list of all of the contaminants requiring more charcoal for control than tetrafluoro ethylene (thru Section 16). This design point was chosen for investigation because (1) it represented a point where the weight for a regenerable charcoal removal technique increased significantly as additional contaminants were considered, (2) fair justification existed for the presence of vinyl chloride and tetrafluoroethylene, and (3) all contaminants requiring more charcoal than this were only produced by equipment off-gassing and had relatively unsubstantiated production rates, that is, the contaminant hasn't been found in any manned spacecraft or manned simulator test.

Table 7
 REGENERATIVE SORBENT BED
 COMPUTER ANALYSIS RESULTS

<u>Slice 1</u>	Mass of Slice <u>gms/day</u>	Cumulative Mass of Slice <u>gms/day</u>	<u>Slice 9</u>	Mass of Slice <u>gms/day</u>	Cumulative Mass of Slice <u>gms/day</u>
Caprylic Acid Indole* Skatole*	0.0318	0.0318	Methyl Acetate Butyric Acid Freon 113 Ethylene Dichloride	5.4159	21.7588
<u>Slice 2</u>			<u>Slice 10</u>		
Decalin Valeric Acid	0.0532	0.08505	Acetone 1,1 Dichloroethane Ethyl Formate n-Butane Trichloroethylene Chloroform Trans Butane 2 Ethyl Ether Freon 11 Methylene Chloride cis-Butane 2 Propylene Aldehyde Acetic Acid Ethyl Acetylene Acrolein Vinylidene Chloride Ethyl Mercaptan mono Methyl Hydrazine Chloroacetone	53.058	74.8171
<u>Slice 3</u>			<u>Slice 11</u>		
Hexomethylcyclotrisihexane	0.0234	0.1085	Butane-1	1.544	76.36
<u>Slice 4</u>			<u>Slice 12</u>		
Napthalene	0.0421	0.1506	Ethyl Alcohol	5.482	81.84
<u>Slice 5</u>			<u>Slice 13</u>		
O-xylene Octane 1,1,3 Trimethyl Cyclohexane 2,2 Dimethyl Butane Di iso Butyl Ketone Mesitylene Cyclohexanol Ethyl Benzene n-Propyl Acetate 3-Methyl pentane Amyl Alcohol Chlorobenzene Phenol Methyl Cyclohexane 1,2,4 Trimethyl Benzene Methyl Butyrate n-propyl Benzene Trans 1 Methyl 3 Ethyl Cyclohexane Cumane Methyl Isobutyl, Ketone Iso, Amyl Acetate Ethylene Glycol Furfural Methyl Methacrylate Tetrachloroethylene Ethyl Sulphide Methyl Furane Iso Butyl Alcohol Propionic Acid Propyl Mercaptan	1.3689	1.5195	iso-Propyl Alcohol	1.370	83.214
<u>Slice 6</u>			<u>Slice 14</u>		
M-xylene Trans 1,2 Dimethyl Cyclohexene	0.1768	1.6962	1,3 Butadiene iso Butylene Tetrahydrofurane	35.266	118.48
<u>Slice 7</u>			<u>Slice 15</u>		
n-Hexane 1,1 Dimethyl Cyclohexane	0.4197	2.1160	Propane Freon 12 Dimethylsulphide Carbon Disulphide Freon 21 Freon 125 Furan Nitrogen Tetroxide Acetonitrile	253.47	371.95
<u>Slice 8</u>			<u>Slice 16</u>		
Pyruvic Acid n-Butyl Alcohol Toluene n-pentane Hexene-1 Methyl, isopropyl Ketone Cyclohexane Ethyl Acetate 1,4 Dioxane Methyl Chloroform n-propyl alcohol Methyl Ethyl Ketone Benzene Ethyl Isobutyl Ether Carbon Tetrachloride Heptane Styrene Isoprene Freon 114 sec-Butyl Alcohol Pentane-2 Chloropropane iso-Butane Pentane-1 2 Methyl, 1 Butane Cyclopentane Dimethyl Furane Freon 114, Unsymmetrical Valeraldehyde Dimethyl hydrazine Allyl Alcohol	14.2269	16.3429	Propylene Acetaldehyde Vinyl Chloride Tetrafluoroethylene (Design Point)	654.16	1026.107
			<u>Slice 17</u>		
			Methyl Alcohol Cynamid Freon 22 Methyl Chloride	1645.00	2671.11
			<u>Slice 18</u>		
			Ethylene Methyl Acetylene Carbonyl Sulphide	7435.74	10106.85
			<u>Slice 19</u>		
			Ethane Chlorofluoromethane Sulfur Dioxide	12422.21	22529.07
			<u>Slice 20</u>		
			Cyclopropane Freon 23 Chlorine Nitric Oxide	31870.06	54399.13
				Not in program	

*Not included in program but removed by first slice.
 **Only 684 grams required to remove down through tetrafluoroethylene.

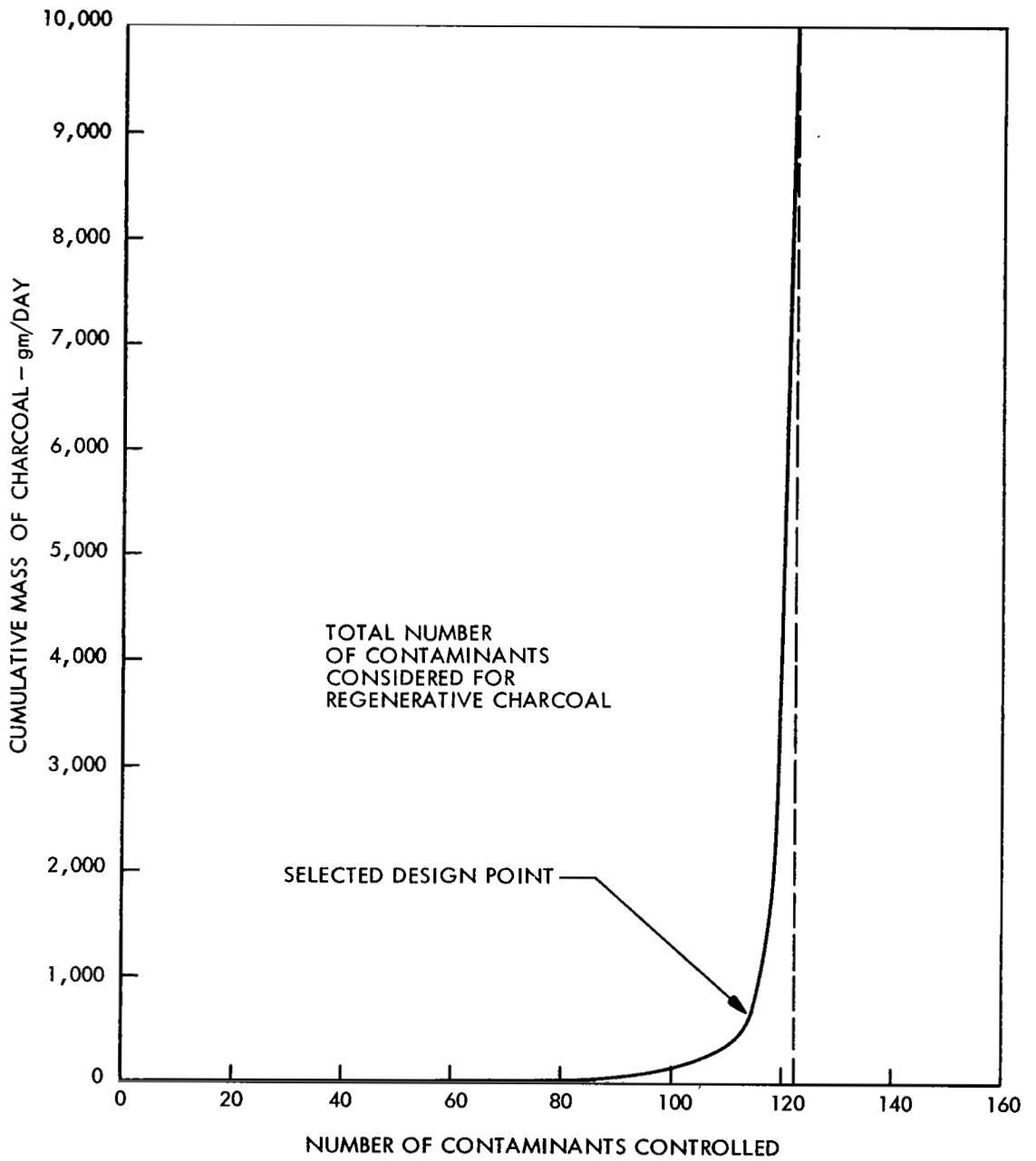


Figure 30 Size of the Regenerative Bed

TABLE 8
 POTENTIAL SOURCES OF CONTAMINANTS REQUIRING EXCESSIVE CHARCOAL FOR CONTROL

Contaminant	Potential Source	Is Source Controllable	Identified in any Manned System	Identified in Apollo 101, 103, & LEM-3
Nitric Oxide	Not known	Yes	Yes	No
Freon 23	Refrigerant Intermediate in organic synthesis	Yes Not known	Yes	No
Chlorofluoromethane	Not known	Not known	Yes	No
Methyl Chloride	Refrigeration	Yes	Yes	No
	Butyl Rubber catalyst solvent	Yes		
	Petroleum refining	Yes		
	Forming agent in styro foam mfg.	Yes		
	Reagent in silicon production	No		
Freon 22	Intermediate in Teflon Mfg.	No	Yes	Yes
Cyanimid	Not known	Not known	No	No

Also listed on this table are (1) potential sources, where they are known, (2) whether or not these sources could be controlled, and (3) whether or not the contaminant has been found in either the LEM or Apollo ground simulation tests since the Apollo fire.

This last item is of particular significance since a great deal of material changes have taken place since that time, and therefore, contaminants that were identified in manned systems prior to that time, but have not been identified since, are probably not potential space station contaminants. In reviewing this list, it appears that Freon 22 is the only one of these contaminants that has been found in either the Apollo or LEM testing. An investigation of the potential source for Freon 22 has indicated that it is an intermediate in the manufacture of Teflon. Discussions with Dupont have revealed that this is the only potential source that they are aware of. Off-gassing studies of Teflon, however, have indicated that Freon 22 is not an off-gassing product. In the analyses conducted of the Apollo S/C 101 and S/C 103, Freon 22 was analyzed by gas chromatography using a poropak column which was unable to separate Freon 12 and Freon 22. Mass spectrometer analysis of the gas chromatograph effluent, however, indicated the presence of both Freon 12 and Freon 22; however, no quantitative reportings have been made. Thus, though Freon 22 may be present its rate probably will not be nearly as great as assumed in this investigation. An analysis was then made to determine what production rate of Freon 22 could be supported by a bed large enough to control all contaminants through tetrafluoroethylene at the design point. The results of this analysis indicated that 37% of the original production rate for Freon 22 could be controlled by the selected bed, since Freon 22 is partially removed in sections upstream of Section 17 (Ref. Table 7). In light of the uncertainties surrounding the source and production rate for Freon 22, this appeared to be a reasonable capability. Thus, the 684 grams/day quantity of charcoal was utilized for the saturated layer portion of the regenerative bed.

System Performance Summary

An evaluation of the flow rate required to remove each of the candidate contaminants revealed that 76 CFM through the fixed bed and 3 CFM through the regenerative bed would control all but 1 contaminant, based on the nominal production rate proposed in Table 1, (monomethyl hydrazine) and all but 8 contaminants based on the proposed maximum production rate (acetic acid, acetonitrile, acrolein, methylene chloride, nitrogen tetroxide, hydrogen fluoride, carbon monoxide, and mono methyl hydrazine). In all of these cases, however, these contaminants had design production rates derived from relatively unsubstantiated equipment off-gassing rates. The 76 CFM flow rate was based on the requirement for removal of pyruvic acid at the nominal production rate. Also, pyruvic acid establishes the size of the fixed bed, since it has a relatively high A value and is only a metabolic contaminant and therefore, its production rate does not change with time, the 76 CFM flow rate is adequate for control of the same contaminants at the maximum production rate except as previously noted. The 3 CFM flow rate was set by the catalytic oxidizer, designed under NAS 1-7433 and NAS 1-6256, and the requirement that the regenerative bed be upstream of the oxidizer to provide effective control of potential catalyst poisons, such as the halogenated hydrocarbons.

A summary of the system performance is presented in Table 9. Included in this table are a list of the contaminants controlled by the system, the removal technique, and the resulting cabin concentration. The contaminant concentrations are presented for both nominal and maximum production rates for both the 3 CFM and 76 CFM flow streams, where applicable. As can be seen from this table, there are 5 contaminants which the regenerative bed is scheduled to control, for which adequate flow is not provided by the regenerative bed at the maximum production rate. These contaminants, however, will be removed in appreciable quantity initially by the fixed bed, when the equipment production rates are at the initial or maximum levels. The capacity reduction of the fixed bed diminishes for these contaminants paralleling the reduction in production rate.

Table 9

SYSTEM PERFORMANCE SUMMARY

Contaminant	(1) Removal Technique	(4) A Value Mol % M	CONCENTRATION				Max. Allow. Conc. Mg/M ³	Initial Removal Provided by Fixed Bed	Adequate Flow Not Provided Initially
			For Average Equip. Prod. Rate, Plus Metabolic		For Max. Equip. Prod. Rate, Plus Metabolic				
			75 CFM N ₂ = 9.9 Mg/M ³	3 CFM N ₂ = 9.8 Mg/M ³	75 CFM N ₂ = 9.9 Mg/M ³	3 CFM N ₂ = 9.8 Mg/M ³			
Acetone	R	18.5		1.04		104	720		
Acetaldehyde	R	30.6		2.56		25.6	36		
Acetic Acid	R	24.8		2.55	0.899	25.5	2.5	+	
Acetylene	O	-		2.55		25.5	6400		
Acetonitrile	R	34.0		2.55	0.895	25.5	7	+	
Acrolein	R	27.2		0.255	0.0895	2.55	0.25	+	
Allyl Alcohol	F	21.9		0.00895		0.0895	0.50		
Ammia	FP	-	1.16			1.820	17.5		
Amyl Acetate	FP	16.0	0.00895		0.0895		53		
Amyl Alcohol	F	15.1	0.00895		0.0895		36		
Benzene	F	20.3	0.0895		0.895		3.2		
n-Butane	R	19.5		2.55		25.5	180		
iso-Butane	F	22.5	0.00895		0.0895	2.55	180		
Butane-1	R	21.0		0.255		25.5	180		
cis-Butane-2	R	24.1		0.255		2.55	180		
trans-Butane-2	R	20.8		2.55		2.55	180		
1,3 Butadiene	R	23.1		2.55		25.5	280		
iso-Butylene	R	27.7		0.255		2.55	180		
n-Butyl Alcohol	F	15.9	0.094				30		
iso-Butyl Alcohol	F	19.4	0.00895		0.0895		30		
sec-Butyl Alcohol	F	21.8	0.00895		0.0895		30		
tert-Butyl Alcohol	R	19.0		0.255		2.55	30		
Butyl Acetate	R	23.0		0.255		2.55	71		
Butraldehyde	R	25.0		0.255		2.55	70		
Butyric Acid	F	26.5	0.00895		0.0895		14		
Carbon Disulphide	R	31.0		0.255		2.55	6		
Carbon Monoxide	CO	-		6.5		29.0	17		
Carbon Tetrachloride	R	20.3	0.0895		0.895		6.5		
Carboxyl Sulphide	FM	-	0.00895		0.0895		25		
Chlorine	FM	-	0.00895		0.0895		30		
Chloroacetone	R	28.3		0.255		2.55	100		
Chlorobenzene	F	15.6	0.00895		0.0895		35		
Chloroform	R	20.2		2.55		25.50	24		
Chloropropane	F	23.0	0.00895		0.0895		84		
Caprylic Acid	F	6.1	0.00358		0.00358		155		
Cumene	F	15.9	0.00895		0.0895		25		
Cyclohexane	F	16.8	0.0895		0.895		100		
Cyclohexene	F	16.8	0.0895		0.895		100		
Cyclohexanol	F	14.7	0.00895		0.0895		20		
Cyclopentane	F	23.9	0.00895		0.0895		100		
Cyclopropane	CO	-		0.255		2.55	100		
Cyanid	R	38.9		0.255		2.55	45		
Decalin	F	7.0	0.00895		0.0895		5.0		
1,1 Dimethyl Cyclohexane	F	18.0	0.00895		0.0895		120		
trans 1,2 Dimethyl Cyclohexane	F	18.0	0.00895		0.0895		120		
2,2 Dimethyl Butane	F	13.1	0.00895		0.0895		93		
Dimethyl Sulphide	R	30.2		0.255		2.55	15		
1,1 Dichloroethane	R	19.0		2.55		25.5	40		
M iso Butyl Ketone	F	12.1	0.00895		0.0895		29		
1,4 Dioxane	F	19.5	0.0895		0.895		36		
Dimethyl Furan	F	24.3	0.00895		0.0895		3.0		
Dimethyl Hydrazine	F	26.8	0.00895		0.0895		0.1		
Ethane	CO	-		2.55		25.5	180		
Ethyl Alcohol	R	22.2		3.04		25.7	190		
Ethyl Acetate	F	18.6	0.0895		0.895		140		
Ethyl Acetylene	R	26.8		0.255		2.55	180		
Ethyl Benzene	F	14.2	0.00895		0.0895		44		
Ethyl Dichloride (1, 2 Dichloro ethane)	R	23.9		0.255		2.55	40		
Ethyl Ether	R	21.2		2.55		25.5	120		
Ethyl Ethyl Ether	F	18.7	0.0895		0.895		200		
Ethyl Formate	R	19.3		2.55		2.55	30		
Ethylene	CO	-		2.55		25.5	180		
Ethylene Glycol	F	20.3	0.00895		0.0895		114		
trans 1, Methyl 3, Ethyl Cyclohexane	F	15.5	0.00895		0.0895		117		
Ethyl Sulphide	F	18.4	0.00895		0.0895		97		
Ethyl Mercaptan	R	27.7		0.102		0.102	2.5		
Freon 11	R	21.3		2.55		25.5	5600		
Freon 12	R	27.6		2.55		25.5	4000		
Freon 21	R	31.1		0.255		2.55	420		
Freon 113	R	23.7		0.255		2.55	142		
Freon 114	F	21.5	0.0895		0.895		300		
Freon 114 unsym	F	25.3	0.00895		0.0895		000		
Freon 125	R	31.8		0.255		2.55	25		
Formaldehyde	FM	-	0.00895		0.0895		25		
Furan	R	31.8		0.255		2.55	3		
Furfural	F	18.2	0.00895		0.0895		2		
Hydrogen	CO	-		8.70		31.80	215		

Table 9 (Continued)

Contaminant	(1) Removal Technique	(4) A Value Mol. CK ML	CONCENTRATION				Max. Allow. Conc. Mg/l ³	Initial Removal Provided by Fixed Bed	Adequate Flow Not Provided Initially
			For Average Equip. Prod. Rate, Plus Metabolic		For Max. Equip. Prod. Rate, Plus Metabolic				
			75 CFM	3 CFM	75 CFM	3 CFM			
			r = 0.9	r = 0.8	r = 0.9	r = 0.8			
		Mg/l ³	Mg/l ³	Mg/l ³	Mg/l ³				
Hydrogen Chloride	FM	-	0.00895		0.0895		0.15		
Hydrogen Fluoride	FM	-	0.00895		0.0895		0.08		
Hydrogen Sulfide	FM	-	0.000032		0.000032		1.5		
Heptane	F	18.8	0.00895		0.0895		200		
Hexene-1	F	15.6	0.0895		0.0895		180		
n-Hexane	F	12.4	0.00895		0.0895		180		
Hexamethylcyclotrisi-hexane	F	10.5	0.00895		0.0895		240		
Indole	F	4.0	0.107		0.107		126		
Isoprene	F	20.9	0.00895		0.0895		140		
Methylene Chloride	R	27.0		2.55		25.5	21	+	
Methyl Acetate	R	18.0		2.55			61		
Methyl Butyrate	F	16.1	0.00895		0.0895		30		
Methyl-1 Butane	F	22.7	0.00895		0.0895		1430		
Methyl Chloroform	F	19.0	0.0895		0.0895		190		
Methyl Furan	F	19.0	0.00895		0.0895		3		
Methyl Ethyl Ketone	F	20.1	0.0895		0.0895		59		
Methyl Isobutyl Ketone	F	16.2	0.00895		0.0895		41		
Methyl Isopropyl Ketone	F	16.2	0.0895		0.0895		70		
Methyl Cyclohexane	F	16.0	0.00895		0.0895		200		
Methyl Acetylene	CO	-		0.255		2.55	155		
Methyl Alcohol	R	34.3		2.73		25.7	26		
3-Methyl Pentane	F	14.6	0.00895		0.0895		295		
Methyl Methacrylate	F	17.7	0.00895		0.0895		41		
Methane	CO	-		260 (3)		950 (3)	1720		
Mesitylene	F	13.3	0.00895		0.0895		2.5		
mono Methyl Hydrazine	R	28.1		0.255		2.55	0.035	(2)	
Methyl Mercaptan	CO	-		0.102		1.02	2		
Naphthalene	F	11.6	0.00895		0.0895		5		
Nitric Oxide	FM	-	0.00895		0.0895		32		
Nitrogen Tetraoxide	R	33.3		0.255		2.55	1.8	+	
Nitrogen Dioxide	FM	-	0.00895		0.0895		0.9		
Nitrous Oxide	FM	-	0.00895		0.0895		235		
Propylene	R	30.2		2.55		25.5	180		
iso-Pentane	F	15.8	0.0895		0.895		295		
n-Pentane	F	15.8	0.0895		0.895		295		
Pentene-1	F	22.3	0.00895		0.0895		180		
Pentene-2	F	22.0	0.00895		0.0895		180		
Propane	R	11.6		2.55		25.5	180		
n-Propyl Acetate	F	14.9	0.00895		0.0895		84		
n-Propyl Alcohol	F	20.7	0.0895		0.895		75		
iso-Propyl Alcohol	R	23.0		2.55		25.5	98		
n-Propyl Benzene	F	15.7	0.00895		0.0895		44		
iso-Propyl Chloride	R	22.2		0.255		2.55	260		
iso-Propyl Ether	R	13.5		0.255		2.55	120		
Propionaldehyde	R	26.6		0.255		2.55	30		
Propionic Acid	F	20.4	0.00895		0.0895		15		
Propyl Mercaptan	F	21.3	0.00365		0.00365		82		
Propyl Aldehyde	R	24.3		0.255		2.55	10		
Pyruvic Acid	F	16.0	0.899		0.899		0.9		
Phenol	F	16.6	0.00895		0.0895		1.9		
Skatol	F	4.0	0.107		0.107		141		
Sulfur Dioxide	FM	-	0.00895		0.0895		0.8		
Styrene	F	19.9	0.00895		0.0895		42		
Tetrachloroethylene	F	18.4	0.00895		0.0895		67		
Tetrafluoroethylene	R	36.8		0.255		2.55	295		
Tetrahydrofuran	R	29.3		0.255		2.55	59		
Toluene	F	15.5	0.0895		0.895		75		
Trichloroethylene	R	20.0		2.55		25.5	52		
1,2,4 Trimethyl Benzene	F	15.4	0.00895		0.0895		49		
1,1,3 Trimethyl Cyclohex.	F	11.2	0.00895		0.0895		140		
Valeraldehyde	F	25.2	0.00365		0.00365		70		
Valeric Acid	F	11.9	0.00365		0.00365		110		
Vinyl Chloride	R	31.4		2.55		0.255	130		
Vinyl Methyl Ether	F	12.0	0.00895		0.0895		60		
Vinylidene Chloride	R	27.2		0.255		2.55	20		
O-xylene	F	12.0	0.0895		0.895		44		
M-xylene	F	12.3	0.0895		0.895		44		
P-xylene	F	12.3	0.0895		0.895		44		

- (1) Removal Technique Key:
 F - Fixed Charcoal Bed
 R - Regenerative Charcoal Bed
 FP - Fixed Charcoal Bed Phosphoric Acid
 FM - Fixed Charcoal Bed, Moisture
 CS - Pre and Post Sorbent Bed
 CO - Catalytic Oxidizer

(2) Adequate flow is not provided at average or maximum equipment production rates.

(3) Based on r = 0.25.

(4) "A" value presented for contaminants controlled by fixed or regenerative beds.

Two contaminants, however, do not have adequate control at the maximum production rates. These are hydrogen fluoride and carbon monoxide. Both of these contaminants have more than adequate flow for removal, however, at the average production rate. The hydrogen fluoride has a cabin concentration of 0.0895 Mg/M^3 at the maximum production rate as compared with an allowable concentration of 0.080 Mg/M^3 . Thus, the system can support a production rate approximately 10% less than the arbitrary maximum rate of 0.25 gm/day, which does not appear to be of significance, since hydrogen fluoride has not been observed in any manned system test and its presence is based on anticipated space station experiments. The 3 CFM flow requirement for carbon monoxide control was established in the original IHCOS study, utilizing the maximum equipment production rates. At that time, carbon monoxide had an allowable concentration of 29 Mg/M^3 . The allowable carbon monoxide level recommended by the panel on air standards for manned space flight of the National Academy of Sciences Space Science Board is 17 Mg/M^3 . Thus, for the maximum rate case, 3 CFM does not provide adequate control. The production rate for carbon monoxide was based, however, on a substantiated metabolic production rate of 0.4 grams/day for 12 men, an arbitrary 0.25 grams/day nominal equipment rate, and an arbitrary 2.50 grams/day maximum equipment rate. Atmospheric analysis of Apollo S/C 101 and S/C 103 established that there was a significantly higher carbon monoxide concentration during the manned tests than during the unmanned tests. This indicates that carbon monoxide production is primarily metabolic. For these reasons, it appears that the capability of the system to handle a maximum carbon monoxide equipment production rate of 1.5 grams/day at a cabin concentration of 17 Mg/M^3 is entirely adequate.

There is one contaminant for which adequate flow is not provided for either maximum or nominal production rates; this is mono methyl hydrazine. This contaminant has not been found in any manned spacecraft or simulator test, and leakage within or into the manned cabin from external sources such as the reaction control system is not anticipated. Therefore, it appears that the capability of the system to control a production rate of 0.034 grams/day is satisfactory.

MODEL SYSTEM TEST

The long-term Model System Test conducted on a 1/10th scale model of the system was performed for a period of 240 days, beginning on November 11, 1970 and ending on July 9, 1971. This section presents the objectives, apparatus, and procedures used, the results obtained, and a discussion of the results.

Objective

The primary objective of this test effort was to determine the characteristics of the integrated system and to establish the validity of the design methodology.

Apparatus

The test apparatus is presented schematically in Figure 31 and is illustrated in Figures 32 and 33. Listed below are the major items used in the test.

- o Cylinders for gaseous contaminant supply
- o Pressure gauge, regulator and diaphragm pump to measure and control system pressure
- o Inlet and exit sampling septa for obtaining gas samples at the inlet and outlet of various components
- o Catalytic oxidizer containing 57 cc of 1/2% pd. catalyst
- o Preheater for heating gasses entering the catalyst bed
- o Furnace and temperature controller to control catalyst bed temperature
- o Air cooled heat exchanger for cooling exit gas from catalyst bed
- o Diaphragm pumps to maintain gas circulation through the system components
- o Wet test meter to determine system outflow (leakage)
- o F&M gas chromatographs model 720, 1609, 810, 700A and 700B equipped with flame ionization electron capture and thermal conductivity detectors
- o Beckman gas chromatograph model GC 4 with microthermal conductivity and helium ionization detectors
- o Perkin Elmer infrared spectrophotometer Model 521 with 10 meter cell
- o Perkin Elmer Model 202 Spectrophotometer for colorimetric analysis
- o Cambridge Instruments dew point hygrometer
- o Water humidifier for humidity control
- o Pre-sorbent and post-sorbent beds containing 6 x 8 mesh Foote Mineral Co. environmental grade lithium hydroxide

77

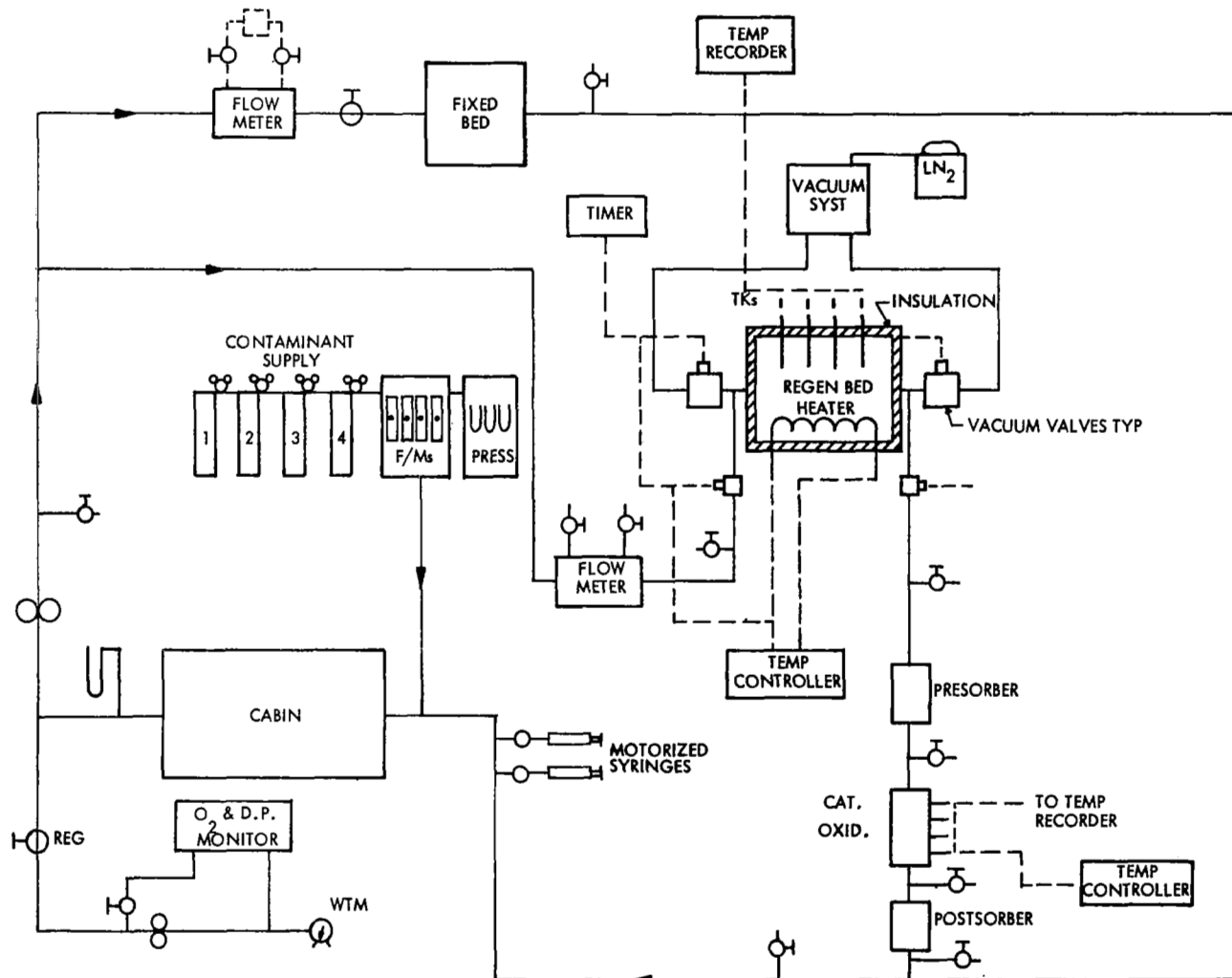


Figure 31 Model System Test Apparatus Schematic

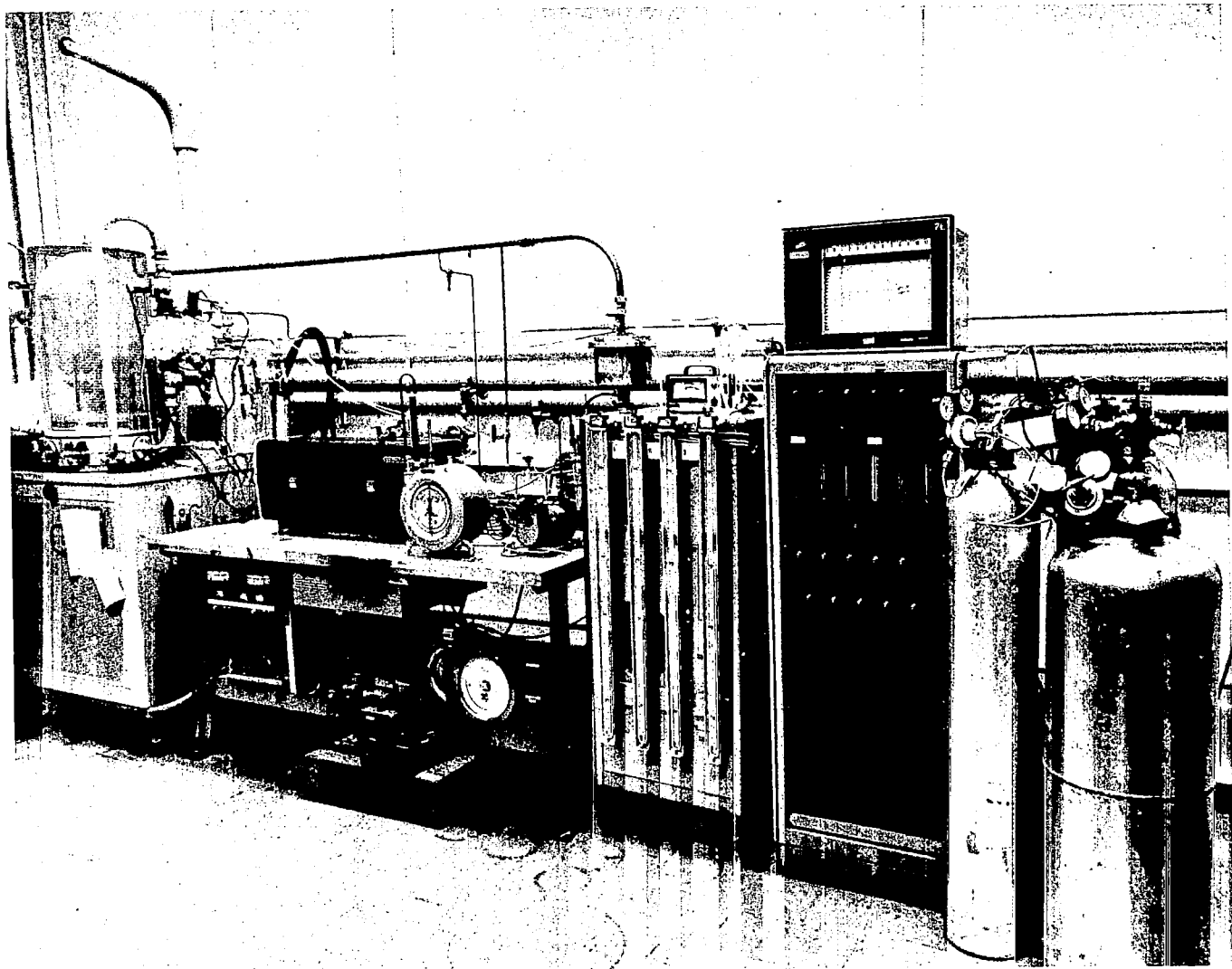


Figure 32 Model System Test Apparatus

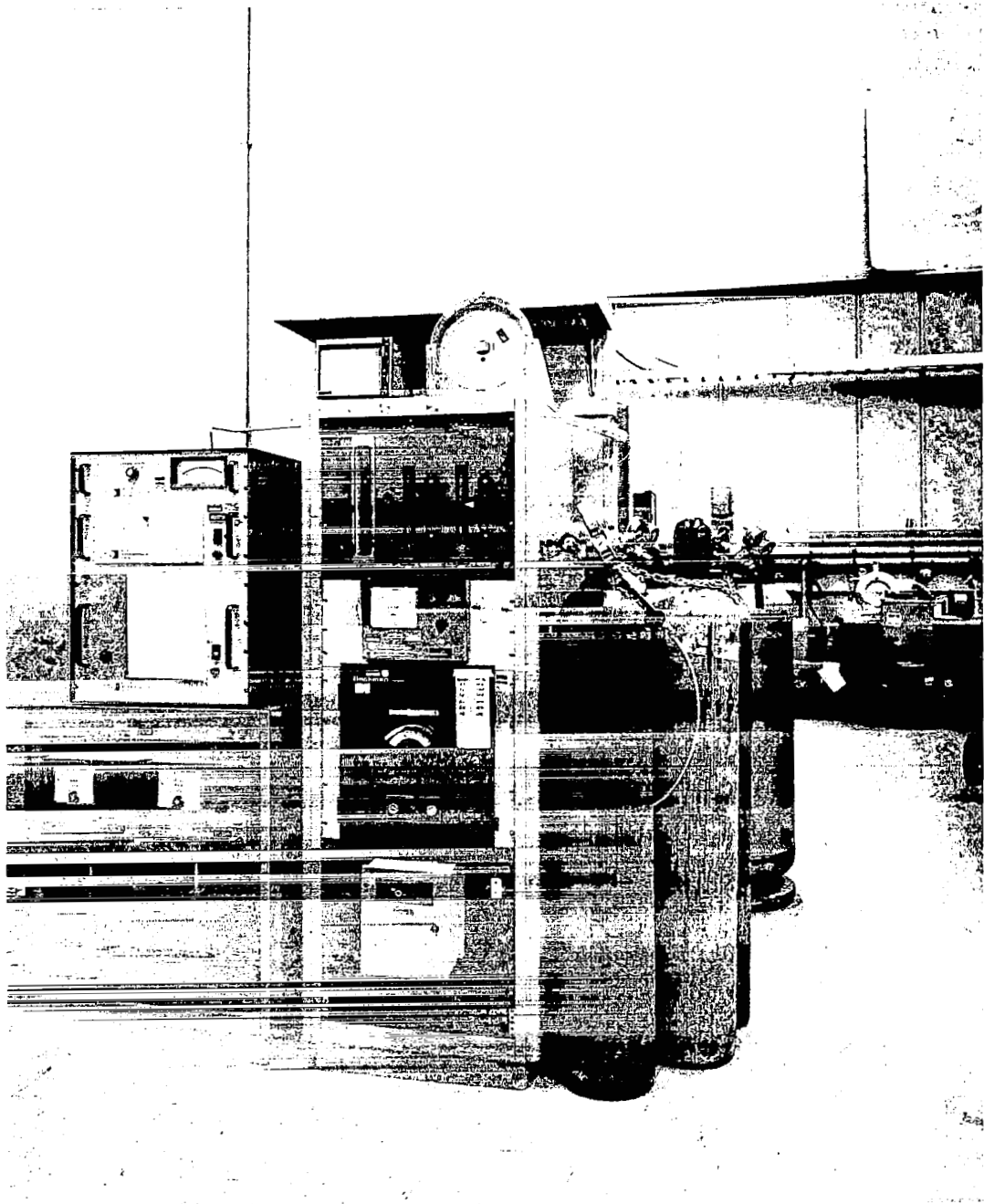


Figure 33 Dew Point and Oxygen Partial Pressure Monitoring Equipment

- o Diaphragm pump, flowmeter and pyrex gas bubblers for colorimetric analysis
- o Motorized syringe and heater for introducing liquid contaminants into the system
- o Beckman oxygen analyzer Model F-3 for monitoring and controlling system oxygen partial pressure
- o CVC vacuum system with 4" diffusion, Welsh Model 1397, roughing pump and liquid nitrogen baffle to simulate space vacuum conditions
- o Liquid nitrogen and automatic level control to provide liquid nitrogen to the vacuum system
- o Regenerative sorbent bed with 0.5 lbs. of Barnebey Cheney BD charcoal with heater and temperature controller
- o Vacuum valves to control flow through the regenerative bed
- o Timer to control the regenerative bed cycle time
- o Fixed sorbent bed containing 3.2 lbs. of 4 x 6 mesh. Barnebey Cheney charcoal impregnated with 2 millimoles of phosphoric acid per gram of charcoal.
- o Hastings mass flow meters, Model LF 20K, to measure the gas flow rates through the fixed bed and regenerative bed
- o Flow meters and manometers to measure the introduction rates of gaseous contaminants
- o Temperature recorder to monitor system temperatures.

Procedure

The long-term model system test was conducted on a 1/10 scale model of the selected system. The system was operated in a closed loop manner in which the inlet and outlet of the contaminant removal components were connected to a simulated cabin.

Gas was circulated through the components of 1/10 the design rate, 0.3 cfm for the catalytic oxidizer regenerative bed and 7.6 CFM for the fixed bed. The system total pressure was maintained at 10 psia and the oxygen partial pressure was maintained at 3.1 psia. The system dewpoint was kept at approximately 50°F. The catalytic oxidizer was operated at a space velocity of 21,000 hr⁻¹ with an average catalyst bed temperature of 680°F. The regenerative sorbent bed was operated on both 24 and 48 hr. cycle times with 2 and 3 hour desorption times.

The input power to the heater was such that the regenerative bed would reach a 200°F bed temperature by the end of the desorption cycle. The desorption vacuum was approximately 5×10^{-5} mm Hg by the end of the desorption cycle. The contaminants introduced into the system and the analytical techniques are described in the following sections.

Selection of Contaminants to be Used in the Model Test

In selecting contaminants to be used in the evaluation of the model system, consideration was given to introducing contaminants into the system that stressed all of the system elements, e.g., fixed charcoal bed, regenerative charcoal bed, and catalytic oxidizer. The selection was based on having a number of contaminants for each device ranging from contaminants easily controlled to contaminants that represented the design limit. Consideration was also given to ease of contaminant introduction as well as the ability to analyze for the individual contaminants at the relatively low levels that were anticipated. The selected contaminants, test introduction rates, anticipated cabin concentration, and maximum allowable concentrations are presented in Table 10. The period of introduction for the various contaminants and the periods of operation for the system components is shown in Figure 34.

Fixed Sorbent Bed

The contaminants used to evaluate the fixed sorbent bed were ammonia, sulfur dioxide, Freon 114, and n-propyl alcohol. Ammonia was selected to establish the effectiveness of the phosphoric acid impregnation on the fixed bed charcoal. Sulfur dioxide was included to verify that the moisture in the fixed bed charcoal would effectively control the acid gasses. Both Freon 114 and n-propyl alcohol were selected as contaminants to be removed by adsorption. Freon 114 represented a catalyst poison that was to be removed by the fixed bed and n-propyl alcohol was used to model pyruvic acid.

Analytical problems in analyzing for pyruvic acid resulted in a search for a substitute compound for test purposes. A prime criteria for the selection of the new material was that it have properties as similar as possible to the pyruvic acid. In determining the adsorption characteristics of a compound upon activated charcoal, two parameters are of particular importance. These are the solubility and the A value. A search of the contaminant list was made to define a material similar in properties which could be easily analyzed. The search was restricted to soluble materials to simulate the same capacity curve on

TABLE 10
CONTAMINANTS USED IN THE MODEL SYSTEM TEST

Removal Device	Contaminant	Nominal Prod. Rate (gm/day)	Anticipated Concentration Mg/M ³	Allowable Concentration Mg/M ³
Fixed Bed	Ammonia	0.325	4	17.5
	Sulfur Dioxide	0.0025	.009	.08
	F 114	0.025	.09	7000.
	n-Propyl Alcohol*	0.250	.90	0.90
Regenerative Bed	Vinyl Chloride	0.025	2.55	130.
	F 12	0.025	2.55	5000.
	F 11	0.025	2.55	5600.
	Acetone	0.102	10.4	720.
Catalytic Oxidizer	Methane	0.60**	157.	1720.
	Carbon Monoxide	0.045***	4.5	17.
	Acetylene	0.025	2.55	6400.
	Ethylene	0.025	2.55	180.
	Ethane	0.025	2.55	180.

* Used to model pyruvic acid.

** Should be 0.995 for the nominal case.

*** Should be 0.065 for the nominal case.

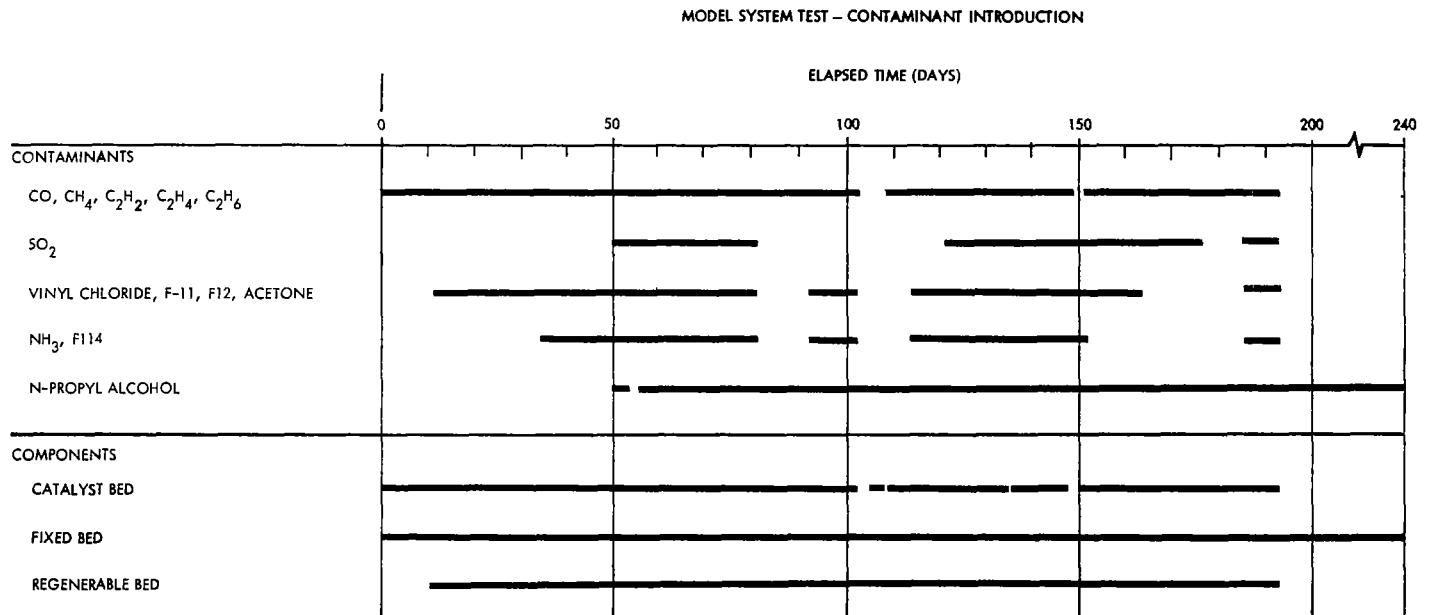


Figure 34 Model System Test Contaminant Introduction

the potential plot. In modeling A value, we observe that:

$$A = \frac{T}{V_m} \log \frac{C_s}{C_i}$$

Of the terms, only C_s and V_m relate directly to the properties of the contaminant. Thus, the value of $(\log C_s)/V_m$ for candidate materials was calculated. This calculation showed that n-propyl alcohol most closely simulates pyruvic acid. As there are no analytical problems associated with this material, it was selected as a substitute. In order to simulate A value, n-propyl alcohol was introduced at the same rate as pyruvic acid.

The selection of Freon 114 was based upon the desirability of selecting a material which is marginally adsorbed by the fixed bed. Freon 114 was selected on the basis of ease of analysis and for the fact that it requires a major portion of the fixed charcoal bed for adsorption. Further, its control in introduction is simplified by its being a gas. Freon 114 is an insoluble contaminant that will be blocked by water.

Regenerative Bed

The contaminants selected for evaluation of the regenerative bed were acetone, Freon 11, Freon 12, and vinyl chloride. Three of these contaminants are known catalyst poisons. Vinyl chloride and Freon 12 were used in the evaluations of the isotope heated catalytic oxidizer tested during NAS 1-7433. Both of these contaminants demonstrated that they would poison the catalyst if allowed to enter in appreciable quantities.

Vinyl chloride is at the design point of the bed in terms of breakthrough. As can be seen from Table 7, vinyl chloride requires the full 684 grams/day. Freon 12 should be removed in the previous slice, which is approximately the mid-point of the bed. Freon 11 and acetone should be removed in the 10th slice, or about 12 per cent of the way through the bed.

Catalytic Oxidizer

The contaminants selected to evaluate the catalytic oxidizer were the same competing hydrocarbons used to evaluate the catalytic oxidizer in the previous 180-day tests of this component. These were methane, carbon monoxide,

acetylene, ethylene, and ethane. Methane establishes the required operating temperature for the catalytic oxidizer, and carbon monoxide establishes the required flow at the maximum production rate. The production rates presented in Table 9 represent the nominal case. The production rate shown for carbon monoxide and methane is about 70% of the desired value due to mixing errors in the contaminant blend. However, the anticipated cabin concentration shown in Table 10 is based on the actual production rate, and hence, bed performance can be based on this concentration.

Chemical Analysis Techniques

Carbon monoxide levels were monitored by gas chromatography using both a Beckman GC-4 equipped with a helium ionization detector and a modified F&M Model 1609 equipped with a catalytic converter (to reduce carbon monoxide to methane) located ahead of a flame ionization detector. Ethylene, acetylene, ethane, and methane were analyzed by gas chromatographic temperature programming techniques. A 90% 13X and 10% 5A molecular sieve 30/60 mesh mix was used for separating the components on a 10 ft. x 1/8 inch O.D. stainless steel column. Temperature programming conditions were at 10°C/minute and from 110°C to 220°C.

The Freons 11, 12, and 114 were monitored by using an F&M Model 810 gas chromatograph equipped with an electron capture detector. A 30 ft. x 1/8 in. O.D. stainless steel column packed with 20% SE-30 on 60/80 chromosorb W was used for separating the components from the samples taken. Oven temperature was maintained at 22°C. Vinyl chloride was analyzed by using an F&M Model 700 flame ionization detector gas chromatograph equipped with a Model 810 electrometer. A 20 ft. x 1/8 in. O.D. stainless steel column packed with 30% equal mixture of di-2-ethyl hexyl sebacate and bis-2-(2-methoxyethyl) adipate on 60/80 chromosorb W operated at 50°C oven temperature was used for separating the vinyl chloride from the other components in the samples.

Both acetone and n-propyl alcohol were analyzed by using another F&M Model 700 flame ionization detector gas chromatograph equipped with a Model 810 electrometer. A 6 ft. x 1/8 in. O.D. stainless steel column packed with 20% Hallcomid M on 60/80 mesh chromosorb W operated at 65°C oven temperature was used for

resolving these contaminants from each other and the other constituents present in the samples.

Samples were obtained from each of the various sampling locations in the system with evacuated 500 cc bottles or directly with two or more 5 cc gas tight syringe samples equipped with 7.6 cm length needles. Quantification was accomplished by calibrating the gas chromatographs by direct injection techniques. Direct comparisons of peak area (height x width at half-height integration method) or peak height of samples with standard samples at the approximate concentration levels were made. Standard curves relating peak area or height versus detector response were plotted.

The colorimetric analysis technique used for measuring SO_2 is described by Lyshkow (Ref. 6). This method was followed over the previous method described by Jacobs (Ref. 7) for eliminating the highly poisonous tetrachloro-mercurate absorbing solution. A hydrochloride and bleached solution containing pararosaniline was used as the absorbing and developing reagent. Standardization was performed against known sodium bisulfite concentration levels. Absorption readings were made at 560 m, 20 cc. Samples were collected by a bubbler system consisting of three 100 cc volume pyrex glass impingers arranged in series and connected by minimal lengths of clear tygon tubing. The first and third impingers were protective traps for the middle impinger containing the absorbing reagent. The impinger was filled with 20 cc absorbing reagent and the system atmosphere was passed through the absorbing reagent at approximately 100 cc per minute. Sampling time varied, depending upon the concentration and contaminant being analyzed. A wet test-meter was used to measure total volume consumed. A Perkin-Elmer Model 202 ultraviolet-visible spectrophotometer equipped with 5 cm path cells (20 cc volume) were used for determining the concentration levels. Conventional calibration techniques were used to obtain quantified data.

Ammonia analysis was performed by using the colorimetric technique described in previous studies (Ref. 8). 0.1N sulfuric acid was used as the absorbing reagent and a combination alkaline phenol and hypochlorite was used as the dye reagent. Ammonium sulfate was used for standardization. Measurements were made at 610 m.

Nitrous oxide samples were obtained from the sampling points in the system by drawing the enclosed atmosphere slowly into an evacuated 10-meter path folded infrared cell. After equilibrium between the cell and system pressure had been reached, infrared scans were made in the 2400-2000 cm^{-1} region. Nitrous oxide concentrations were determined by standard methods. Sample absorption readings were compared against calibration curves obtained on known nitrous oxide levels.

Results

The system dew point data is presented in Figure 35. Methane, carbon monoxide, acetylene, ethylene, and ethane inlet concentration and catalytic oxidizer removal efficiency data are presented in Figures 36, 37, 38, 39, and 40. Acetone, Freon 11, Freon 12 and vinyl chloride inlet concentration and regenerative bed removal efficiency data are presented in Figures 41, 42, 43, and 44.

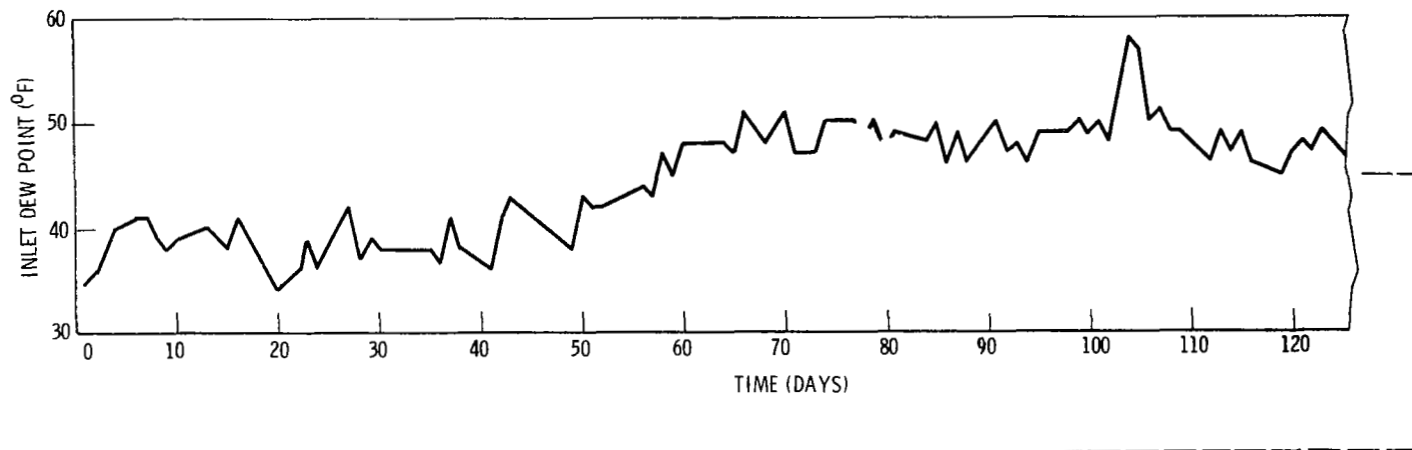
Ammonia, sulfur dioxide, n-propyl alcohol and Freon 114 concentration and fixed bed removal efficiency data are presented in Figures 45, 46, 47, and 48. Figure 48 also presents the regenerative bed removal efficiency for Freon 114. Freon 11, Freon 12, Freon 114 and vinyl chloride catalytic oxidizer inlet concentration data are presented in Figure 49. Nitrous oxide catalytic oxidizer effluent concentration data are presented in Figure 50. Freon 12 regenerative bed effluent concentration data are presented in Figure 51. Sulfur dioxide, catalytic oxidizer inlet concentration data are presented in Figure 52.

Discussion

During the long-term test investigations were conducted relative to the performance of the catalytic oxidizer, regenerative bed and fixed bed. The following sections discuss the results of the tests pertinent to these investigations.

Catalytic Oxidizer

The catalytic oxidizer operated satisfactorily for the first 75 days of the test at which time methane removal efficiency started to decay. The methane removal efficiency dropped to zero on the 79th through 82nd day of the test, Ref.



88

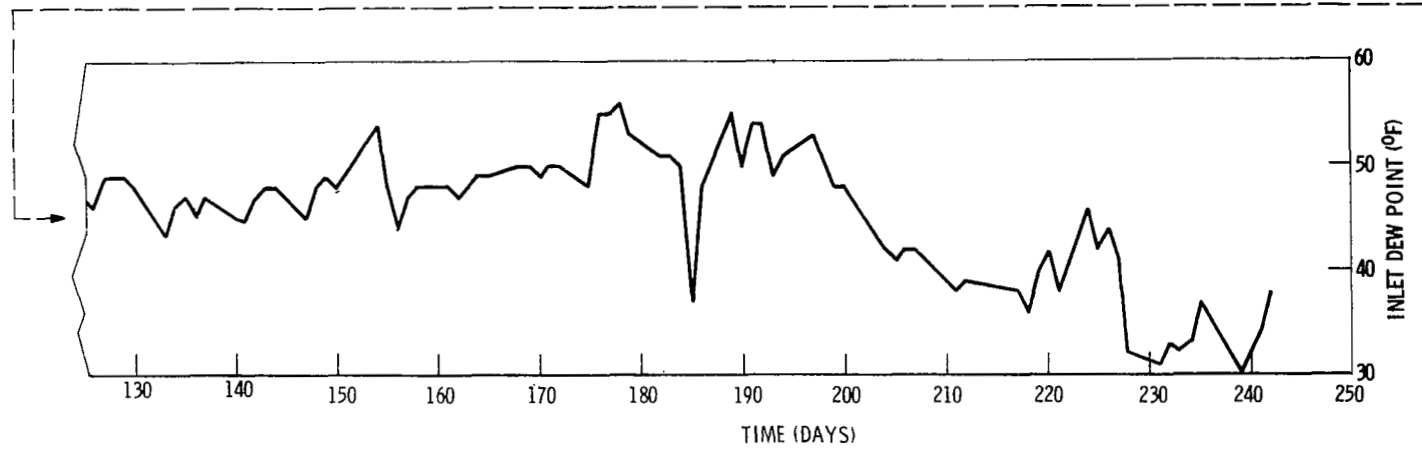


Figure 35 System Dew Point Temperature

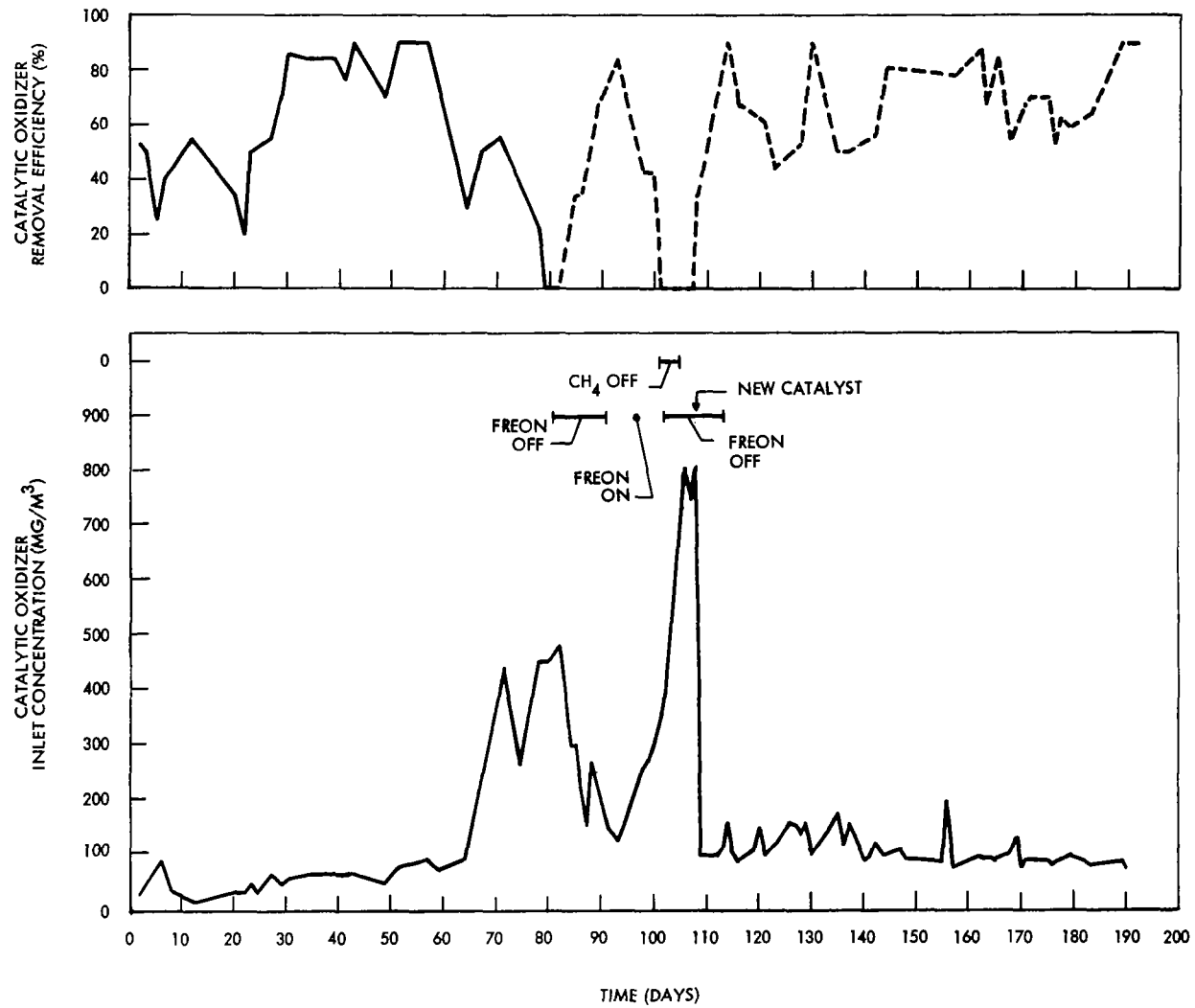


Figure 36 Methane Performance

06

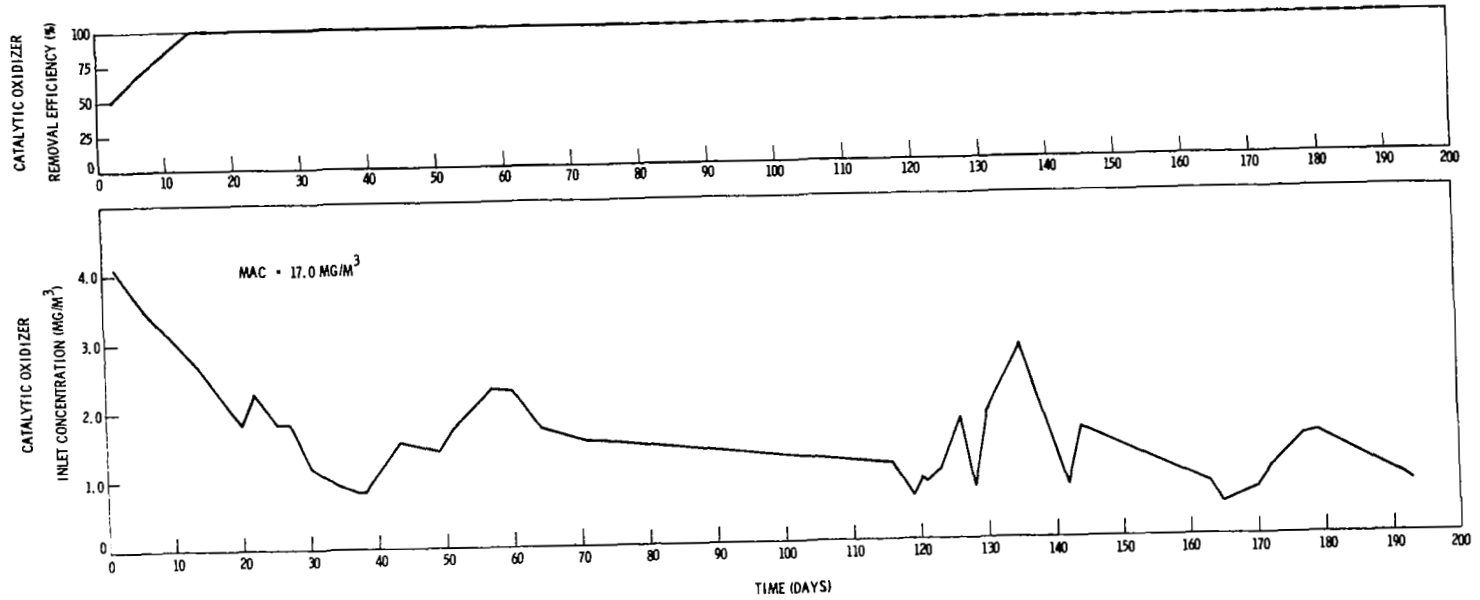


Figure 37 Carbon Monoxide Performance

T6

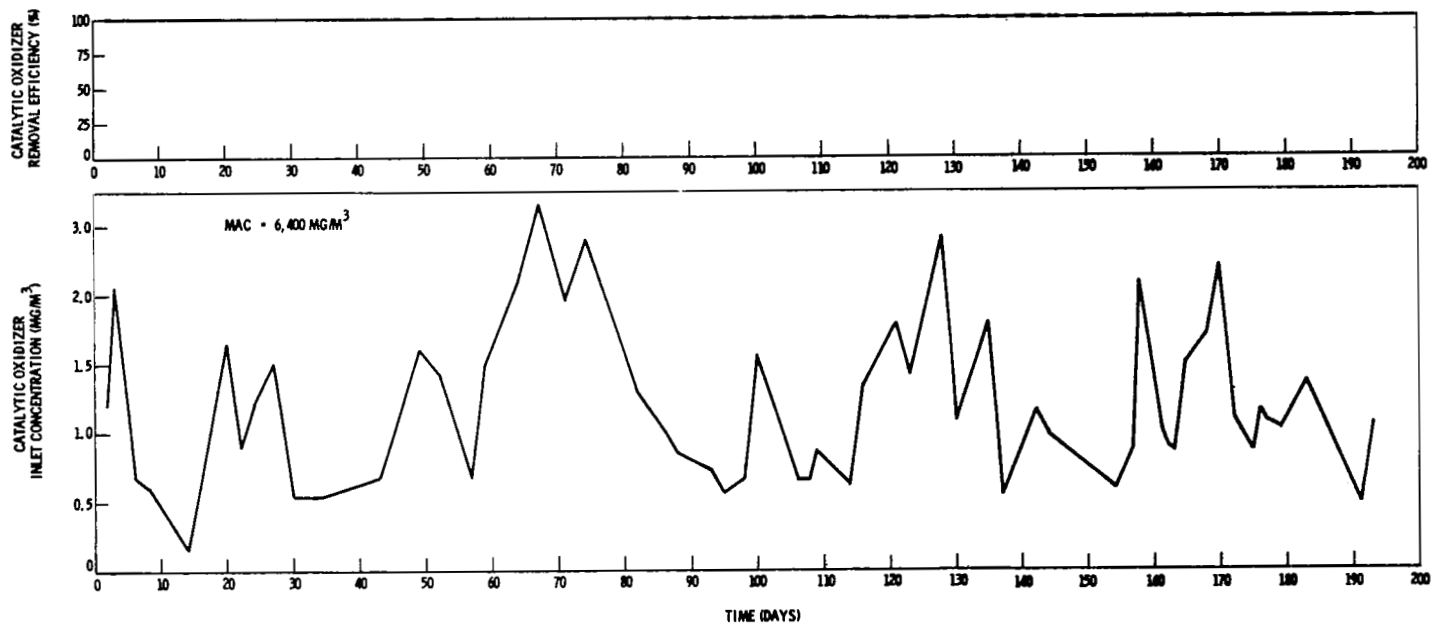


Figure 38 Acetylene Performance

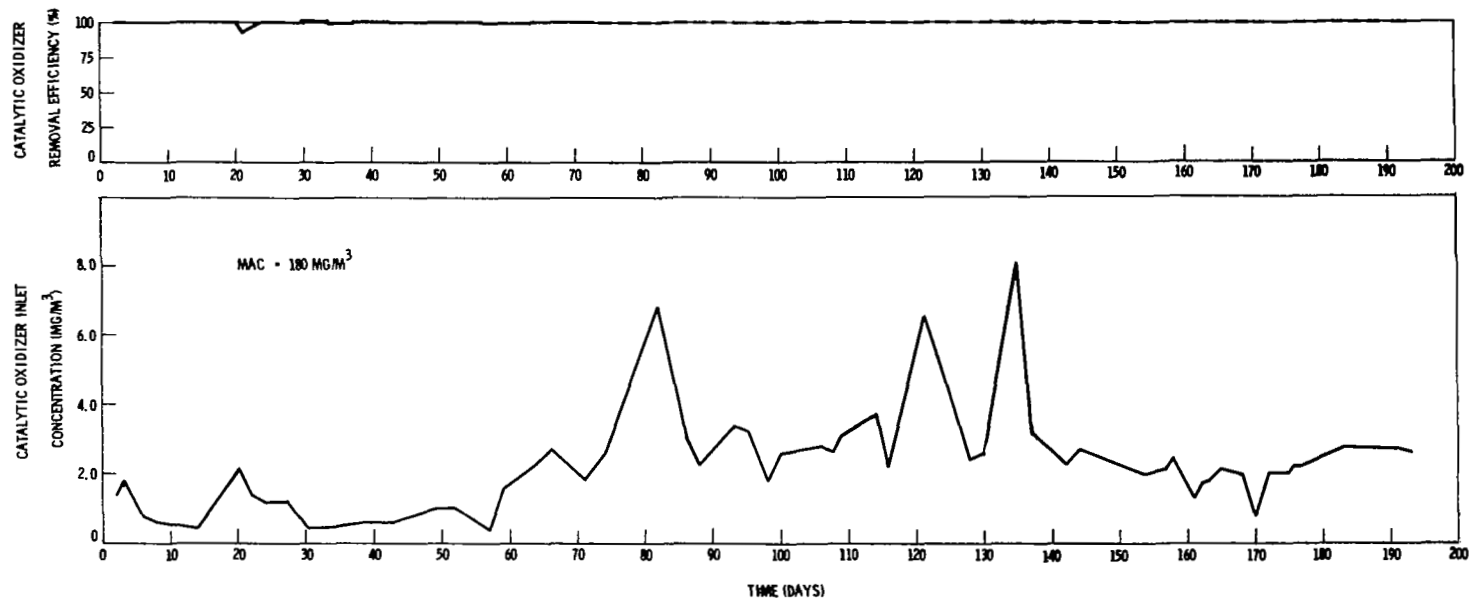


Figure 39 Ethylene Performance

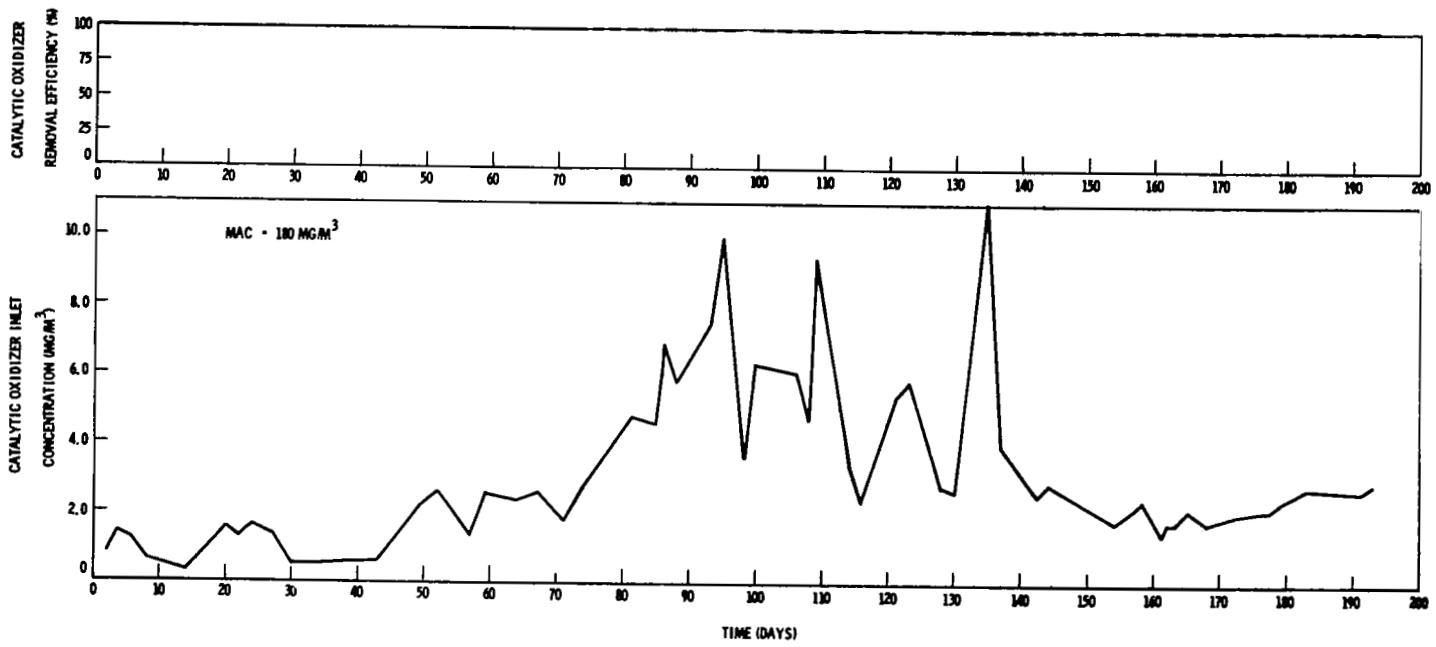


Figure 40 Ethane Performance

t16

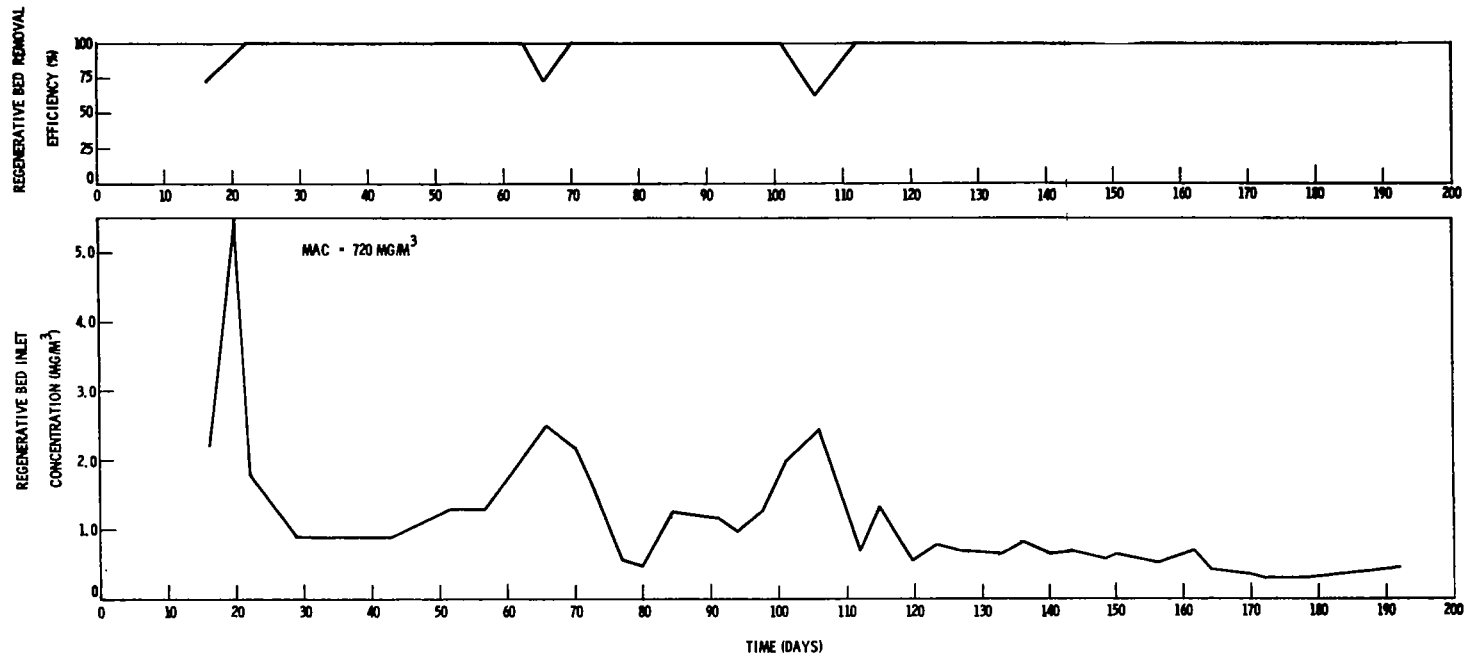


Figure 41 Acetone Performance

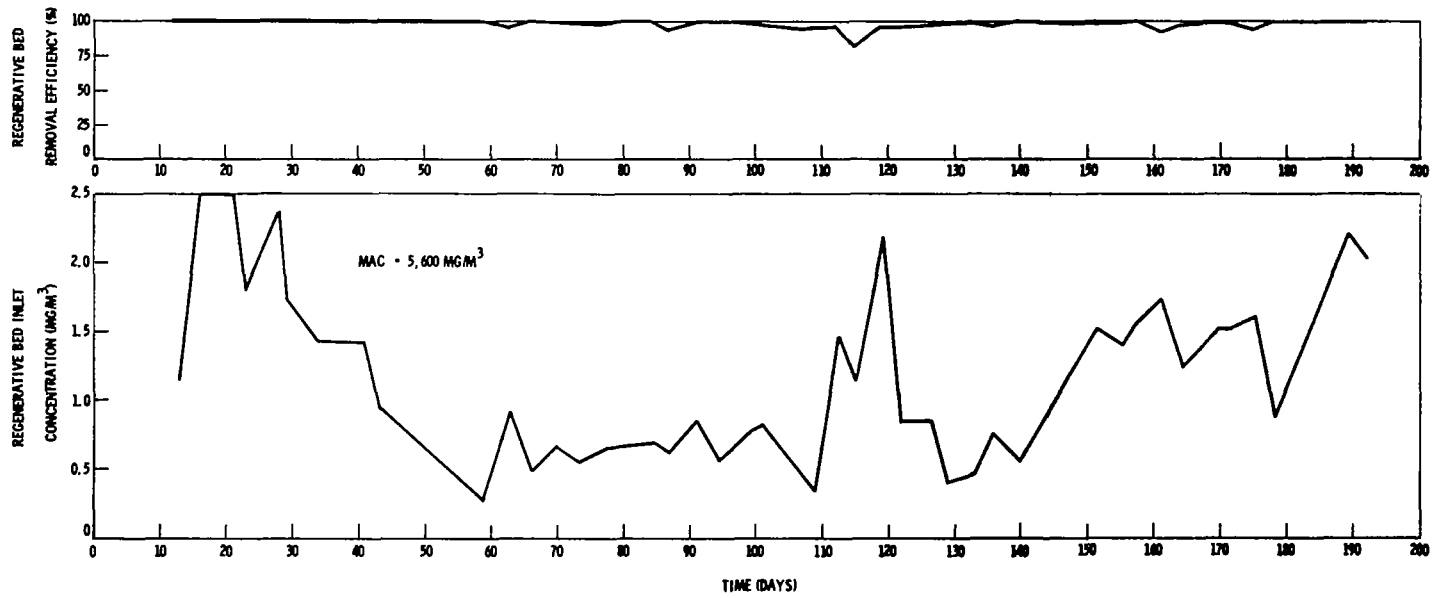


Figure 42 Freon 11 Performance

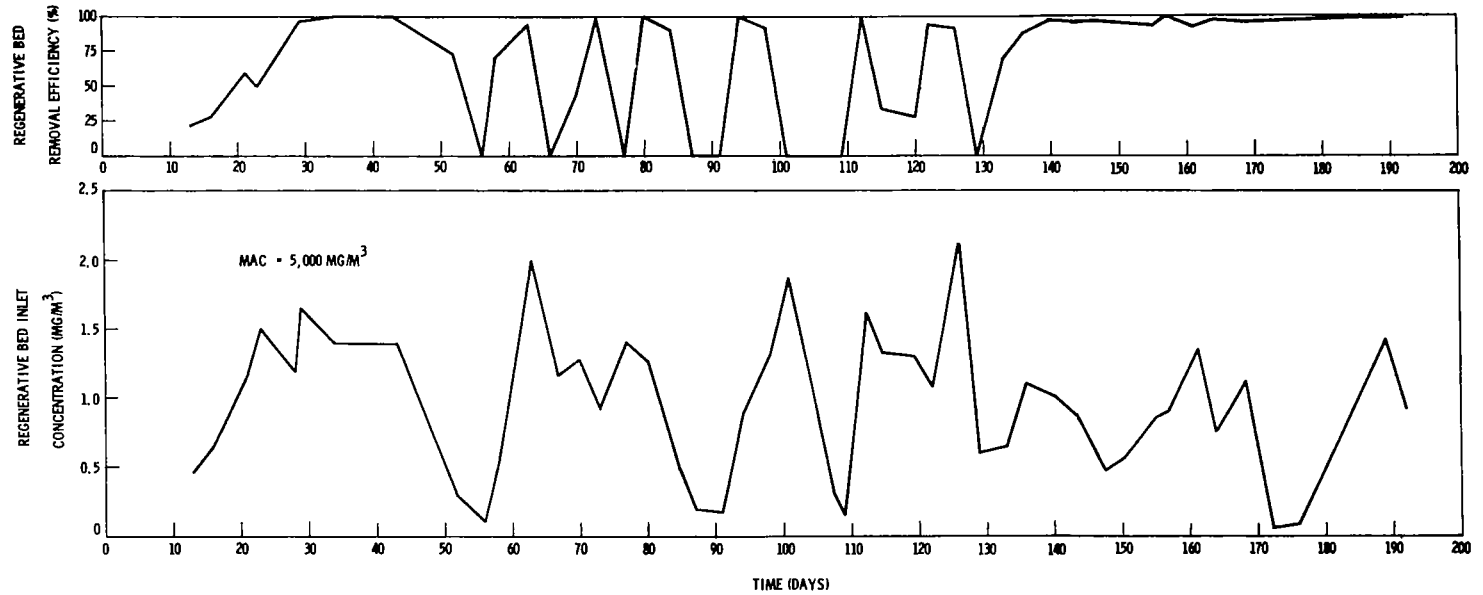


Figure 43 Freon 12 Performance

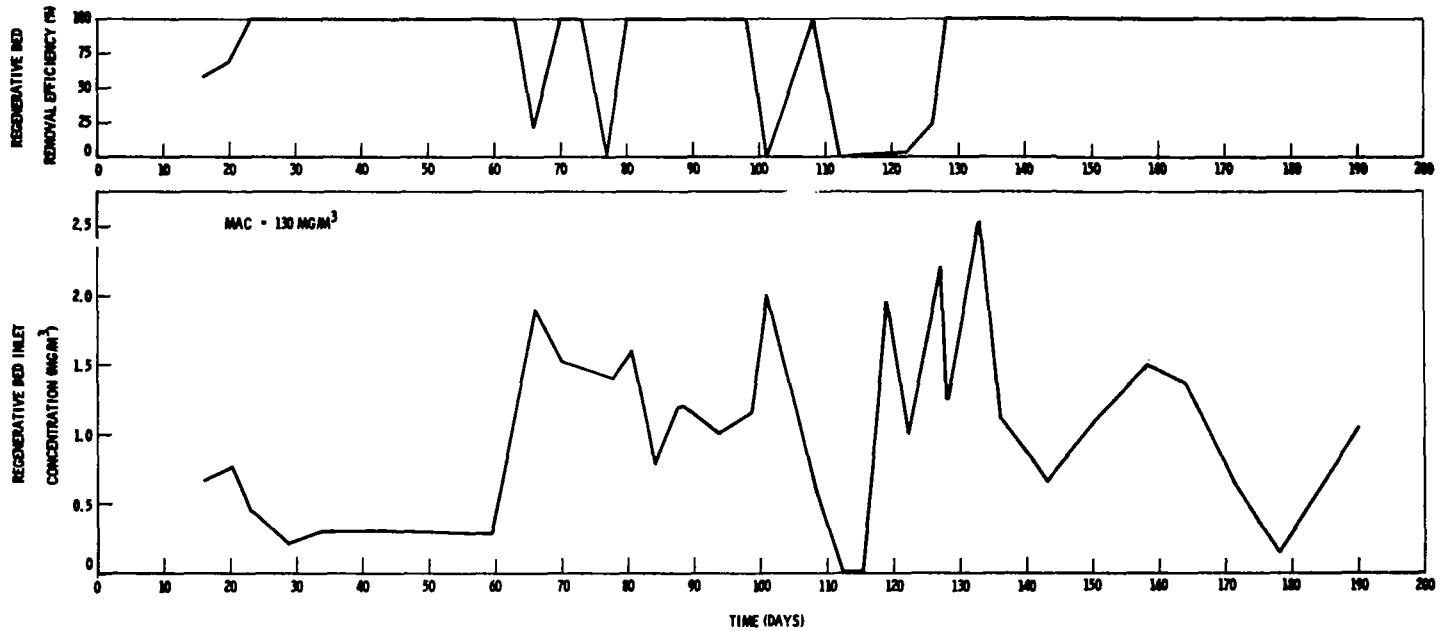


Figure 44 Vinyl Chloride Performance

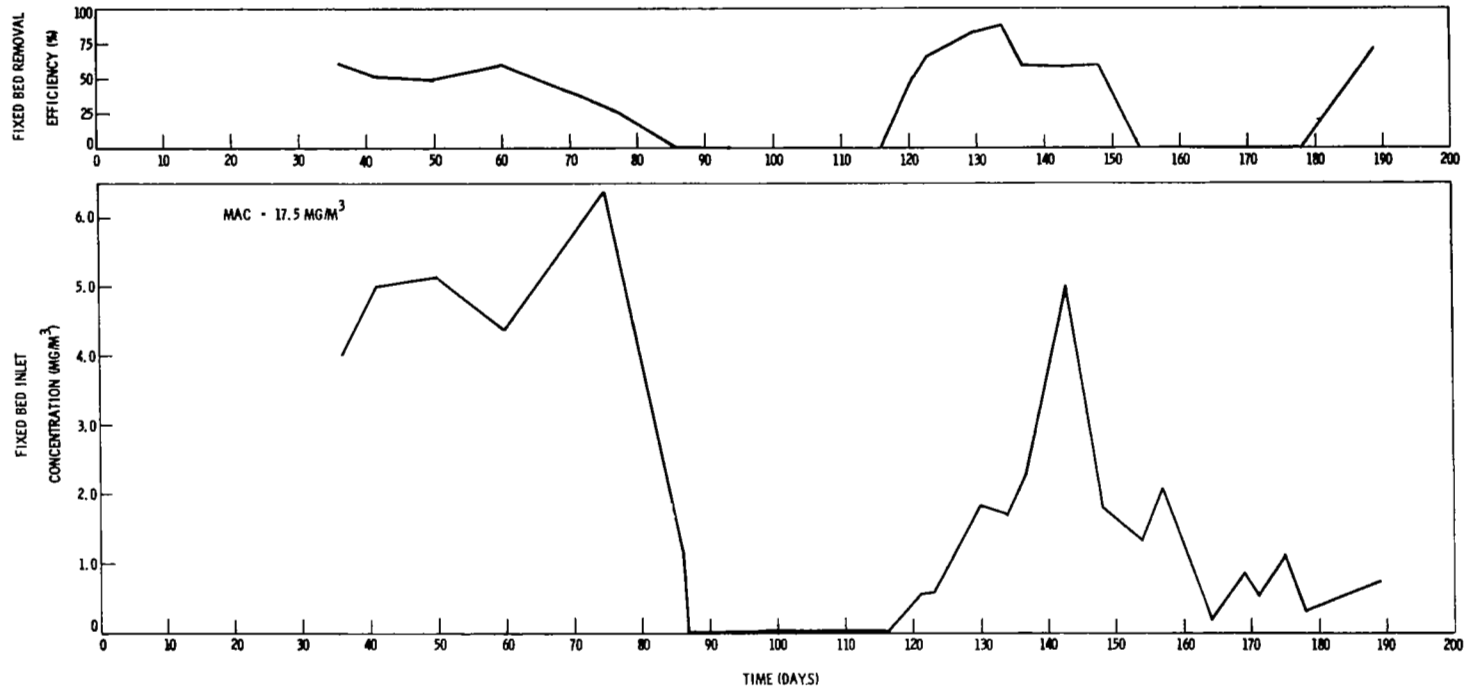


Figure 45 Ammonia Performance

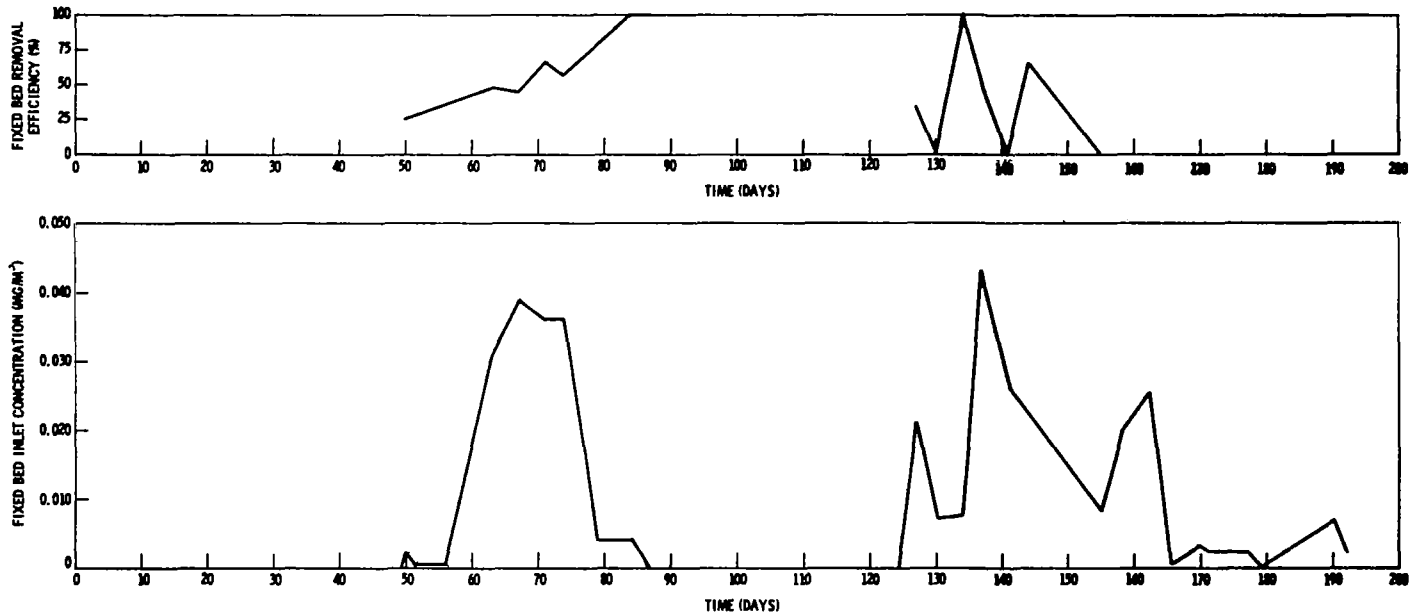
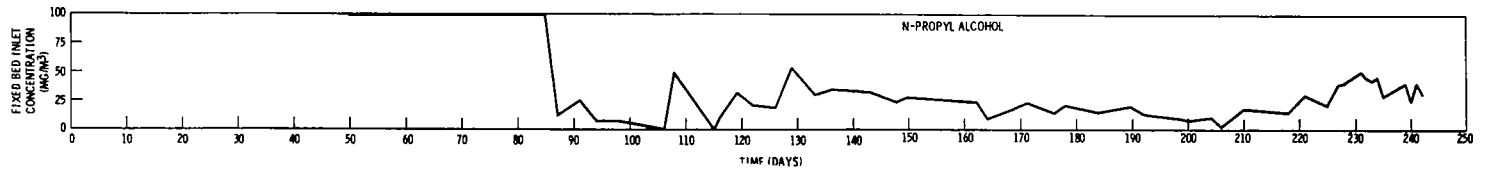


Figure 46 Sulfur Dioxide Performance



001

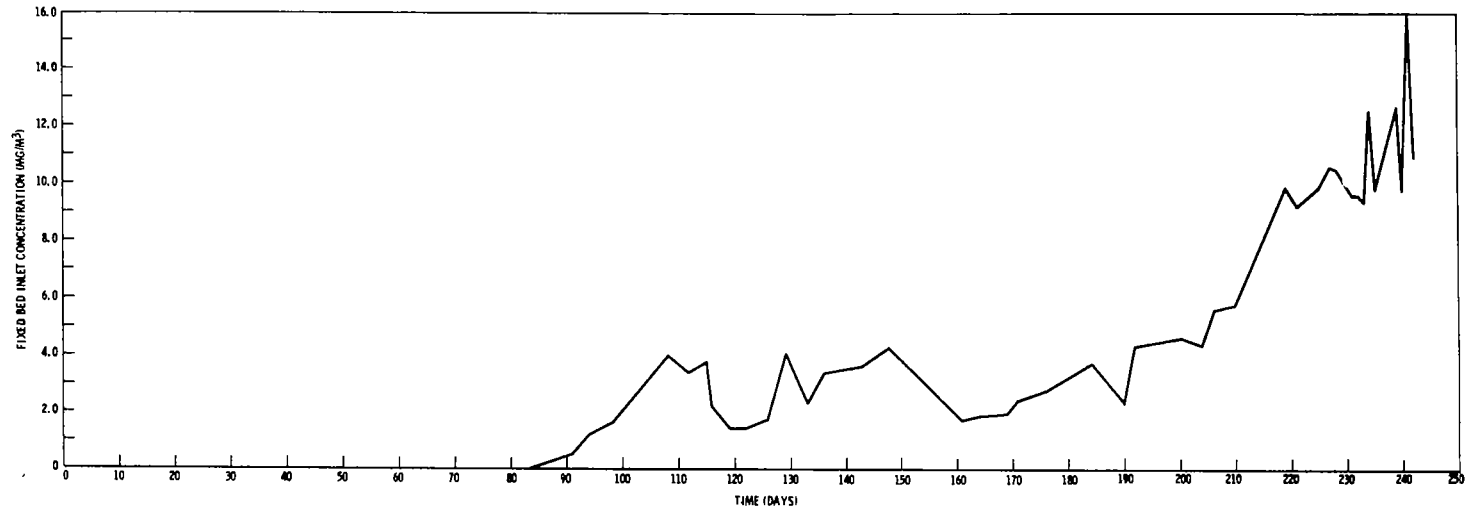


Figure 47 N-Propyl Alcohol Performance

101

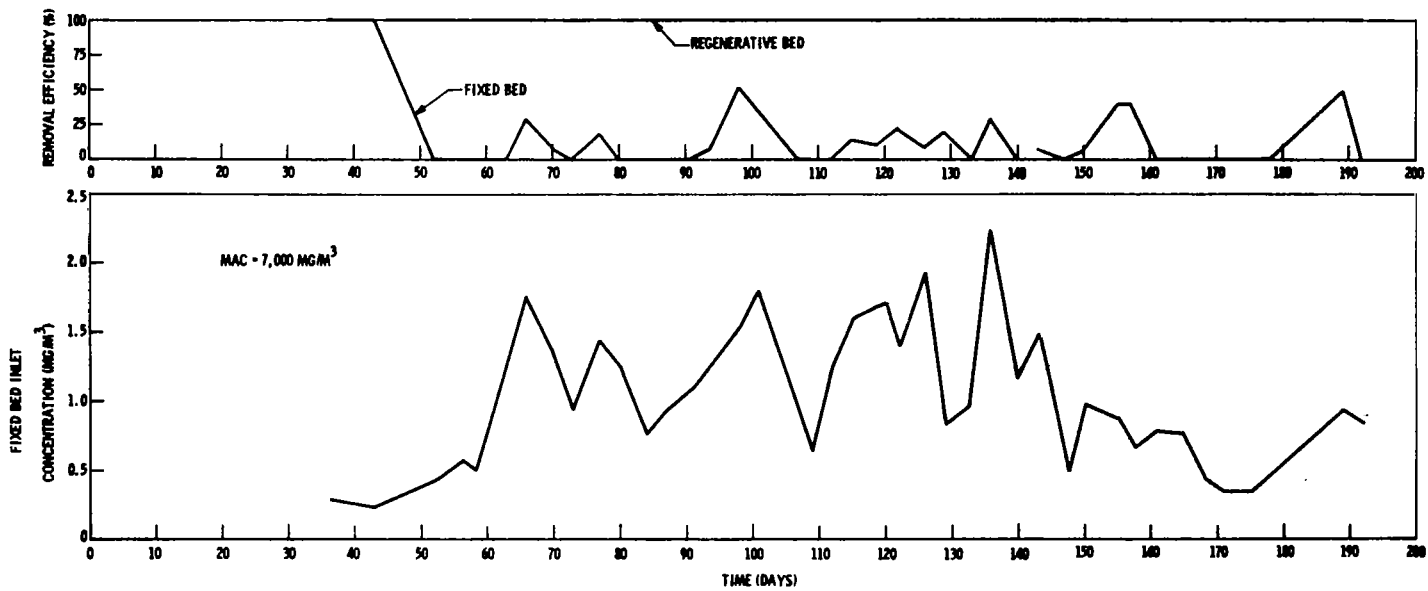


Figure 48 Freon 114 Performance

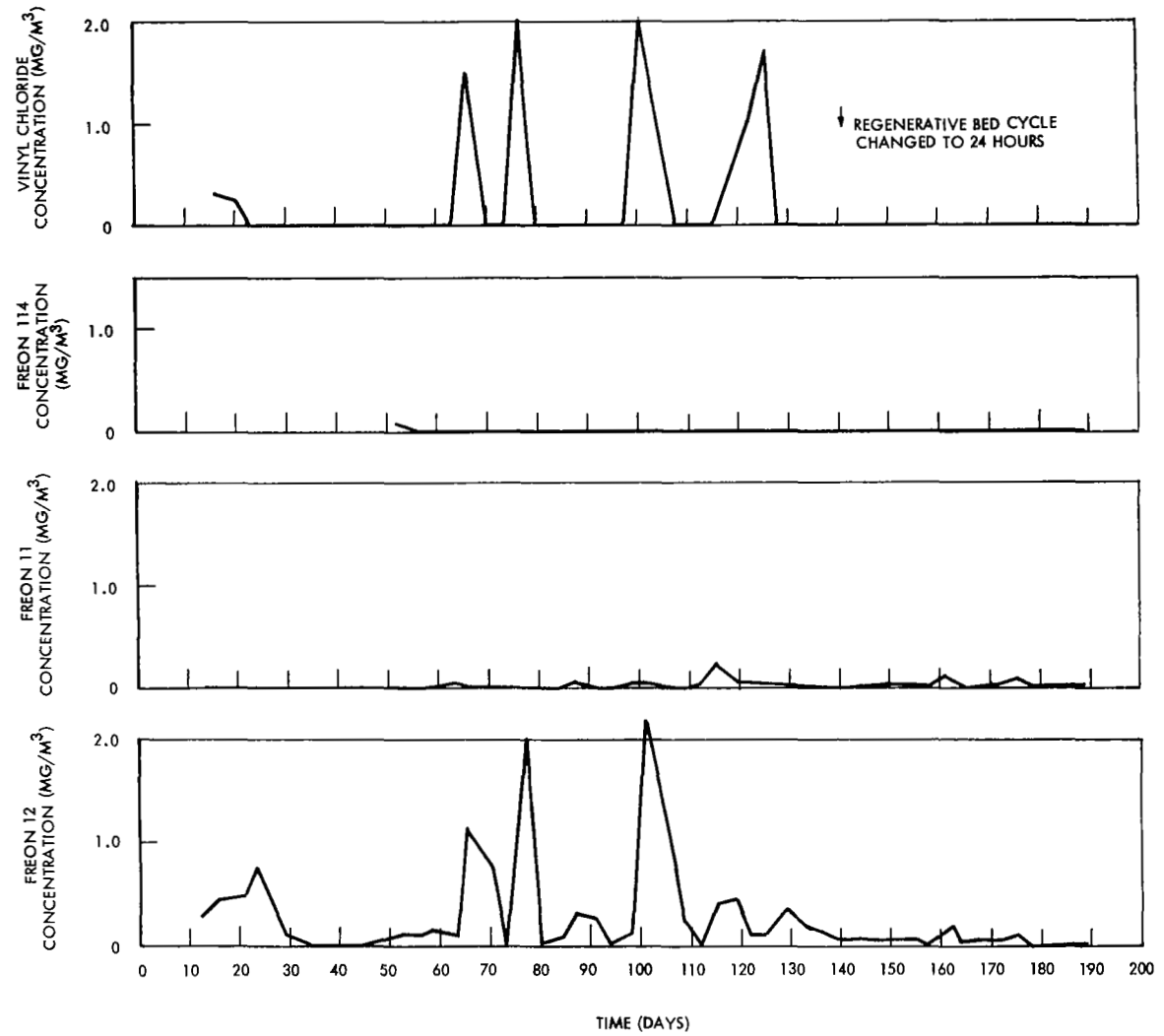


Figure 49 Hydrogenated Hydrocarbon Inlet Concentration to the Catalytic Oxidizer

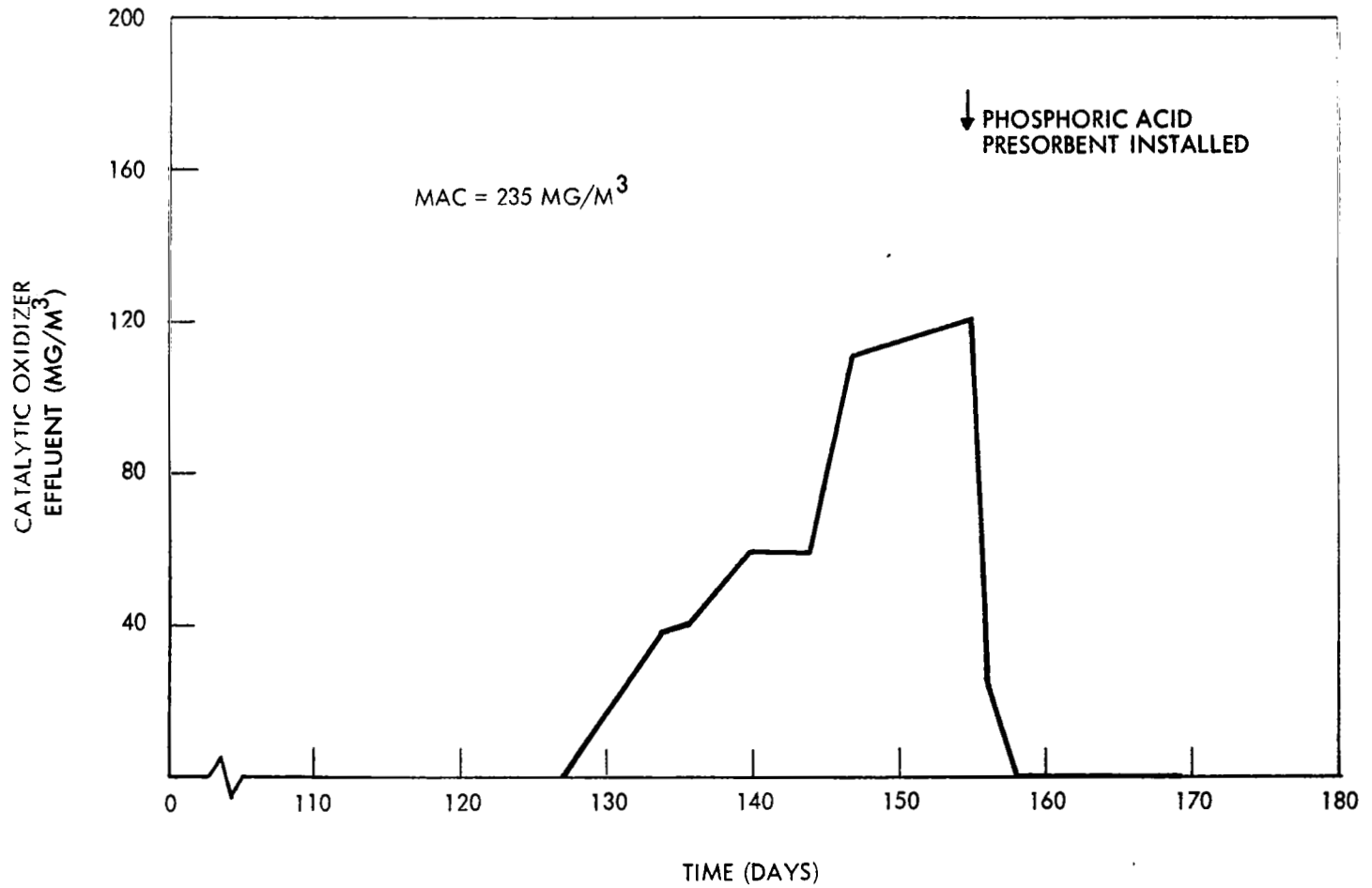


Figure 50 Nitrous Oxide Effluent Concentration from the Catalytic Oxidizer

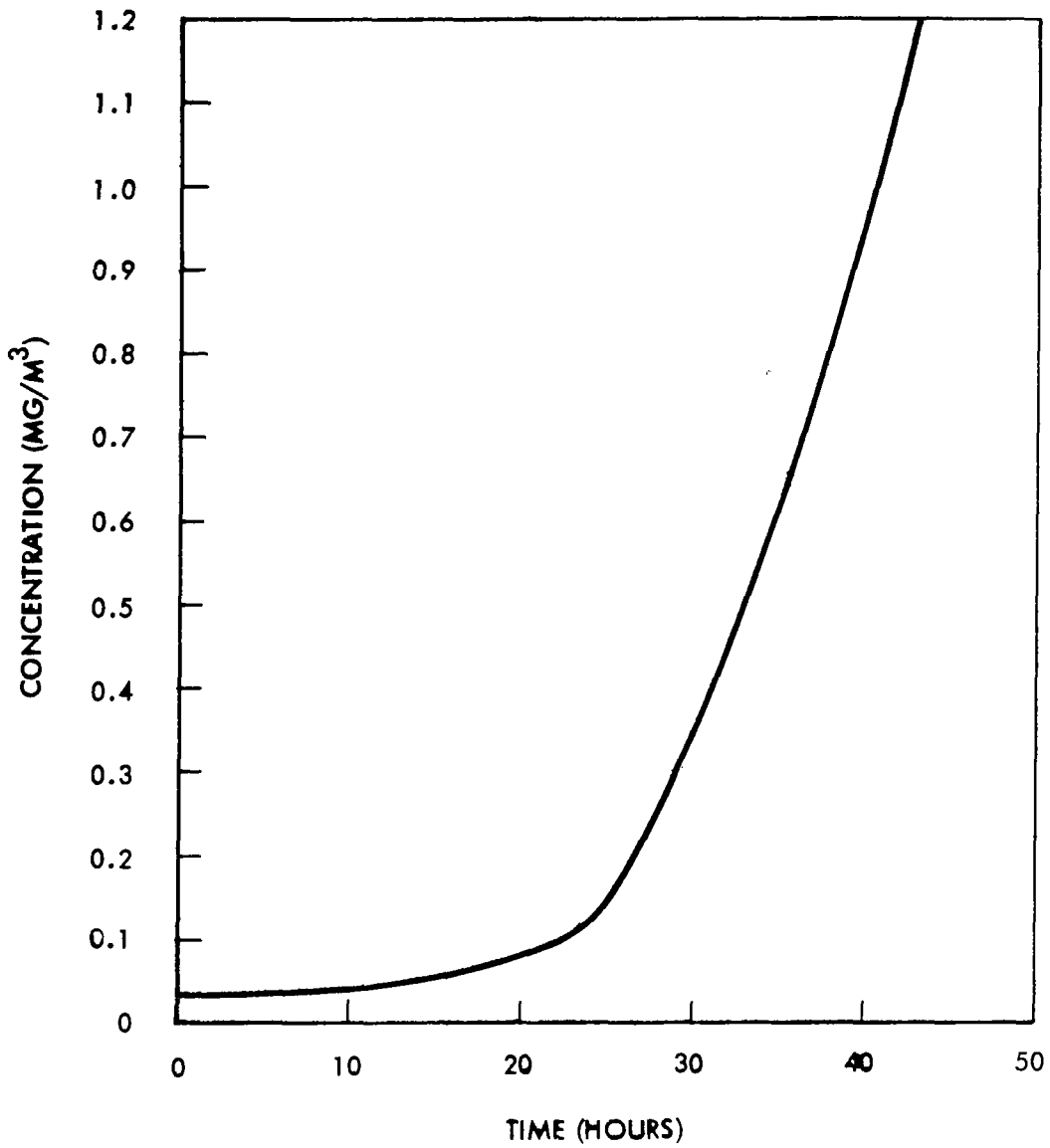
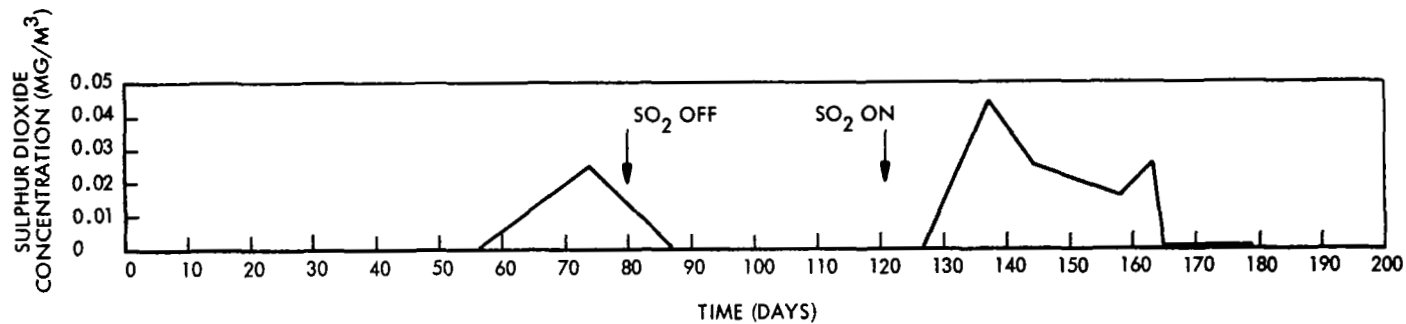


Figure 51 Freon 12 Effluent Concentration from the Regenerative Test Day 141



* Figure 52 Sulfur Dioxide Inlet Concentration to the Catalytic Oxidizer

Figure 36. The efficiency recovered for a brief period and then returned to zero between the 101st and 108th day. On the 108th day of the test, the catalyst was changed and the test was continued through 193 days with the catalytic oxidizer working successfully. The removal efficiency of the other hydrocarbons (acetylene, ethane and ethylene) and carbon monoxide remained at a satisfactory level throughout the test, Ref. Figures 37, 38, 39, and 40.

It was originally suspected that the catalyst poisoning for methane was caused by a failure of the lithium hydroxide bed to adequately control the level of sulfur dioxide entering the catalyst bed. Sulfur dioxide was observed to be entering the catalytic oxidizer at very low concentrations ($\sim 0.03 \text{ Mg/M}^3$) between the 56th and 87th day of the test, Ref. Figure 52. This conclusion was based on the fact that the dew point of the gas entering the lithium hydroxide presorbent was reduced approximately 13°F due to the moisture removed by the regenerative charcoal bed. In an attempt to correct this situation, the lithium hydroxide canister was relocated to a position upstream of the regenerative charcoal bed, where the gas moisture content would be higher. This change was made at the same time the catalyst was replaced. Subsequent observations indicated that sulfur dioxide was still entering the catalytic oxidizer even after relocation of the lithium hydroxide. The inlet concentration of sulfur dioxide to the catalytic oxidizer was still quite low as in the previous exposure. Sulfur dioxide was observed entering the catalytic oxidizer between the 127th and 165th day of the test. During this period of exposure, no catalyst poisoning occurred. However, this fact was not recognized for some time. The recovery of the catalytic oxidizer performance after its replacement was not detected immediately because at the time the catalyst was replaced, a change was made in the gas sampling technique which resulted in erroneously high contaminant concentrations at the catalytic oxidizer exit. This gas sampling error was caused by the use of 500 cc evacuated flasks in lieu of the previously used tight syringe. The evacuated flask was used at this point to increase the sensitivity of the analysis by obtaining a larger sample. The larger sample, however, caused gas to be drawn into the flask not only from the catalytic oxidizer effluent but also from the fixed sorbent

bed exit. This was due to the close proximity and small volume of gas between these two points. This type of sampling error did not occur at other points in the system. By mixing gas from the fixed sorbent bed exit with the catalytic oxidizer exit, a higher catalytic oxidizer exit concentration reading was obtained, resulting in apparent reduced removal efficiencies. Since this error occurred at the same time as a catalyst replacement, it was initially assumed that the new catalyst was also poisoned. The cause of this problem did not become apparent until the 188th day, at which time the analyses were taken with the small volume gas tight syringes. During the period from the time the catalyst was replaced until the sampling error was discovered, a number of different attempts were made to determine the cause of the assumed catalyst poisoning. These attempts included turning various contaminants on and off, adding sorbent beds upstream of the catalyst, and by-passing the regenerative bed. The degree of mixing brought about by the use of the 500 cc evacuated flasks was established, Ref. Appendix C, and then used to correct the removal efficiency data between the period after the catalyst was replaced and day 189. The catalytic oxidizer was operated for another week to confirm the removal efficiency data.

When it was recognized that the catalyst performance was satisfactory following the catalyst replacement that took place on the 108th day, it also became apparent that sulfur dioxide could not be the cause of the catalyst poisoning. Additional investigation revealed that the two periods of catalyst poisoning coincided with periods of high Freon 12 and vinyl chloride inlet concentrations, Ref. Figure 49. The reason that it was not initially recognized that Freon and vinyl chloride were the cause of the catalyst poisoning was that in both instances, when the methane conversion efficiency dropped to zero, it remained at zero for a period of time after the Freon and vinyl chloride concentrations had dropped. This several day lag had not been previously noted.

As can be seen in Figure 50, on test day 127, nitrous oxide was observed in the system. The nitrous oxide concentration continued to rise from this point on. A phosphoric acid impregnated charcoal bed was placed upstream of the catalytic oxidizer on day 154 to ensure that no ammonia would enter the catalytic oxidizer. It was reasoned that oxidation of ammonia appeared to be the most logical source for the nitrous oxide even though previous tests

had indicated no oxidation of ammonia with this catalyst. The nitrous oxide concentration in the system decayed immediately after the phosphoric acid bed was placed at the catalytic oxidizer inlet, confirming that oxidation of ammonia was probably the problem. The reason that previous tests with this catalyst did not reveal any nitrous oxide formation was probably due to the fact that they were open loop tests. In these previous tests, no measurable change in ammonia concentration occurred across the catalyst bed. If, however, a slight oxidation of ammonia occurred and the system was closed as this system was, then the product of oxidation would build up in concentration. This is what occurred in this test, and by the 127th day a measurable concentration of nitrous oxide was reached. No additional nitrous oxide was observed after the phosphoric acid impregnated charcoal was placed at the catalytic oxidizer inlet.

Regenerative Bed

The regenerative bed was operated for 193 days. During this period of time there were only two changes in the operating parameters. The first of these changes was on the 60th day when the desorption time was increased from 2 to 3 hours. This was done because the bed temperature at the end of the desorption cycle had dropped below 200°F due to a planned increase in system dewpoint and hence an increased charcoal moisture load. Therefore, additional time was provided to heat the bed to the desired temperature.

The removal efficiency for acetone and Freon 11 remained at 100% throughout the test with the exception of one or two occasions where partial breakthrough occurred, Ref. Figures 41 and 42. Vinyl chloride and Freon 12 breakthrough was also noted occasionally near the end of the regenerative bed cycle, Ref. Figures 43 and 44. Since the sampling period was random, causing samples to be taken at the beginning of a new bed cycle and some samples to be taken near the end of the cycle, it was decided to make a careful survey of the regenerative bed outlet concentration as a function of time.

The results of this analysis, presented in Figure 51, which was conducted on the day 141 indicated that the outlet concentration from the bed remains at less than 5% of the inlet concentration for the first 24 hours of the cycle. After this, the outlet concentration rises rapidly with complete breakthrough occurring after 48 hours. Based on these data, it appeared that better protection

of the catalyst could be obtained by changing the cycle time to every 24 hours. This change was made on the 141st day, and no contaminant breakthrough was subsequently observed.

Fixed Bed

The fixed bed was operated for 240 days. N-propyl alcohol which was used to model pyruvic acid in the model system test was removed by the fixed bed at a 100% removal efficiency until the 85th day of the test, Reference Figure 47. At that time, the removal efficiency decayed to about 25% and the system concentration rose to a value somewhere between 1 and 4 Mg/M³, where it remained until about test day 200. After test day 200, the concentration of n-propyl alcohol increased again, reaching a value of 10.0 Mg/M³ on test day 219. It continued at about this level until test day 227. At this point in the test, it was decided to reduce the flow rate through the main sorbent bed to establish the effect on the removal efficiency and removal rate of n-propyl alcohol.

It was suggested that the initial determination in adsorption zone length for the fixed bed was in error and a modification was made in the system flow rate to attempt to verify this conclusion. Since the adsorption zone length is a function of velocity, variations in system flow rate would alter the bed velocity and hence the adsorption zone length. The fixed bed design is based on an adsorption zone length of 1.0 inch and a saturated layer 7.0 inches in length, and hence the predominant portion of the bed (86%) is devoted to the saturated layer. It was reasoned that if these lengths were correct, then a significant decrease in the adsorption zone length, brought about by a decrease in velocity, would probably not cause a major change in performance of this point in time. On test day 227, the flow rate through the fixed bed was decreased by a factor of 4. The result of this change was approximately a two-fold increase in removal rate indicating that a significant portion of the bed must be devoted to the adsorption zone. These results, though entirely qualitative in nature, were conclusive enough to prompt additional analytical investigation into the possibility that the adsorption zone length was in error. These investigations resulted in a quantitative confirmation of this fact and are discussed in detail in a subsequent section.

Breakthrough of Freon 114 through the fixed bed was also premature indicating that the initial capacity or adsorption length, data for insoluble contaminants was in error. This, however, had no impact on the system configuration since none of the insoluble contaminants require more than 3 CFM for control and thus adequate removal is provided by the regenerative bed as was the case for Freon 114 during this test. The regenerable bed removal efficiency for Freon 114 was 100% throughout the test.

Sulfur dioxide was controlled satisfactorily throughout the test. The data on removal efficiency per pass was erratic, as can be seen in Figure 46. However, the average system sulfur dioxide concentration remained in the neighborhood of 0.025 Mg/M^3 and did not show an increasing or decreasing trend. This concentration is equivalent to a removal efficiency per pass of approximately 15%. Sulfur dioxide input to the system was terminated on the 193rd day of the test.

Ammonia removal by the fixed bed was satisfactory during the first 75 days of the test, Ref. Figure 45. During the period between the 75th and 105th day, the removal efficiency dropped and the system concentration rose to 12.0 Mg/M^3 . At this time, the ammonia was turned off for a few days while problems with the catalyst were being investigated. When ammonia introduction was resumed, the system concentration varied between 1.5 and 4.0 Mg/M^3 for the remainder of the test. The removal efficiency data was erratic; however, the system concentration did not show an increasing or decreasing trend. The removal efficiencies corresponding to the system concentrations of 1.5 and 4.0 Mg/M^3 are 80 and 30%. These efficiencies are more than adequate for ammonia removal. The allowable concentration for ammonia is 17.5 Mg/M^3 . Thus, it can be concluded that the selected quantity of phosphoric acid impregnation of the charcoal provides adequate ammonia removal.

MODIFICATIONS TO THE DESIGN PROCEDURE

In reviewing the data of the model system test, it appears that the proposed design methodology requires modification to account for the required increase in the regenerative bed cycle time and the premature breakthrough of Freon 11 and n-propyl alcohol in the fixed bed. The test results were reviewed and it was subsequently concluded that a single modification to the procedure could correlate all of the experimental observations.

The first step in this investigation was to determine if the performance variation was related to the adsorption zone or the saturated layer. The saturated layer portion of the charcoal bed was considered initially in the event that the potential plot capacity data could have been in error. However, an examination of the potential plot revealed that no reasonable shift in the potential plot line could explain the discrepancies observed in the test. Furthermore, the potential plot data have been confirmed by numerous experimental investigations and hence, is not likely to be in error by a significant amount.

An examination was then made of the data and procedure used to establish the adsorption zone length and the following conclusions were reached. As discussed previously, the adsorption zone length (I) defined by I. M. Klotz, can be expressed as:

$$I = I_t + I_r$$

Where I_t is a function of the diffusion rate of adsorption molecules from the gas stream to the carbon surface and I_r is a function of processes occurring within the pores of the carbon. Klotz further stated that for high molecule weight vapors $I = I_t$ with little contribution from I_r while for lighter molecules, it is small relative to I_r . Since it varies as $U^{0.4}$ (where U equals velocity), and I_r varies as $U^{1.0}$, then the adsorption zone varies somewhere between $U^{0.4}$ and $U^{1.0}$. The experimental data taken by MSAR on adsorption zone length was taken at a linear velocity of 1.3 ft/min and the selected designs utilized different velocities, therefore, the data on adsorption zone length had to be corrected. A velocity correlation of $U^{0.5}$ was utilized, since this best fits MSAR experimental evidence to date.

Examination of the long-term test results, however, reveals that a different exponent would have provided a better correlation.

In reviewing the data for the regenerative bed, Table 11, it can be seen that the saturated layer was approximately 50% of what was originally anticipated, since the cycle time had to be increased from 48 hours to 24 hours.

Table 11
Zone Lengths for the Regenerative
Bed Based on Freon 12 Performance

<u>Length</u>	<u>Anticipated</u>	<u>Actual*</u>
Saturated Layer	8.5 inches	4.25 inches
Adsorption Zone	1.5 inches	5.75 inches
Total	10.0 inches	10.0 inches

*Based on full size bed.

This meant that the adsorption zone was 5.75 inches instead of the originally anticipated 1.5 inches. Based on this data, a velocity correlation of $U^{1.0}$ provides close agreement with the original MSAR adsorption zone length data.

Reviewing the fixed bed data in Figure 47, it can be seen that n-propyl alcohol broke through after 35 days of n-propyl alcohol introduction at which time the removal efficiency remained near 25% gradually diminishing. This indicates that the saturated layer was only 1.36 inches in length as opposed to the originally anticipated 7.0 inches. As can be seen in Table 12, this results in an adsorption zone length of 6.64 inches. Utilizing this adsorption zone length and referring to the MSAR adsorption zone length data, a velocity correlation factor of $U^{1.0}$ was confirmed.

Table 12
Zone Lengths for the Fixed Bed Based
On N-propyl Alcohol Performance

	<u>Anticipated</u>	<u>Actual</u>	<u>Corrected for Final Design</u>
Saturated Layer	7.0 inches	1.36 inches	7.0 inches
Adsorption Zone	1.0	6.64 "	6.64 "
Total	8.0	8.0 "	13.64 "

Consideration of the Freon 114 data indicates the following: Freon 114 breakthrough occurred almost immediately, as can be seen in Figure 48, indicating that the entire bed was required for the adsorption zone. Utilizing a velocity correlation factor of $U^{1.0}$ and the MSAR adsorption zone data, an adsorption zone length of 9.0 inches for Freon 114 was obtained which is in excess of the 8.0 inch bed length and confirms the initial breakthrough of Freon 114.

Thus it can be concluded, based on the regenerative bed and fixed bed test results that the design procedure should be modified to utilize a velocity correlation factor of $U^{1.0}$ in determining adsorption zone lengths. This is a general agreement with the theory of Klotz who postulated that for lighter weight molecules, the adsorption zone length is predominantly controlled by I_r which is a function of $U^{1.0}$ power. The impact of this change on the system design would be a modification in the cycle time of the regenerative bed from 48 hours to 24 hours as stated previously, and a modification in the length of the fixed bed. The details of the fixed bed modification are presented in Table 11. Since the required saturated layer of the fixed bed is 7.0 inches in length and the experimental data indicated that the adsorption zone length is 6.64 inches in length, the total bed length is then 13.64 inches. No additional modifications need to be made to the fixed bed to account for the increased adsorption zone length for Freon 114 since the 13.64 inch total length would provide over 4 inches of saturated layer for this contaminant which is more than adequate.

The long term test results indicated a need to control the level of ammonia entering the catalytic oxidizer. This was due to the observed formation of nitrous oxide when ammonia was allowed to enter the catalytic oxidizer. Eliminating ammonia from the catalytic oxidizer inlet during the test stopped the formation of ammonia.

In the selected system, the high flow (76 CFM) fixed bed and the low flow (3 CFM) components are in parallel paths. This was done to provide greater flexibility in system arrangement and to eliminate the need to pass the high flow rate through a pressure drop equivalent to that of the low flow components

which would be required in a series arrangement. In the parallel arrangement, the regenerative charcoal bed does not have the protection of the fixed sorbent bed and thus, the size of the regenerative bed was increased to accommodate contaminants not amenable to desorption that would be controlled by the fixed bed in a series arrangement.

The quantity of charcoal required for this is approximately 1 pound. This same quantity of charcoal impregnated with phosphoric acid to the same level as the fixed bed (2 millimoles of phosphoric acid per gram of charcoal) would provide adequate protection for ammonia entering the catalytic oxidizer. Thus, it is recommended that in the final design that the first 1# or 20% of the regenerative charcoal bed be impregnated with phosphoric acid. MSAR experience indicates that no problem exists in exposing the phosphoric acid to the regeneration conditions of temperature and vacuum.

SYSTEM DESIGN

The following sections describe the design characteristics of the catalytic oxidizer, the pre- and post-sorbent beds, the fixed bed and the regenerative bed.

Catalytic Oxidizer

The catalytic oxidizer assembly is shown in Figure 53. The catalytic oxidizer is 14.50 inches long, excluding end fittings, and 7.62 inches in diameter. The weight of the unit is approximately 20.9 lb. The unit consists of an outer shield, molded insulation, and an inner body. The inner body is made up of a regenerative heat exchanger, catalyst canister and radio-isotope heat source.

The regenerative heat exchanger is a 5-pass cross-counter flow, stainless steel plate fin heat exchanger. The cold end is bolted to one end of the cylindrical aluminum shield. The hot end of the heat exchanger terminates in a machined flange that mates with the catalyst canister. The gas ports are sealed with Parker metallic face seals. This heat exchanger has a very small fin and parting sheet thickness to reduce core conduction losses. In addition, the fin height is very low to obtain high heat transfer coefficients. The center fin passage on the cold side is 0.146 inches high which allows for the passage of instrumentation leads through the heat exchanger. This eliminates the requirement for high temperature electrical penetrations into the catalyst canister. Sintered metal plates are provided at the cold outlet and hot inlet cone face to assure good flow distribution.

The catalyst canister is a cylindrical unit that contains the 0.5 percent palladium catalyst and the radioisotope heat source. The catalyst is easily replaceable from the end opposite the heat exchanger by unbolting the end of the shield, removing the insulation section, unbolting the end of the catalyst canister, removing the screens and pouring the catalyst out. New catalyst can then be put in the unit and the unit reassembled in the reverse order. The catalyst canister body is furnace-brazed and entirely constructed of

nickel. The radioisotope is mounted in the center of the catalyst canister where it is supported by posts projecting from either end of the isotope source. One post is slotted and held in place with a key to prevent rotational movement of the isotope heat source. The other post is cylindrical, and fits into a socket located on the end of the catalyst canister away from the heat exchanger. Axial movement is limited with a Belleville spring placed in this socket. This spring also allows for thermal expansion of the isotope. Straight fins are provided on the isotope heat source to control the maximum isotope heat source temperature.

The isotope heat source consists of the following components: liner, strength member, cladding, reentry member, and structural module. The liner provides a compatible container for the fuel. The strength member provides protection during impact and contains the pressure caused by the helium buildup. Cladding is provided for oxidation protection. A pyrolytic graphite shell provides aerothermal reentry protection. The structural module which contains the radial fins provides oxidation protection and heat transfer surface area.

The catalyst material is located in eight compartments located between the fins of the isotope heat source. A perforated steel plate and screen is placed at one end of the catalyst compartment and a screen is located at the other end to prevent the catalyst material from entering the heat exchanger. A machined cover is located at the end of the catalyst canister away from the heat exchanger to provide access to the isotope heat source and catalyst material. This flange is held in place with bolts and sealed with a Parker metal face seal.

The entire area between the inner body and the shield is filled with molded insulation (Johns Manville Min-K 1301). The insulation is molded in five pieces; four half-cylindrical sections to insulate the catalyst canister and the heat exchanger, and one to insulate the catalyst canister cover.

The aluminum outer shield separates at the catalyst cover and canister plane to allow access to the insulation and inner body of the unit. The aluminum outer shield is also attached to the cold end of the regenerative heat exchanger. The shield is painted white to provide a high emittance, and thus reduce its surface temperature.

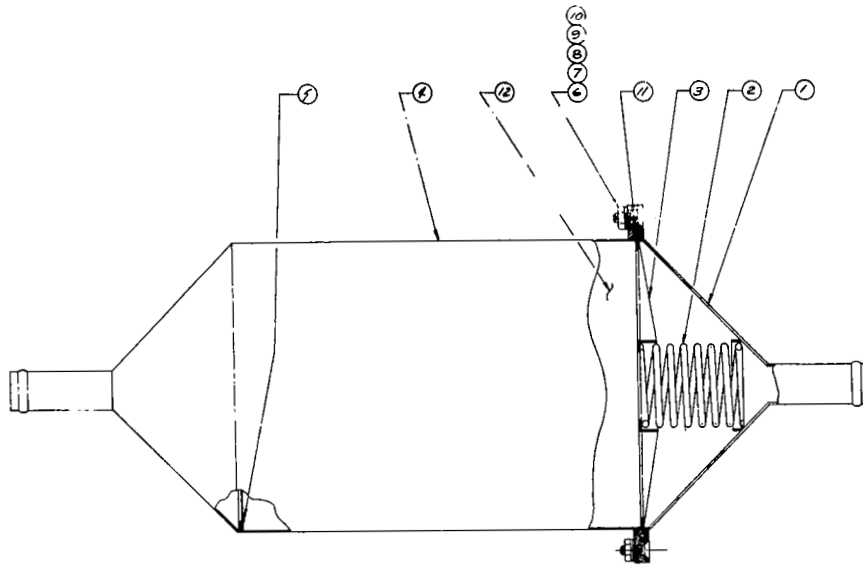
Fitting ends on the cold end of the regenerative heat exchanger are per MS33666-12, for tube connections. An electrical feed-through is also located at the cold end of the heat exchanger for instrumentation leads and for the electrical leads of the optional electrically heated simulated isotope. The instrumentation and electrical leads pass through the inlet gas passage of the regenerative heat exchanger. Instrumentation consists of recording gas temperatures at the inlet of the catalyst bed and the isotope surface temperature.

Pre- and Post-Sorbent Canisters

The pre- and post-sorbent canisters are shown in Figures 54 and 55. The units are constructed of 321 stainless steel and consist of a cylindrical body with a flange, housing an "O" ring seal on one end and a 45° cone outlet duct on the other end; a flanged 45° cone inlet duct is used for the cover. The flange on the cover mates and is bolted to the flange on the body. A 235 mesh screened ring is located in the outlet end of the body to retain the sorbent in the body. A screened ring backed by a compression spring is used to compress the sorbent material and keep it from channeling. The spring is compressed between the cover on one end and the screened ring and sorbent material on the other end. The mated sealing flange is used as a mounting ring.

Fixed Bed

The fixed bed assembly presented in Figure 56 consists of a 14 x 17 inch diameter shell with 45° conical ends, a 12 x 12 mesh stainless steel screen assembly at each end of the sorbent bed and a 100-pound spring acting against one of the screens to maintain compression on the sorbent material. The outlet end is bolted to the body through flanges and a silicone rubber gasket,



2. RECOMMENDED VENDOR 100% MINERAL
 CO. EXTON PENN.
 1. INSTALL FASTENERS PER IAC-0581
 NOTE:

CHANGE EFFECT		REVISION	
NO.	DESCRIPTION	NO.	DESCRIPTION

QTY REQD	CODE POINT	PART OR IDENTIFYING NO.	NOMENCLATURE OR DESCRIPTION	REMARKS OR NOTE	SPECIFICATION	ZONE	ITEM NO.
2			"SORBENT"	L10H	EMS SWS		12
1		2-162	"D" RING	SANDWICH PLATE MIL-M-8887 SPECIFIED SIZE 2	ARMORER SERIAL CO CULVER CITY OHIO		11
1/6		LS8889-3	NUT				10
1/6		MS3523-73	LOCK WASHER				9
1/6		HW60C10C	WASHER				8
8		LS87175-10	SCREW				7
8		LS87175-5	SCREW				6
1		BE100-24-305	SCREW/COVER				5
1		BE100-23-305	BODY				4
1		BE100-22-305	COUNTERSINK PLATE				3
1		BE100-21	SAFING				2
1		BE100-20-305	COVER				1

LIST OF MATERIAL OR PARTS LIST

INTERPRET THIS DRAWING PER STANDARDS IN MIL-C-12227	DATE 10/14/88	POST-SORBENT CANISTER IACOS
UNLESS OTHERWISE SPECIFIED	DR 12 W/14	
TOLERANCES UNLESS OTHERWISE SPECIFIED	DIMS ± .015 DIA ± .010 ANGLES ± .5°	
FINISH SURF STRENGTH WELDING QUALITY	CHECKED SUPPLY APPROVED	
NEXT AMBY APPLICATION	USED ON REQ/AMBY	CODE POINT NO. 06887 D DRAWING NO. BE100-25 SHEET 1 OF 1

Figure 55 Post-Sorbent Canister

and terminates in a 3.0 inch diameter tubing end. A 400-cycle, 115 VAC, 1-phase blower is flange-mounted to the inlet end and will deliver 76 scfm air at 2.0 inches of water pressure. The sorbent bed is 56 pounds of 4 x 6 mesh activated charcoal. Mounting provisions for the assembly are incorporated in the body flange.

Regenerative Bed

The regenerative bed, presented in Figure 57, contains a thermally insulated housing, screens at each end of a sorbent bed, an electrical heater and electrically operated valves on inlet and outlet air flow and vacuum ports.

The housing is a welded stainless steel construction consisting of a 10 inch x 6 inch diameter shell bolted through flanges to 45° conical ends. Each end includes a 3/4 air-flow port and a 1-1/2 inch evacuation port. 28 VDC solenoid-operated valves are flange-mounted to each port to provide periodic evacuation of the housing interior by closing the air-flow ports and opening the evacuation ports. The exterior of the housing is covered with "Min-K" insulating material and an outer aluminum shell. The 71-watt stainless steel heater is located within the sorbent bed. The heater element is finned and its terminals are wired to a hermetic-seal-mounted electrical connector with 14-gauge high-temperature wires. The sorbent bed is 5.2 pounds of 6 x 12 mesh activated charcoal and is retained at each end by a 200-mesh stainless steel screen assembly. A 15 lb spring acting against the inlet screen assembly maintains compression on the sorbent material.

CONCLUSIONS

The program for the development of a sorber trace contaminant control system has resulted in the design of an integrated trace contaminant control system for use in a space station. The system sized for 12 men, has the capability of controlling all of the contaminants anticipated to be present in a typical space station. The use of regenerative charcoal has a major impact on reducing the required charcoal quantity. A fixed bed system satisfying the same requirements needs approximately 500 lb of charcoal, whereas the proposed system utilizes approximately 59 lb of charcoal. The model system test results indicated that a combined regenerable sorbent bed and lithium hydroxide presorbent bed can be used to successfully eliminate potential catalyst poisons. These results also demonstrated that the catalytic oxidizer will successfully control the hydrocarbon contaminants that are not amenable to removal by the charcoal beds.

The final system requires a total of 125 watts of power. The weight of the catalytic oxidizer is 20.9 lb. The pre- and post-sorbent lithium hydroxide canisters weigh 7.7 lb, the fixed charcoal bed weighs 62 lb, and the regenerative charcoal bed weighs 6.6 lb.

REFERENCES

1. Atmospheric Contaminants in Spacecraft Report of the Panel on Air Standards for Manned Space Flight of the Space Sciences Board, National Academy of Sciences, October 1968.
2. R. A. Dora, et al "Monitoring of the Bioeffluents of Man to Establish Space Vehicle Environmental Control Requirements", Aerospace Medical Association Preprints 36th Annual Meeting, April 1965, New York.
3. C. A. Spezia, "Toxic Contamination of Manned Spacecraft Cabins: A Review of the Problem", Lockheed California Company, Burbank, LR 17744, April 1964.
4. M. Polanyi Verh. dtsch, phys. Ges. 1b, 1012, 1914.
5. Klotz, I.M., Chapter 8 of Summary Technical Report of Division 10, "The Adsorption Wave", NDRC 1946.
6. N. A. Lyshkow, J. Pollution Control Assoc., 17, 687, 1967.
7. M. B. Jacobs, The Chemical Analysis of Air Pollutants, Interscience Publishers, Inc., New York, 1960.
8. T. M. Olcott, Development and Design of an Isotope Heated Catalytic Oxidizer, Trace Contaminant Control System, NASA CR 66739, Feb. 1969.

APPENDIX A
ADSORPTIVE CAPACITIES

Adsorptive Capacities, Contaminant Adsorbed Singly

Adsorptive capacities were determined by (1) weight gain of the carbon with dry nitrogen used as carrier gas, (2) weight gain under vacuum (static CCl_4 activity tests) and (3) by use of the effluent concentration curve. In the last case, the conditions were reduced, pressure at 10 lb/in^2 and 30% O_2 - 70% N_2 carrier gas at relative humidities of 34% and 50%.

Table A-1 presents a summary of the adsorptive capacity data for single contaminants. Figures A-1 through A-5 and Tables A-2 through A-9 present the effluent concentration curves for acetone on S154 and G1 and for Freon 11 on G1.

The differences in adsorptive capacities for the four carbons are due to differences in pore structure. Since the super-activated carbon has the largest total micropore volume, it has the largest adsorptive capacity at the high concentrations, i.e., low A values. BPL has the smallest total micropore volume and, therefore, the smallest adsorptive capacities at low A values. At higher A, in the range of interest to spacecraft application, BPL and BD carbons exhibit higher adsorptive capacities than the superactivated and G1 carbon. This is an indication that the mean micropore diameters of BPL and BD are smaller than those of the superactivated and G1. The superactivated carbon is the poorest of the carbons in the higher A value region.

The presence of moisture in the carbon at the 37% RH equilibration level appears to have little or no effect on the adsorptive capacity of S154 for acetone. The adsorptive capacity was $0.0092 \text{ cm}^3 \text{ liq/g}$ for Run 25 at 34% RH gas stream and $0.0097 \text{ cm}^3 \text{ liq/g}$ for Run 27 at 0% RH gas stream. Run 25 was a regenerated carbon which had lost a small part of its adsorptive capacity; hence, the effect of moisture at this RH level is less than the capacity difference would indicate.

TABLE A-1
 ADSORPTIVE CAPACITIES SINGLE CONTAMINANTS

<u>Based on Weights Gain</u>	<u>Carbon</u>	<u>Conditions</u>	<u>mg</u>	<u>A</u>
n-Octane	S154	N ₂ , 9.9 (mg/l) C ₁	749	1.5
Methyl cyclohexane	BPL	N ₂ , 15.8 (mg/l) C ₁	319	2.5
Methyl cyclohexane	G1	N ₂ , 13.7 (mg/l) C ₁	450	2.6
Ter-Amyl alcohol	G1	N ₂ , 29.5 (mg/l) C ₁	596	1.1
Carbon Tetrachloride	S154	Vacuum, 0.16 p/p _o	1540	2.3
Carbon Tetrachloride	BPL	Vacuum, 0.16 p/p _o	670	2.3
Carbon Tetrachloride	G1	Vacuum, 0.16 p/p _o	1000	2.3

A-2

Based on Effluent Concentration
 (10 psia, 30% O₂ - 70% N₂)

Table No., Fig. No.

Acetone, Run 27	S154	0% RH	7.3	17.6	A3	A1
Acetone, Run 25	S154	34% RH	6.9	17.6	A2	A1
Acetone, Run 29	G1	50% RH	13.0	17.6	A4	A2
Freon 11, Run 47, 49	G1	0% RH	1.80	23.0	A6	A3
Freon 11, Run 46	G1	50% RH	1.26		A5	A3
Freon 11, Run 66	G1 with H ₃ PO ₄	50% RH	0.61		A7	A4
Freon 11, Run 67	G1 with H ₃ PO ₄	50% RH	0.81		A9	A5
Freon 11, Run 71	G1 with H ₃ PO ₄	50% RH	0.87		A8	A4

A-3

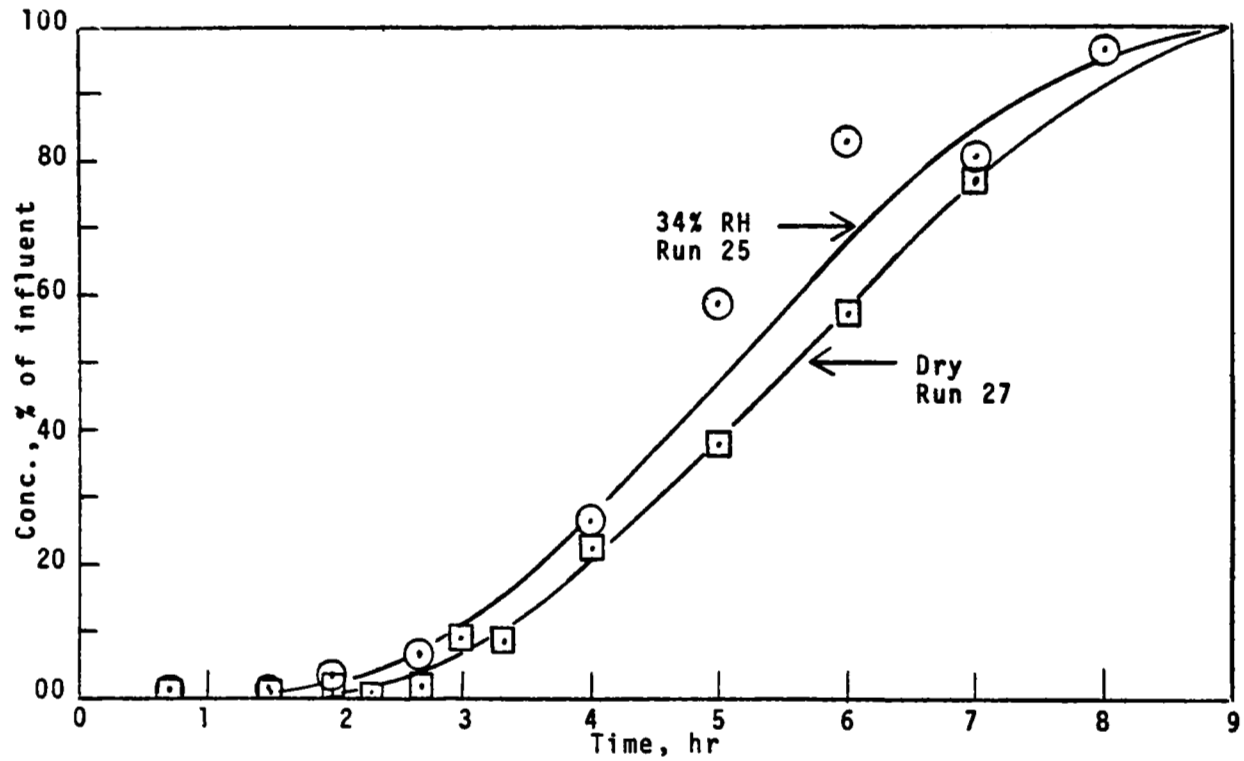


Figure A-1 Effluent Concentration Curves for Runs 25 and 27, Acetone on GI

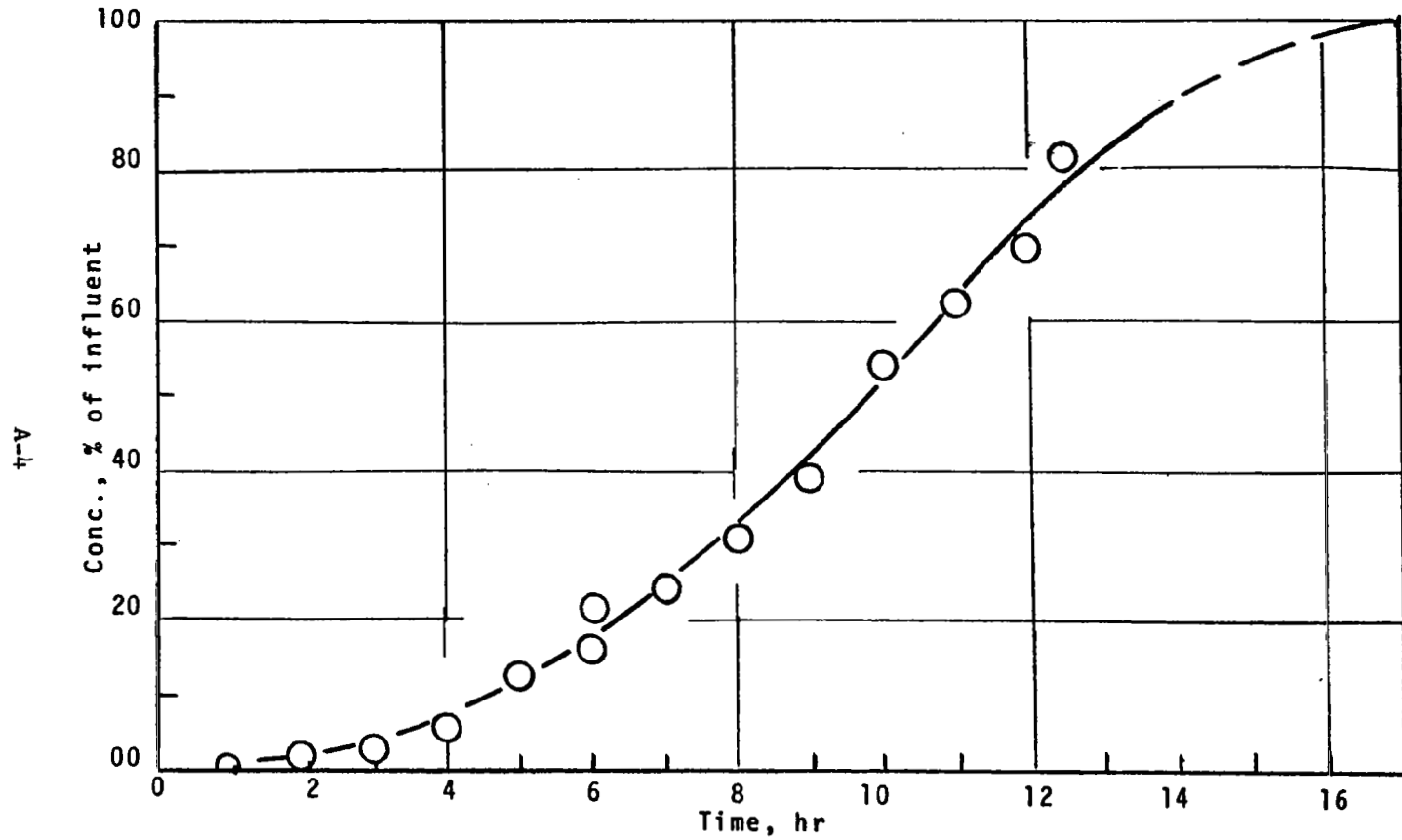


Figure A-2 Effluent Concentration Curve for Run 29

A-5

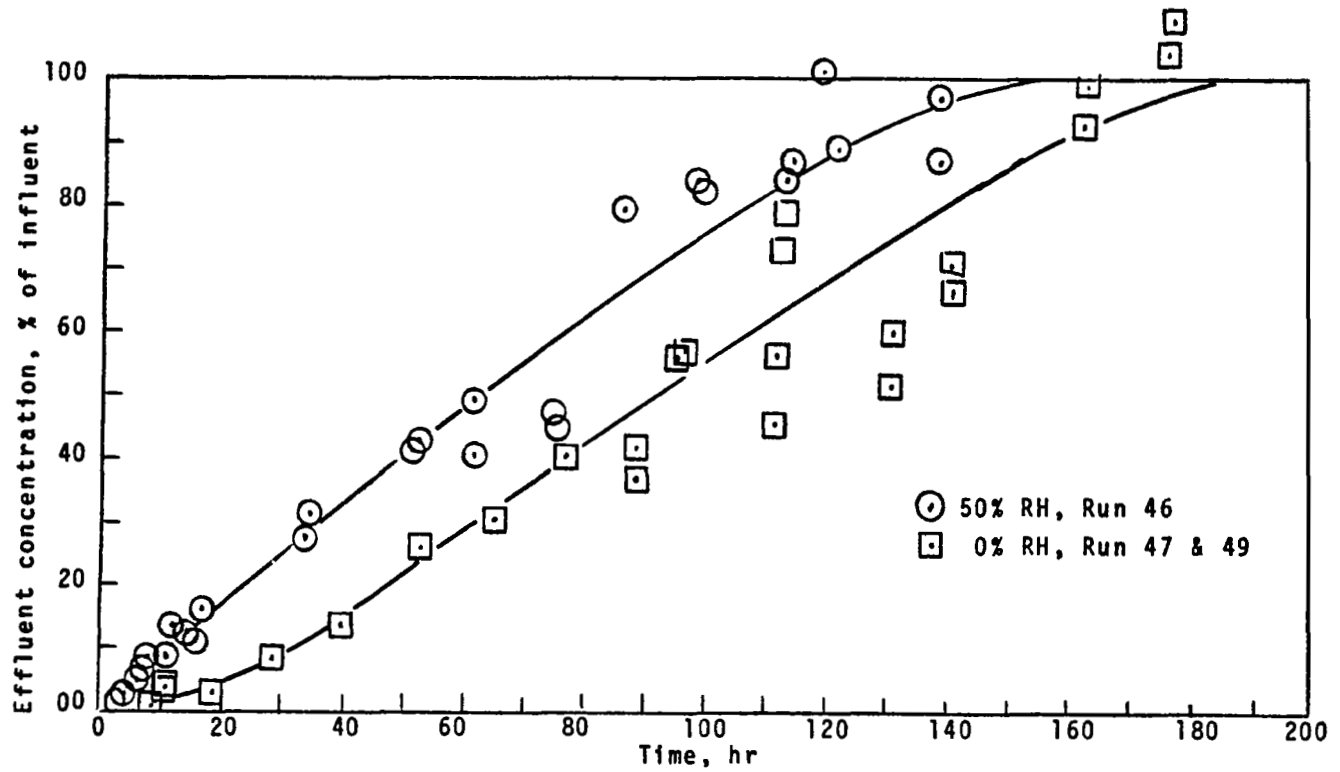


Figure A-3 Effluent Concentration Curves for Freon 11 on Barnebey Cheney GI Carbon

A-6

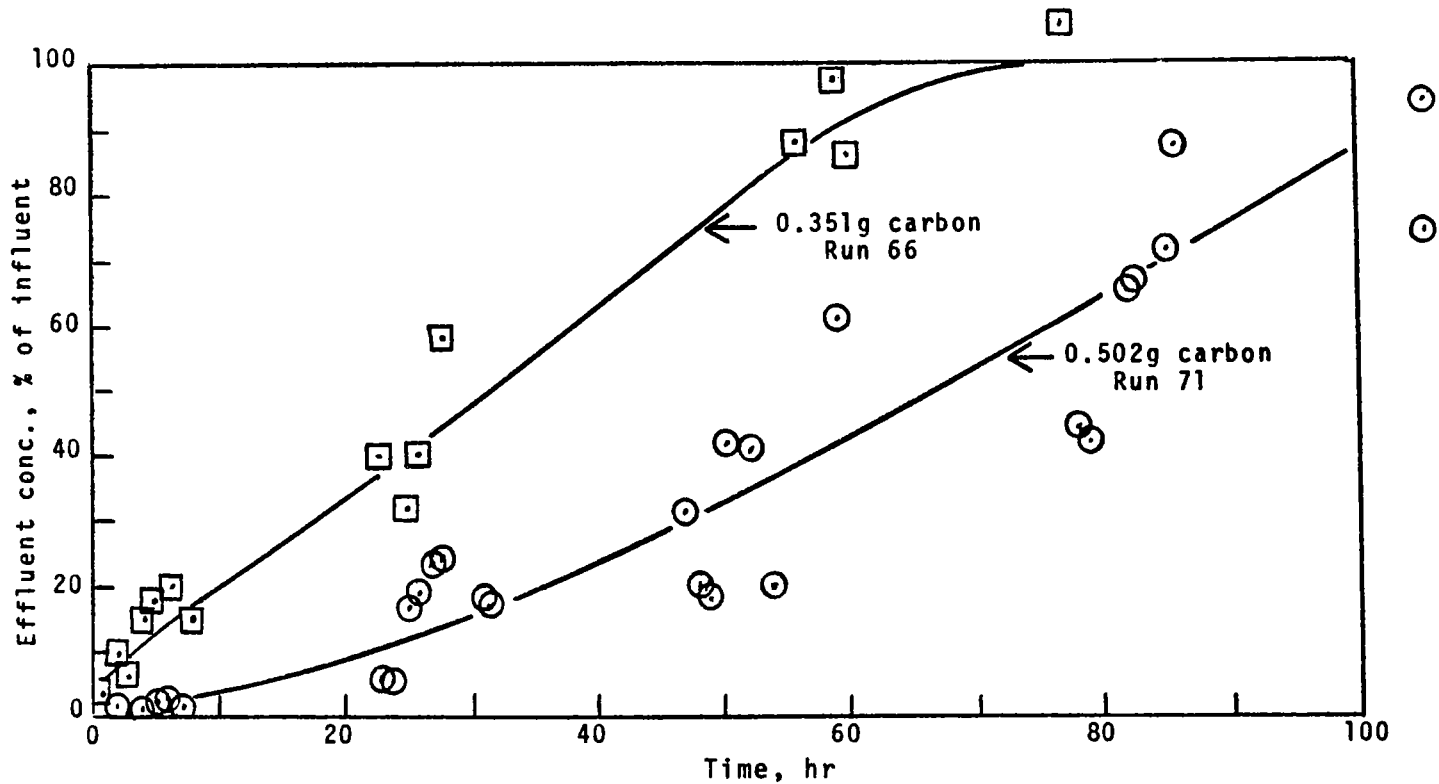


Figure A-4 Effluent Concentration Curves for Freon 11 on H_3PO_4 Treated Barnebey Cheney Carbon

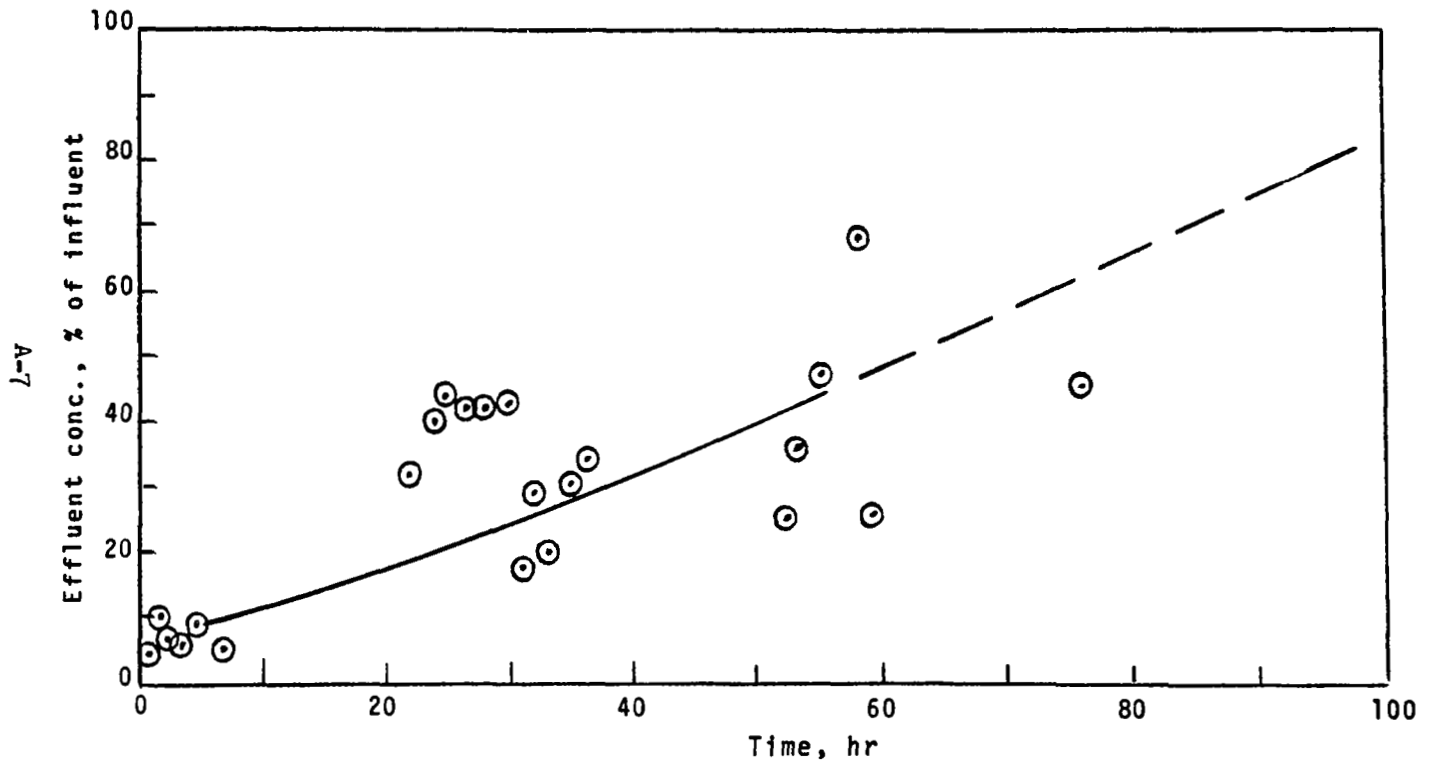


Figure A-5 Effluent Concentration Curve for Freon 11 on H_3PO_4 Treated Barnebey Cheney GI Carbon, Run 67

TABLE A-2
 ADSORPTIVE CAPACITY OF S154 FOR ACETONE,
 34% RH, RUN 25

Weight of carbon	2.711 g
Carrier gas	30% O ₂ and 70% N ₂
Pressure	10 lb/in ² (ads.)
Gas flow	2.83 L/min (52 ft ³ /min)
Acetone conc.	0.021 mg/g
Relative humidity	34%
Adsorption temp.	ambient (25°C)

Effluent concentration data

<u>Time</u> <u>min</u>	<u>Concentration, % of influent</u>
40	0.0
90	1.2
120	3.1
140	---
160	6.8
180	---
200	---
240	26.4
300	58.8
360	82.5
420	80.3
480	96.0

Adsorptive capacity, q 6.9 mg/g, 0.0092 cm³ liq/g
 A = 17.6

TABLE A-3
 ADSORPTIVE CAPACITY OF S154, FOR ACETONE,
 WITH DRY CARRIER GAS, RUN 27

Weight of carbon	2.72 g
Carrier gas	30% O ₂ and 70% N ₂
Pressure	10 lb/in ² (abs.)
Gas flow	2.83 L/min (52 ft ³ /min)
Acetone conc.	0.021 mg/g

Effluent Concentration Data

<u>Time, min</u>	<u>Concentration, % of influent</u>
0	0.0
40	1.1
90	0.6
120	2.2
140	0.7
160	2.0
180	8.8
200	8.6
240	22.2
300	37.2
360	56.9
420	76.4

Adsorptive capacity, $q = 7.3 \text{ mg/g}; 0.0097 \text{ cm}^3 \text{ liq/q}$

A = 17.6

TABLE A-4
 ADSORPTIVE CAPACITY OF BARNEBEY CHENEY G1, FOR
 ACETONE, 50% RH, RUN 29

Weight of carbon	2.701 g
Carrier gas	30% O ₂ and 70% N ₂
Pressure	10 lb/in ²
Gas flow	2.83 L/min (52 ft ³ /min)
Acetone conc.	0.021 mg/g

Effluent concentration data

<u>Time, hr</u>	<u>Concentration, % of influent</u>
1	0.1
2	1.3
3	2.6
4	6.2
5	12.5
6	21.5
6	15.7
7	23.6
8	31.7
9	39.4
10	56.4
11	61.8
12	69.8
12.5	81.6

Adsorptive capacity, $q = 13.0 \text{ mg/g}$, $0.0173 \text{ cm}^3 \text{ liq/g}$

$A = 17.6$

TABLE A-5
 ADSORPTIVE CAPACITY OF BARNEBEY CHENEY G1,
 FOR FREON 11, 50% RH CARRIER GAS, RUN 46

Weight of carbon 0.350 g
 Carrier gas .30% O₂ and 70% N₂
 Pressure 10 lb/in²
 Gas flow 0.11 L/min (3 ft³/min)
 Freon 11 conc. 0.00103 mg/g

<u>Time, hr</u>	<u>Effluent conc., % of influent</u>	<u>Time, hr</u>	<u>Effluent conc., % of influent</u>
0.2	1.7	18	44.3
0.3	1.3	34	27.2
1.0	0.8	35	31.4
1.5	1.0	52	41.2
2.0	1.3	53	43.2
2.5	1.8	62	49.6
4.0	2.6	62	40.9
5.0	3.8	75	47.3
6.0	5.4	76	45.0
6.2	4.5	86	46.1
7	6.2	87	79.6
8	8.2	99	84.7
9	8.3	99	84.6
10	7.7	100	82.9
11	8.1	114	84.0
12	13.8	115	87.3
13	11.1	120	101.5
14	12.3	123	89.5
16	11.5	139	87.2
17	16.5	139	97.3

TABLE A-6
 ADSORPTIVE CAPACITY OF BARBEREY CHENEY G1, FOR
 FREON 11, 50% RH CARRIER GAS, RUNS 47 AND 49

Weight of carbon	0.351 g
Carrier gas	30% O ₂ and 70% N ₂
Pressure	10 lb/in ²
Gas flow	0.11 L/min (3 ft ³ /min)
Freon 11 conc.	0.00103 mg/g

<u>Time, hr.</u>	<u>Effluent conc., % of influent</u>	<u>Time, hr</u>	<u>Effluent conc., % of influent</u>
1	2.3	96	56.7
2	1.7	97	57.2
3	0.2	112	45.4
4	0.3	112	56.2
5	0.9	113	73.2
5	1.9	113	79.6
6	1.0	131	60.0
7	2.0	131	51.2
8	2.3	141	71.4
9	3.3	141	66.8
10	3.4	155	57.5
11	4.6	155	60.4
Run 49		163	93.0
		164	99.6
2	0.3	177	104.0
19	3.0	178	109.5
29	8.5		
40	13.7		
53	26.0		
65	30.6		
77	40.4		
89	42.0		
89	36.6		

TABLE A-7
 ADSORPTIVE CAPACITY OF PHOSPHORIC ACID TREATED
 BARNEBEY CHENEY G1, FOR FREON 11, 50% RH, RUN 66

Carbon weight	0.351 g
Carrier gas	30% O ₂ and 70% N ₂
Pressure	10 lb/in ²
Gas flow	0.11 L/min (3 ft ³ /min)
Freon 11 conc.	0.00103 mg/g
Amount H ₃ PO ₄	10% of carbon weight

<u>Time, hr</u>	<u>Effluent conc., % of influent</u>	<u>Time, hr</u>	<u>Effluent conc., % of influent</u>
1	4	28	58
2	10	29	74
3	6	31	103
4	15	56	88
5	18	59	98
6.5	20	60	86
8	15	77	106
23	48	78	115
25	32		
26	40		

TABLE A-8
 ADSORPTIVE CAPACITY OF PHOSPHORIC ACID TREATED
 BARNEBEY CHENEY G1, FOR FREON 11, 50% RH, RUN 71

Carbon weight 0.502 g
 Carrier gas 30% O₂ and 70% N₂
 Pressure 10 lb/in²
 Gas flow 0.11 L/min (3 ft³/min)
 Freon 11 conc. 0.00103 mg/g
 Amount H₃PO₄ 10% of carbon weight

<u>Time, hr</u>	<u>Effluent conc., % of influent</u>	<u>Time, hr</u>	<u>Effluent conc., % of influent</u>
2	1.6	55	79
4	1.2	56	113
5	2.3	58	105
6	2.3	59	61
7	1.3	60	119
23	5.5	61	99
24	5.0	78	44
25	16	79	42
26	19	82	66
27	23	82.5	67
28	24	85	72
31	18	85.5	87
31.5	17	101	54
47	31	102	54
48	20	106	74
49	18	106	93
50	42	107	59
52	41		
53	67		
54	20		

TABLE A-9
 ADSORPTIVE CAPACITY OF PHOSPHORIC ACID TREATED
 BARNEBEY CHENEY G1, FOR FREON 11, 50% RH, RUN 67

Carbon weight	0.503 g
Carrier gas	30% O ₂ and 70% N ₂
Pressure	10 lb/in ²
Gas flow	0.11 L/min (3 ft ³ /min)
Freon 11 conc.	0.00103 mg/g
Amount H ₃ PO ₄	10% of carbon weight

<u>Time, hr</u>	<u>Effluent conc. % of influent</u>	<u>Time, hr</u>	<u>Effluent conc. % of influent</u>
1	3.8	35	30
2	9.5	36	34
3	5.8	52	25
4	5.2	53	36
5	8.5	55	47
7	4.9	58	68
22	32	59	26
24	40	76	46
25	44		
27	42		
28	42		
30	43		
31	17		
32	29		
33	20		

Adsorptive capacity studies with Freon 11 on G1 carbon show that moisture at the 50% RH equilibration level and H_3PO_4 treatment of the carbon lowers the adsorptive capacity. Moisture in the gas stream lowers the capacity by 30% from 1.80 to 1.26 mg/g. The carbon impregnated with 10% by weight of H_3PO_4 further lowers the capacity from 1.26 to 0.76 mg/g, or another 40%.

Adsorption of acetone was not significantly affected by moisture, and, since acetone is soluble in water, this fact suggests that water soluble contaminants may not be greatly affected at the 37% or 50% RH level. Moisture pick-up at the 37% RH level can be expected to be about 1% by weight and, at the 50% RH level, about 2% by weight. For low V_m , nonwater-soluble contaminants, such as Freon 11, this small amount of water reduces the adsorptive capacity.

The H_3PO_4 impregnant is required in the carbon to attain adequate retention of ammonia. For the treated carbon adsorption runs, one millimole of H_3PO_4 was added per gram of G1 carbon from a saturated aqueous solution. The amount of solution and concentration was adjusted so that the carbon just soaked up the solution without the granules becoming externally wet. The treated carbon was then dried at 150°C until successive weighings showed that the water had been evaporated. This treatment gave a carbon with 10% H_3PO_4 by weight.

Adsorptive Capacities, Contaminant Mixtures

The effects which the contaminant mixtures would have on their adsorptive capacities were studied with acetone, Freon 11 and methyl cyclohexane. The data on these adsorption runs are shown in Figures A-6 and A-7 and in Tables A-10 and A-11.

When acetone is adsorbed singly, the carbon capacity for acetone is 16.1 mg/g, and, singly for Freon 11, it is 1.26 mg/g. Two separate one gram quantities of carbon can then adsorb 17.4 g of acetone and Freon 11 combined. Per gram of carbon, the adsorbed amount of acetone and Freon 11 is 8.7 g.

When acetone and Freon 11 are adsorbed as a mixture, the adsorptive capacity of each decrease. Acetone capacity decreases only slightly and Freon 11 by 44%. The combined weight of acetone and Freon 11 that can be adsorbed on

A-17

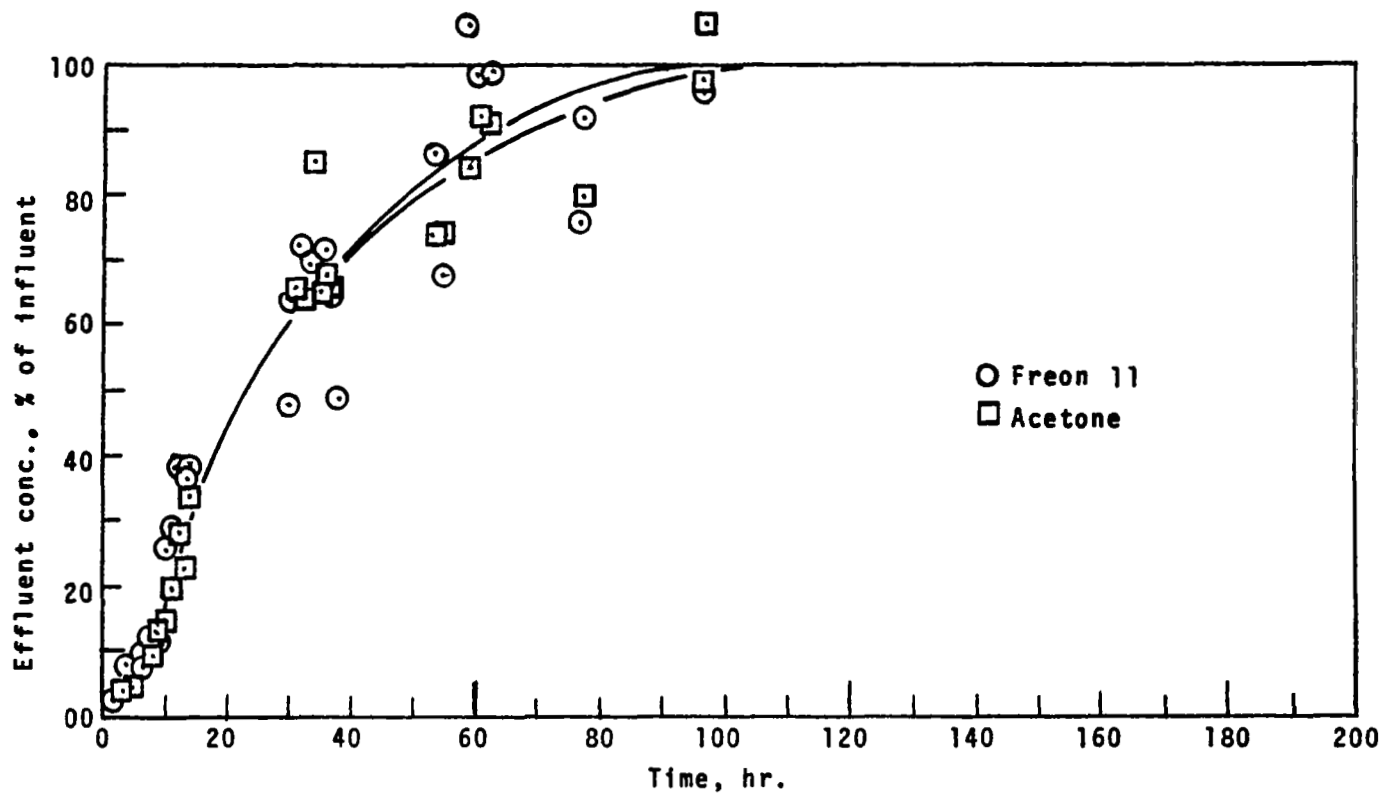


Figure A-6 Effluent Concentration Curves for Freon 11 and Acetone Mixture on Barnebey Cheney GI, 0.350 g of Carbon, Run 48

A-18

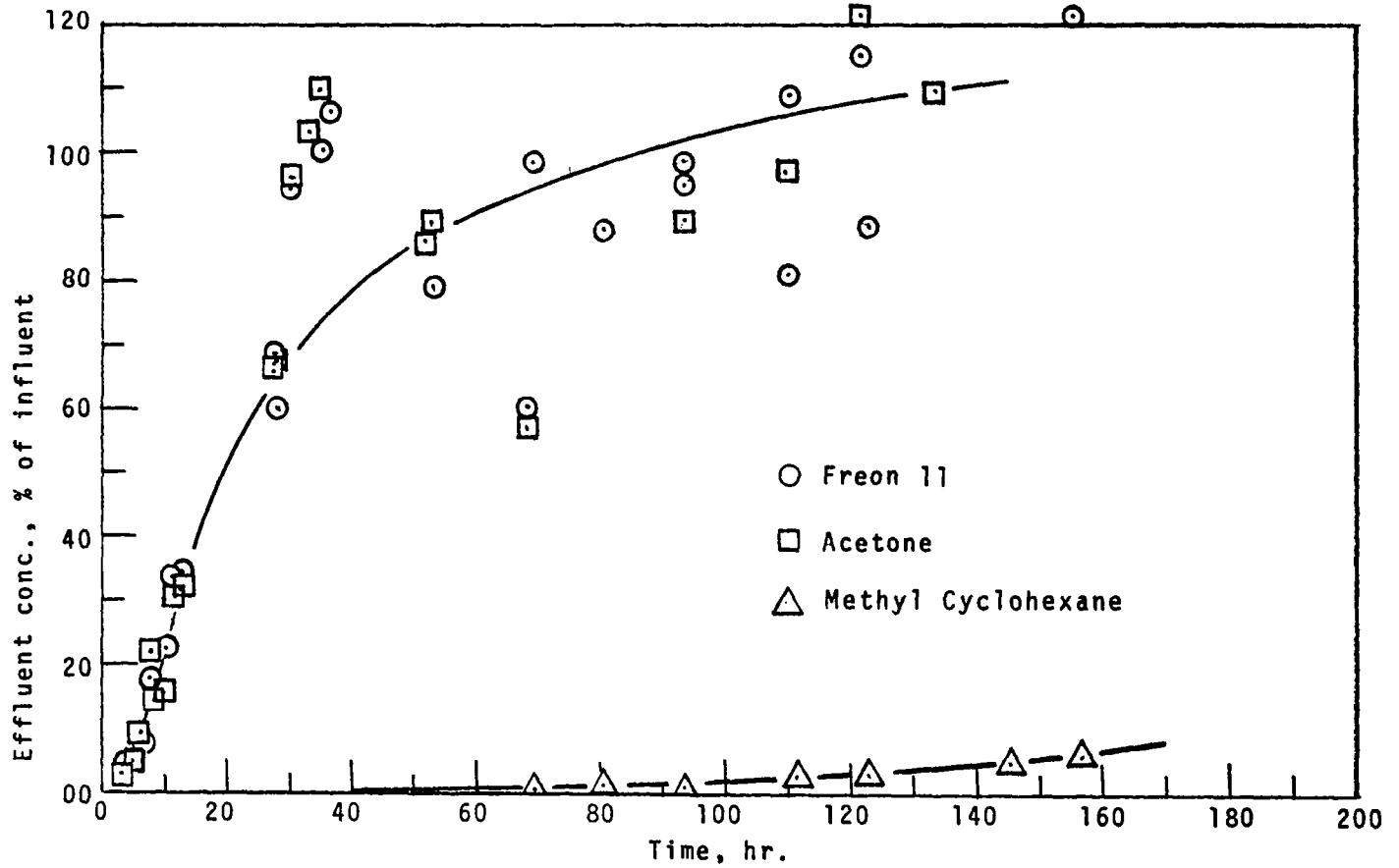


Figure A-7 Effluent Concentration Curves for Adsorption of Mixture of Methylcyclohexane, Freon 11 and Acetone on BC-G1, 0.352 g Carbon, Run 50

TABLE A-10
 ACETONE AND FREON 11 MIXTURE

Eff. conc., % of influent

Run 48 0.350 g

<u>Time, hr</u>	<u>Acetone</u>	<u>Freon</u>	<u>Time, hr</u>	<u>Acetone</u>	<u>Freon</u>
8	12.3	9.2	36	68.4	65.7
9	11.7	13.3	37	63.8	77.5
10	25.6	14.4	37		66.6
11	28.5	19.4	38	48.5	
12	38.7	28.5	54	85.9	73.4
13	37.6	22.2	55	67.2	73.4
14	36.0	33.0	59	106.1	83.5
14	38.7	32.9	61	99.9	91.4
30	47.6		62	99.1	90.8
31	63.6	65.1	77	75.7	91.2
32	71.9	64.6	78	91.4	79.7
34	59.3	83.5	97	97.2	97.7
36	71.0	65.2	97	95.6	106.1

TABLE A-11
 ACETONE, FREON 11, METHYL CYCLOHEXANE MIXTURE

Effluent conc., % of influent

Run 50, 0.352 g

<u>Time, hr</u>	<u>Acetone</u>	<u>Freon 11</u>	<u>MCH</u>
1.0	0.45	1.5	
1.5	0.71	1.4	
2.5	2.3	3.6	
4.5	4.8	5.0	
6	8.6	7.1	
7	21.4	17.7	
8	14.5	17.8	
9.5	15.8	22.5	
11	30.2	33.5	
12.5	31.4	34.7	
27.5	66.2	68.9	
28	68.2	60.2	
30.5	95.4	94.5	
33	102.8	117.4	
35.5	110.5	100.4	
36	100.8	106.3	
52.5	85.8	78.6	
53	89.6	79.1	
68	57.3	60.5	
69		98.4	0.60
80		88.4	0.69
81			0.70
93	89.2	98.7	
93.5		94.7	0.77
110	96.9	109.3	
111		80.9	2.6
122	121.6	115.8	2.7
122.5		88.6	
133		185.4	
133.5	108.7		
145		184.8	4.2
156		153.5	5.4

the same one gram of carbon is 15.7 g, or 1.8 times more than when each was adsorbed singly. This means that they can coexist to a considerable degree on the carbon surface. This is a steady state condition, i.e., it will not change with adsorption time. Figure A-6 shows the effluent concentration curves for the two contaminants. At 90-hr adsorption time, both effluent concentrations reach 100% of influent; hence, the 0.350 g carbon layer no longer takes part in removing these two contaminants from the air stream.

When methyl cyclohexane is added to the mixture, the adsorptive capacity for acetone and Freon 11 again decreases, but steady state adsorptive capacities could not be determined, since the runs were not conducted long enough to bring the methyl cyclohexane effluent concentration up to its influent concentration.

APPENDIX B
EXPERIMENTAL PROCEDURE FOR THE CARBON BED PERFORMANCE STUDIES

Equipment and Experimental Procedures

Adsorption Apparatus

Presented in Figure B-1 is a sketch of the adsorption apparatus used to determine the adsorptive capacities and critical bed depths of selected contaminants on coconut based carbons.

Since very low contaminant concentrations were being studied, special precautions were exercised in constructing the line to exclude extraneous contaminants which could utilize part of the carbon capacity and/or interfere with the analyses of the contaminants under study. Structural parts coming in contact with the contaminant gas stream were limited to glass, stainless steel and Teflon. New flowmeters, valves, tubing and stopcocks were purchased. All components were then cleaned with water, acetone, trichloroethane and acetone, in that order, and then dried in an oven at 150°C or flamed out with a hand torch where appropriate. Valves and flowmeters were disassembled for the cleaning operation. Prior to actual adsorption runs, nitrogen was run through the unit for at least 12 hr with periodic flaming of the steel tubing.

The oxygen and nitrogen gases contained extraneous contaminants; hence, it was necessary to install the activated carbon traps as shown in the upper left section of the sketch. A Barnebey-Cheney G1 coconut carbon was used. It was dried for several hours at 150°C before charging to the flasks.

Some uncertainty existed in that the distilled water, for the humidifier, may contain organic contaminants. To remove possible organics, the water was redistilled from a potassium permanganate solution.

Tubing shown by a single line was 1/4 inch 316 stainless steel, and all fittings were Swagelock type except where connections were made to pressure gauges and metal to glass. Tubing shown by double line were either 8 mm Pyrex glass or plastic, as in the connections to the pumps. Metal to glass connections

B-2

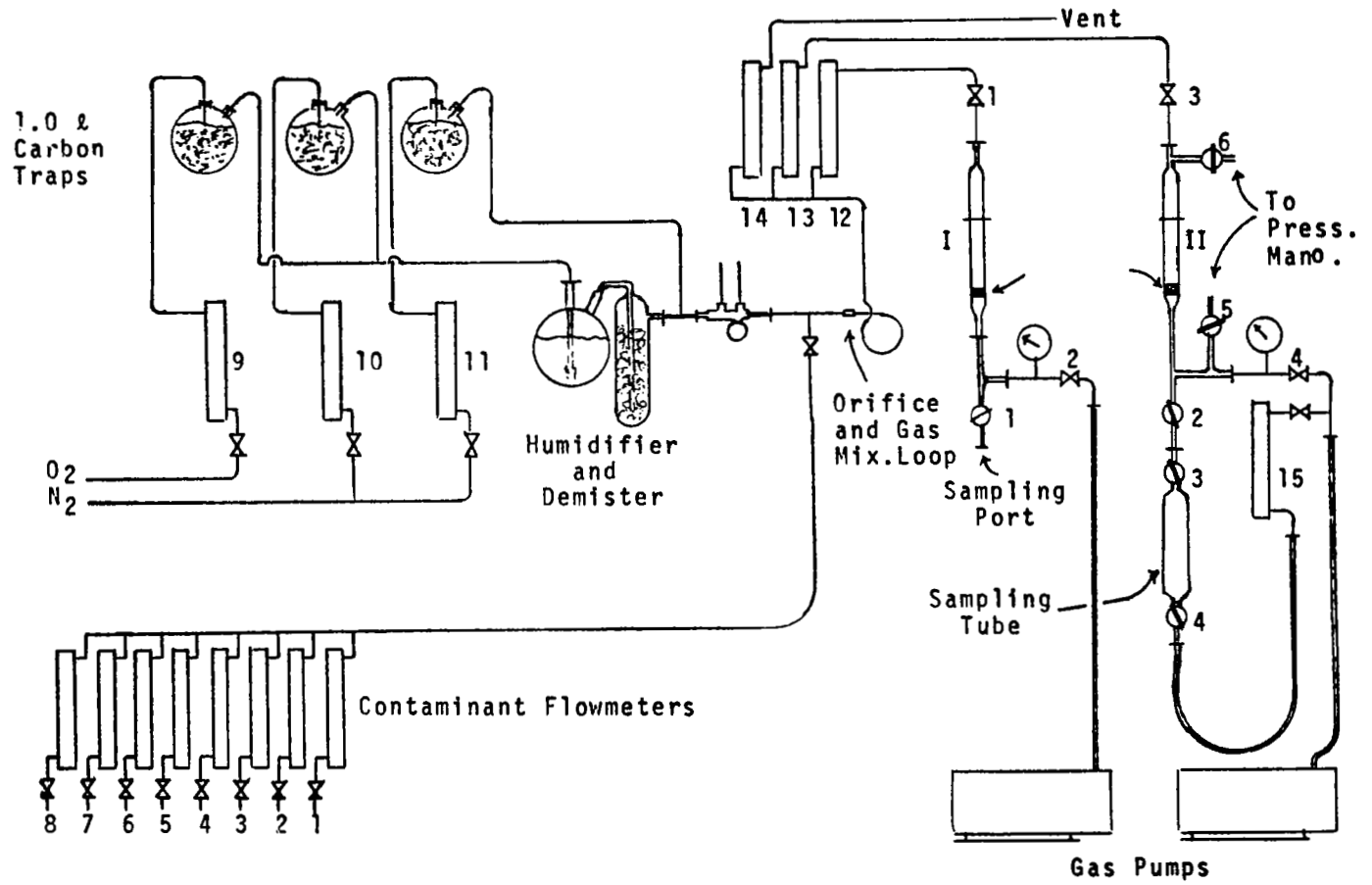


Figure B-1 Adsorption Apparatus

and glass to glass connections which needed to be frequently unconnected, such as the carbon adsorption and effluent gas sampling tubes, were all "O" ring type. These were held together with clamps with screw tighteners. Stopcocks coming in contact with the gas-stream were Teflon bore type. Glass stopcocks requiring lubricants were avoided.

The bank of flowmeters at the lower left were for metering prepared contaminant mixtures of known concentration from pressurized cylinders. Upper limit on the flowmeters was 55 cc/min for nitrogen. The contaminant mixtures were purchased from Matheson Gas Products. The contaminant cylinder attached to each flowmeter had the following type contaminant and concentration.

Table B-1 - Contaminant Mixtures

<u>Flowmeter</u>	<u>Contaminant</u>	<u>Conc. in nitrogen, Vol. %</u>
1	Genetron 23	0.12
2	Freon 11	0.0005
3	Acetone	0.29
4	Methyl chloride	0.0024
5	Cyclopentane	0.022
6	Methyl cyclohexane	0.012
7	Ammonia	0.085
8	Methyl mercaptan	0.0029

The metered gas flow from any one, or from any combination of, cylinders was then diluted further to the required concentrations with the humidified oxygen-nitrogen mixture metered through flowmeters 9, 10, and 11. These flowmeters were sized so that oxygen-nitrogen mixtures (30% O₂ - 70% N₂) at 73% relative humidity could be generated up to total flows of 2.3 L/min at atmospheric pressure.

To insure complete mixing of the contaminant and diluent gas streams, the combined mixture was passed through an orifice and then through a coil as indicated in the drawing.

Excess gas mixture was generated and the excess vented through Flowmeter 14. The required amount for the tests were drawn through Flowmeter 12 for Adsorption Tube I and through Flowmeter 13 for Adsorption Tube II.

Valves 1 and 2 were used to control the flow through Adsorption Tube I and Valves 3 and 4 for Adsorption Tube II. At Valves 1 and 2, the pressure decreases from atmospheric down to 9.5 in. of mercury negative pressure. When atmospheric pressure is 14.7 lb/in², the reduced pressure is the 10 lb/in² absolute as specified for these experiments. The reduction in pressure increases flow rate by the factor 14.7/10 and reduces all concentrations by 10/14.7. Relative humidity decreases from 73% to the 50% specified for the experiments.

Figure B-2 gives the details of the type adsorption tube used.

The chromatographic method was used to determine influent and effluent concentrations of the carbon beds. Gas samples were collected in 200 to 300 cc volume sampling tubes, attached to the unit as shown in the drawing. Stopcocks 3 and 4 of the sampling tube had Teflon bores, the upper concentration was "O" ring type and the lower a tapered ground glass type.

The sampling procedure consisted of (1) evacuate sampling tube, (2) expand effluent gas into tube until 10 lb/in² absolute pressure is attained (this was done without changing pressure or flow rate through carbon bed), (3) direct total effluent flow through tube at required rate and 10 lb/in² pressure for five minutes, and (4) close off Stopcock 4 and allow pressure to build up to atmospheric. As the pressure approaches atmospheric, the flow through carbon bed slows down and concentration increases. This introduced a small error in the concentration determinations because of adsorption rate change over the carbon bed. The alternative procedure would have been to fill the sampling tubes to 10 lb/in² absolute and run the risk of air leaking into the sampling tubes through the Teflon bore stopcocks.

Analytical Procedures

The analysis of the influent and effluent concentration was performed by gas chromatography. Two instruments were used for the various analysis.

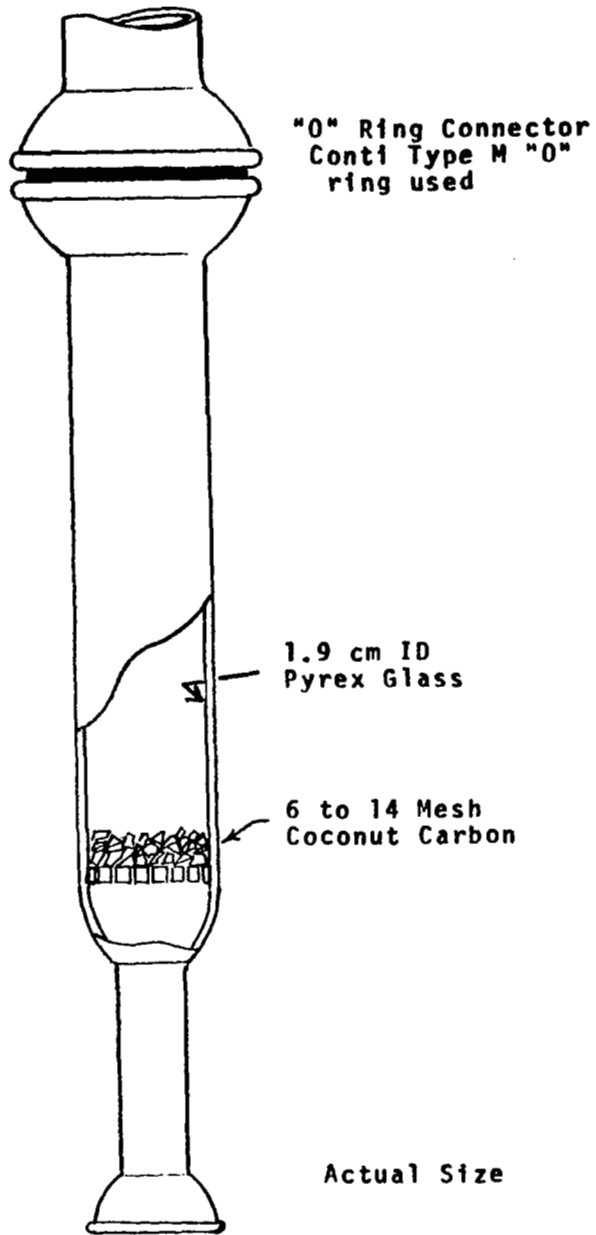


Figure B-2 Adsorption Tube

A Hewlett Packard Research Gas Chromatograph Model 5750 with dual flame ionization detectors was used for the analysis of the hydrocarbon compounds, and an F & M Model 810 with an electron capture detector was used for the Freon compounds. Three columns were used for the various analysis - 6 ft x 4 mm I.D. glass 100-120 Mesh Porapak QS; 6 ft x 1/8 in O.D. stainless steel 80-100 mesh Porapak and 6 ft x 1/8 in stainless steel 10% UCC-W982 on 80-100 mesh Diatoport S. The required detection limits were attained for the hydrocarbons by a concentration technique whereby all the contaminant contained in the 200-300 ml sample tubes was concentrated on a short pre-column and injected into the analytical column. Sample size was determined by the calibrated volume for each sample tube with the appropriate temperature and pressure corrections.

The contaminant concentration system is shown in Figure B-3. A 10 x 1/8 inch O.D. stainless steel tube packed with 45/60 mesh DMCS treated Chromosorb P was used instead of the usual small sample volume tube on the chromatograph valve. A Carle Instruments, Inc. micro volume valve No. 2014 was used in this system. This type valve is stainless steel with glass and ceramic filled Teflon sliders. The valve and all connecting transfer lines were maintained at above ambient temperature. The sample inlet was fitted with an "O"-ring connector to accept the gas sampling tubes. The "normal" sample outlet line was attached to a vacuum manifold. The analysis was initiated by attaching the glass sample tube to the "O" ring connector on the switching valve. The valve trap and inlet lines were evacuated and a liquid nitrogen bath was placed around the sorption trap. By evacuating the sample through the trap, the contaminants were concentrated in the trap and the non-condensibles were exhausted through the pump.

The valve was then switched to allow the helium carrier gas to sweep through the trap into the chromatograph. The liquid nitrogen bath was replaced with a hot water bath and the contaminant was injected into the chromatograph by the rapid heat-up and carrier gas purge of the trap.

The sample concentration method was not required for the analysis of Freon since the electron capture detector had the required sensitivity. The samples were removed from the sample tubes and injected into the chromatograph



B-7

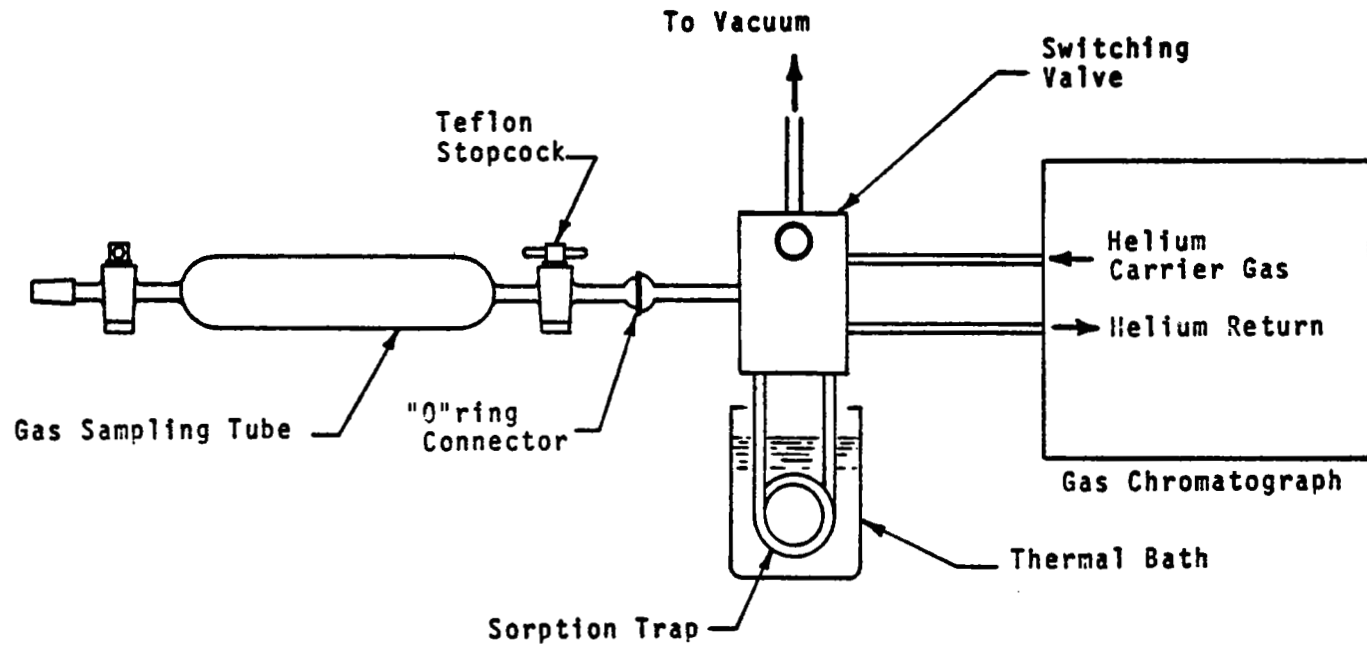


Figure B-3 Sample Concentration and Injection System

with a gas-tight syringe. The system used for this method consisted of a stainless steel "tee" fitted with a silicon rubber septum and an "O" ring connector before introducing a sample, the "tee" was evacuated. The sample was then admitted to the "tee", and a sample was taken with the syringe through the septum. The sample (usually 1/2 cc) was then injected into the chromatograph.

The analytical systems were calibrated by determining the specific mass response factor for each contaminant of interest. The compound of interest in a suitable solvent was injected into the chromatograph, and the response was related to the amount injected. Typical precision for five response factor determinations during a working day was a relative standard deviation of 4%.

The sampling and calibration methods were cross-checked with gas standards mixed in 75 liter mylar bags using pre-purified nitrogen as the diluent. The standard mixes were then sampled and analyzed by the routine method.

Sensitivities attained in all cases were adequate for the experimental specification of at least 1% of the influent concentration.

APPENDIX C
Derivation of Methane Removal Efficiency Correction Factor

The following section presents a derivation of the methane removal efficiency correction factor that was applied during the period that the 500 cc evacuated flask was used for sampling at the catalytic oxidizer effluent.

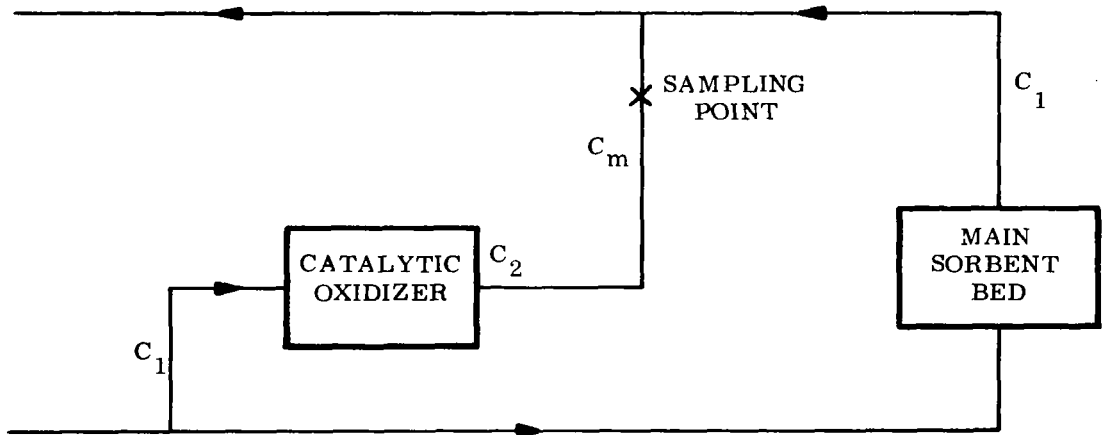


Figure C-1

Location of Catalytic Oxidizer
Effluent Sampling Point

Figure C-1 presents the location of the catalytic oxidizer sampling point. C_1 represents the concentration of methane entering the catalytic oxidizer which is also equal to the methane concentration leaving the main sorbent bed since no methane removal occurs in the main sorbent bed. C_2 represents the concentration of methane leaving the catalytic oxidizer. C_m represents the concentration of contaminant occurring in the 500 cc flask.

Performing a mass balance where M_1 equals the quantity of sample drawn in from the main sorbent exit and M_2 represents the quantity of sample drawn in from the catalytic oxidizer exit we have:

$$\text{Eqn. C-1} \quad (C_m)(M_1 + M_2) = C_2M_2 + C_1M_1$$

If we let C' designate acetylene concentrations we have:

$$\text{Eqn. C-2} \quad (C'M)(M_1 + M_2) = C_2'M_2 + C_1'M_1$$

However for acetylene $C_2' = 0$

therefore:

$$\text{Eqn. C-3} \quad M_1 = \frac{CM'}{C_2} (M_1 + M_2)$$

and:

$$\text{Eqn. C-4} \quad M_2 = (M_1 + M_2) \left(1 - \frac{CM'}{C_1}\right)$$

Substituting equation C-3 and C-4 into equation C-1 and solving for C_2 we have:

$$\text{Eqn. C-5} \quad C_2 = \frac{CM - C_1 \left(\frac{CM'}{C_1}\right)}{1 - \frac{CM'}{CM_1}}$$

The actual methane removal efficiency is:

$$\text{Eqn. C-6} \quad R_r = \frac{C_1 - C_2}{C_1}$$



Substituting equation C-5 for C2 we have:

$$\text{Eqn. C-7} \quad \eta_r = \frac{\frac{C_1 - C_M}{C_1}}{\frac{C_1' - C_M'}{C_1'}}$$

However $\frac{C_1 - C_M}{C_1}$ is the measured methane removal efficiency and

$\frac{C_1' - C_M'}{C_1'}$ is the measured acetylene removal efficiency. Therefore

the actual methane removal efficiency is:

$$\text{Eqn. C-8} \quad \eta_r = \frac{\text{Measured Methane } \eta_r}{\text{Measured Acetylene } \eta_r}$$

APPENDIX D
CHARCOAL BED ADSORPTION PROGRAM

Charcoal Bed Performance Analysis

The saturation capacity of activated charcoal for any singly adsorbed material can be estimated from potential adsorption theory. When tests have been conducted with multiple contaminants at spacecraft concentration levels, a displacement effect has been observed in which materials having a low A value will displace those having a higher A value from adsorption sites. If the difference in A values exceeds some critical value, total displacement is observed. Based upon these observations, this computer program was generated to estimate the required quantity of activated charcoal for control of multiple contaminants.

The program scans all contaminants by A value and then orders them from the lowest to highest value. It then calculates the quantity of sorbent required to remove the most strongly adsorbed substance. Using experimental potential plot data, the capacity of this sorbent section for additional substances is then estimated on the assumption that their capacity is less than saturation and is assumed linear with A value difference up to the critical A value. The program then proceeds to the next contaminant which is not yet completely removed and repeats the calculation. This process is continued until all of the listed contaminants have been completely adsorbed.

In these calculations three potential plots would be used: (1) for water insoluble contaminants on phosphoric acid, impregnated charcoal, (2) for water insoluble contaminants on charcoal without phosphoric acid, and (3) for water soluble contaminants on charcoal, either with or without phosphoric acid.

In order to assess the sensitivity of the critical sizing parameters, A critical, flow rate, time, and contaminant loadings would be inputs to the program. The program would be used to generate the various designs for an optimization study.

Equipment Configuration

The main storage module of each 1108 computer contains 65,536 words of 36 bits. The EXEC II controller requires 12,288 words, leaving 53,248 words of core available to the programmer. The OXNIP program uses only 1,594 words. The hardware structure includes two FASTRAND II mass storage units. Each FASTRAND unit has a storage capacity of 22,020,096₁₀ words and a transfer rate of 25,590 words per second.

The 1108 EXEC II system and the LMSC accounting routine accept certain specific cards on any job being submitted for processing. All control cards begin with a (master space) which is a 7-8 punch in Column 1. Figure D-1 shows the deck setup. All necessary blanks are indicated by _b.

The RUN card serves as an LMSC accounting record and a job initiation card. It includes a run identification number and estimated run time and page count. The sample run used 23 seconds and 50 pages. The LID control card is used to provide additional accounting information for the 1108 system. Each run must contain a LID control card and a RUN card or the run will be aborted.

The FRN control card calls in the FORTRAN V compiler and the FORTRAN deck is then compiled. To execute the FORTRAN V compiled program, the XQT control card is used with the F option. The EOF control card signals the end of the deck. Figure D-2 presents the table input data.

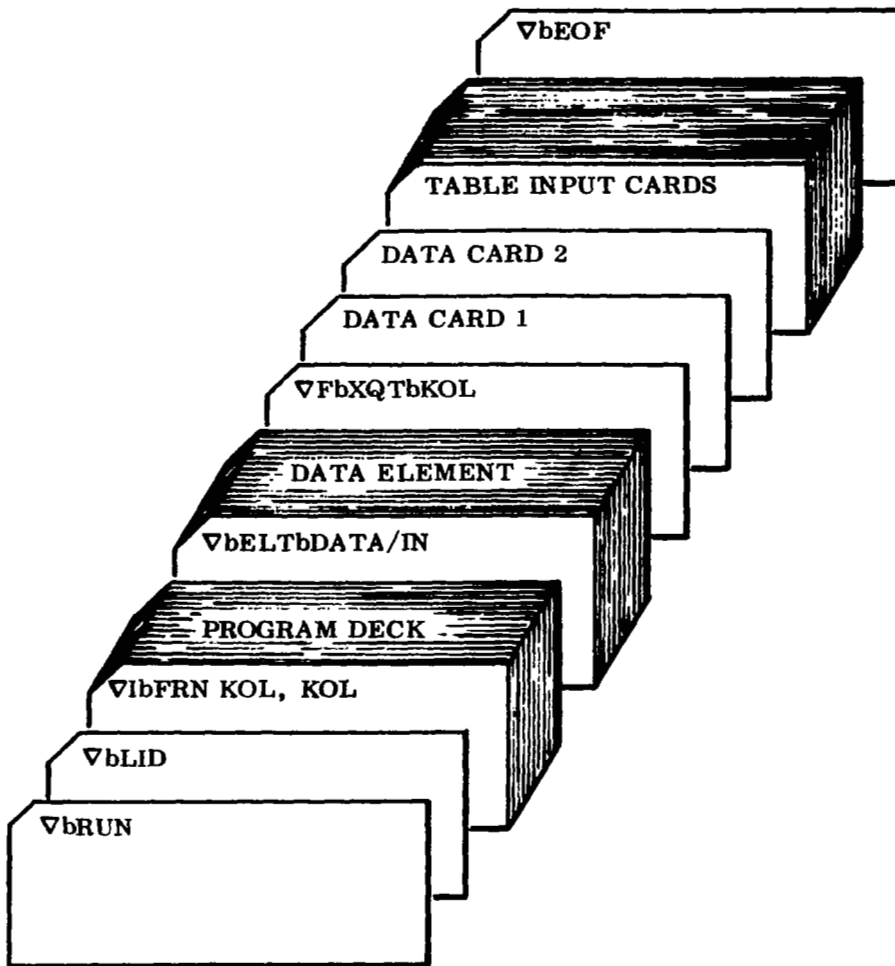


Figure D-1 System Card Sequence - 1108

DATA CARD INPUT

FORTRAN SYMBOL	DESCRIPTION	UNITS
AVC	A value cut-off	$\frac{\text{MOL, } ^\circ\text{K}}{\text{ml.}}$
DA	Δ A Critical	$\frac{\text{MOL, } ^\circ\text{K}}{\text{ml.}}$
ETA	Removal efficiency = $\frac{C_{in} - C_{out}}{C_{in}}$	None
F	Temperature	$^\circ\text{F}$
QQ	Flow Rate	$\text{Ft.}^3/\text{min.}$
R	Multiplier for production rate	None
TAU	Time	Days

FLAG SYMBOLS

FORTRAN SYMBOL	DESCRIPTION	UNITS
KFLAG	0 for intermediate output for each slice. 1 suppresses intermediate output.	

TABLE INPUT (See Figure 2-2)

FORTRAN SYMBOL	DESCRIPTION	UNITS
TA(1,)	Potential parameter	$\frac{\text{MOL, } ^\circ\text{K}}{\text{ml}}$
TQ(1,)	Saturation Capacity (Soluble Contaminants)	cc./gm.
TA(2,)	Potential Parameter	$\frac{\text{MOL, } ^\circ\text{K}}{\text{ml.}}$
TQ(2,)	Saturation Capacity (Insoluble Contaminants)	cc/gm.

DATA ELEMENT FOR nth CONTAMINANT

FORTRAN SYMBOL	DESCRIPTION	UNITS
NAME(6,n)	Name	-
MAC(n)	Maximum allowable concentration	mg./M ³
MD(n)	Input production rate	gm/day
MW(n)	Molecular Weight	-
P(n)	Saturation pressure	Atmospheres
RO(n)	Input Density	gm/cc.
VM(n)	Input Molar Volume	MOL/ML
KODE	Solubility Code: 1 = soluble in water 2 = insoluble	

CALCULATED OUTPUT SYMBOLS

FORTRAN SYMBOL	DESCRIPTION	UNITS
A	Potential parameter	$\frac{\text{MOL, } ^\circ\text{K}}{\text{ml.}}$
C(I)	Inlet concentration	mg/M ³
Q	Flow Rate	Ft. ³ /Min.
SLICE	Unit of Charcoal required to remove a given contaminant.	-
MASS	Mass of charcoal in slice	gm.
SWM	Cumulative masses of slices	gm.
LDG CTMT	Lowest A value contaminant fully removed by SLICE.	-
MAS(I)	Mass of adsorbed contaminant	gm.
MR(I)	Mass of remaining contaminant yet to be removed.	gm.

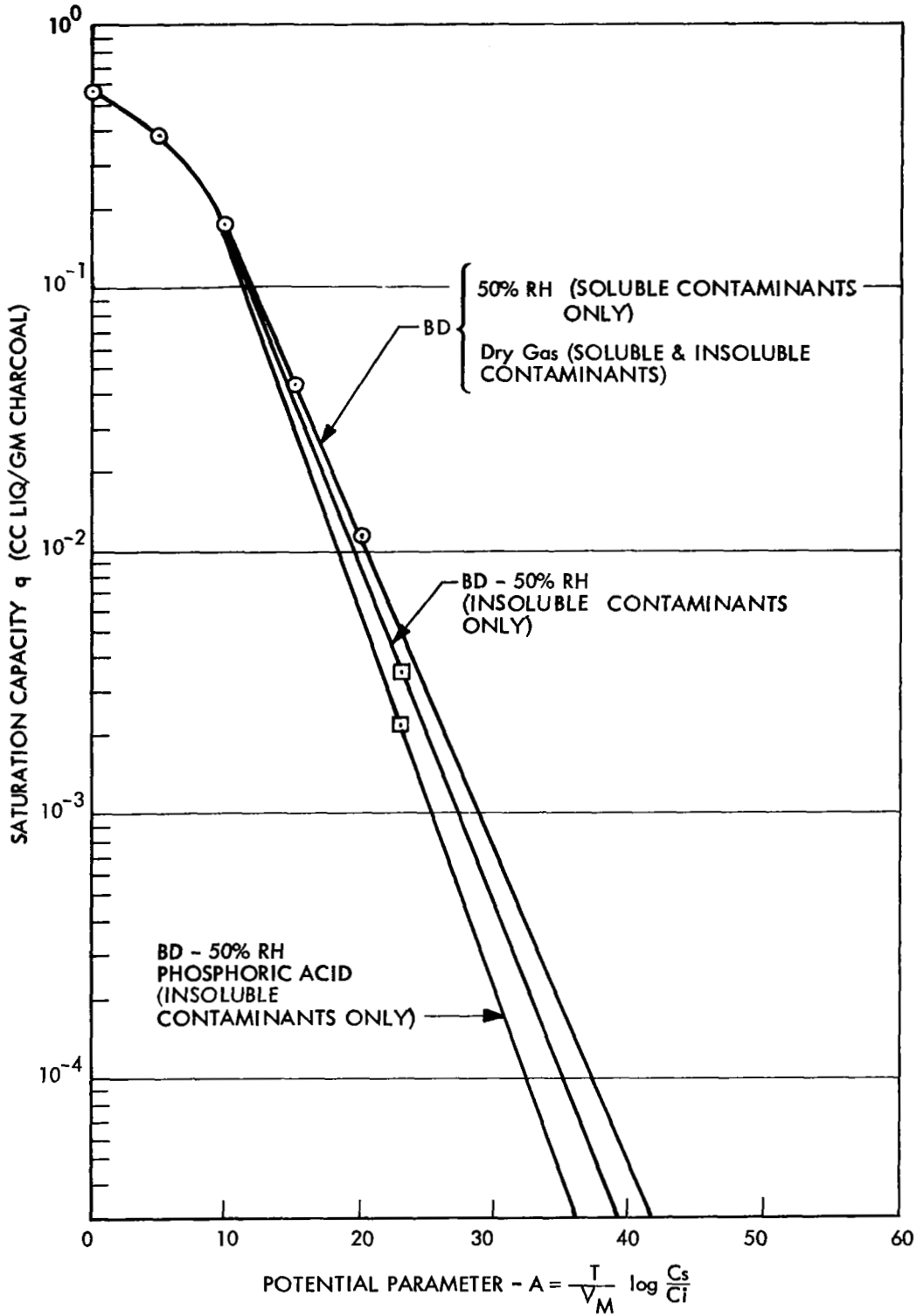


Figure D-2 Potential Plot for Barnebey Cheney BD Carbon

Program Listing

* ELT KOL, I, 711020, 37610

```

000001      DIMENSION NAME(200,10),MD(200),MAC(200),RO(200),VH(200),MH(200),
000002      1P(200),KODE(200),Q(200),A(200),C(200),HDEX(200),MH1(200),WKSP(200)
000003      2,CQ(200),EM(200),MAS(200),MR(200),MH2(200)
000004      DIMENSION AA(20),BB(20)
000005      DIMENSION MPC(200),SMH(200)
000006      COMMON NAME,MD,MAC,RO,VH,MH,P,KODE,EM,NM
000007      I,A,C,QQ
000008      REAL NAME,MAC,MD,MR,MH
000009      REAL MAS
000010      CALL INELT(9,4NDATA,2HIN,$10,K)
000011      CALL SORT1(10,AA,$200)
000012      I=1
000013      IE=0
000014      1 CONTINUE
000015      READ(9,100) (NAME(I,J),J=1,6)
000016      READ(9,102) MD(I),MAC(I),RO(I),VH(I),MH(I),P(I),KODE(I)
000017      I=I+1
000018      GO TO 1
000019      10 CONTINUE
000020      NN=I-1
000021      2 READ(5,104) QQ,TAU,F,DA,ETA,AVC,R
000022      WRITE(6,116)
000023      WRITE(6,122)
000024      READ(5,118) KFLAG
000025      WRITE(6,124) QQ,TAU,F,DA,ETA,AVC,R
000026      IF (QQ .EQ. 0) GO TO 12
000027      DO 14 I=1,NN
000028      C(I)=24.5*MD(I)*R/(QQ*ETA)
000029      IF (C(I) .GT. MAC(I)) CALL ELIST(C(I),IE,I,NAME(I,1))
000030      14 CONTINUE
000031      GO TO 18
000032      12 DO 16 I=1,NN
000033      BQ(I)=24.5*(MD(I)*R)/(MAC(I)*ETA)
000034      16 C(I)=MAC(I)
000035      WRITE(6,126)
000036      DO 56 I=1,NN
000037      WRITE(6,128) (NAME(I,L),L=1,6),BQ(I),C(I)
000038      56 CONTINUE
000039      18 CONTINUE
000040      T=(F+459.6)/1.8
000041      DO 20 I=1,NN
000042      CO=P(I)
000043      A(I)=T/VH(I)*ALOG10(CO/C(I))
000044      CALL LU10(I),A(I),KODE(I)
000045      EH(I)=TAU*MD(I)*R
000046      MR(I)=EH(I)
000047      20 CONTINUE
000048      CALL LIST
000049      REMIND 2
000050      NITEMS=NN+100000
000051      DO 30 I=1,NN
000052      AA(I)=A(I)
000053      DO 32 L=2,7
000054      AA(L)=NAME(I,L-1)

```

000055	32 CONTINUE	0055
000056	AA(8)=C(1)	0056
000057	AA(9)=HD(1)	0057
000058	AA(10)=MAC(1)	0058
000059	AA(11)=RO(1)	0059
000060	AA(12)=VM(1)	0060
000061	AA(13)=HM(1)	0061
000062	AA(14)=P(1)	0062
000063	AA(15)=D00L(KODE(1))	0063
000064	AA(16)=EM(1)	0064
000065	AA(17)=MR(1)	0065
000066	AA(18)=Q(1)	0066
000067	CALL SORT2	0067
000068	30 CONTINUE	0068
000069	CALL SORT3	0069
000070	34 CONTINUE	0070
000071	CALL SORT4	0071
000072	WRITE(2) AA	0072
000073	GO TO 34	0073
000074	200 CONTINUE	0074
000075	REWIND 2	0075
000076	DO 38 I=1,NM	0076
000077	READ(2) BB	0077
000078	A(1)=BB(1)	0078
000079	DO 38 L=2,7	0079
000080	NAME(L,L-1)=BB(L)	0080
000081	38 CONTINUE	0081
000082	C(1)=BB(8)	0082
000083	HD(1)=BB(9)	0083
000084	MAC(1)=BB(10)	0084
000085	RO(1)=BB(11)	0085
000086	VM(1)=BB(12)	0086
000087	HM(1)=BB(13)	0087
000088	P(1)=BB(14)	0088
000089	KODE(1)=D00L(BB(15))	0089
000090	EM(1)=BB(16)	0090
000091	MR(1)=BB(17)	0091
000092	Q(1)=BB(18)	0092
000093	36 CONTINUE	0093
000094	WRITE(6,118)	0094
000095	CALL LIST	0095
000096	IF (QQ .EQ. 0.) CALL EXIT	0096
000097	K=1	0097
000098	M=1	0098
000099	N1=1	0099
000100	3 CONTINUE	0100
000101	HN(M)=MR(K)/(RO(K)*Q(K))	0101
000102	SH(M)=SH(M-1)+HN(M)	0102
000103	WRITE(5,114) M,SH(M),SH(M),N1,NAME(N1,LX),LX=1,6)	0103
000104	AM=A(K)	0104
000105	DO 40 J=N1,NM	0105
000106	XN=1.-((A(J)-AM)/DA)	0106
000107	IF (XN .LT. 0.) XN=0.	0107
000108	MAS(J)=SH(M)*RO(J)*Q(J)*XN	0108
000109	MR(J)=MR(J)-MAS(J)	0109
000110	IF (MAS(J) .LE. 0) GO TO 42	0110
000111	IF (J .GE. NM) GO TO 42	0111
000112	40 CONTINUE	0112

000113	42 NN1(M)=N1	0113
000114	JJ=J	0114
000115	DO 44 J=N1,NN	0115
000116	IF (NR(J) .GT. 1.E-5) GO TO 48	0116
000117	NR(J)=0.	0117
000118	44 CONTINUE	0118
000119	GO TO 5	0119
000120	46 N1=J	0120
000121	49 CONTINUE	0121
000122	IF (KFLAO .NE. 0) GO TO 51	0122
000123	WRITE(6,120)	0123
000124	WRITE(6,106) ((NAME(I,L),L=1,6),HAS(I),NR(I),N,1=1,NN)	0124
000125	51 CONTINUE	0125
000126	M=M+1	0126
000127	NL=N1	0127
000128	K=NL	0128
000129	GO TO 3	0129
000130	5 CONTINUE	0130
000131	DO 50 I=1,M	0131
000132	NL=NN1(I1)	0132
000133	LY=I1	0133
000134	DO 52 J=1,LY	0134
000135	NNH=NNH+NN(J)	0135
000136	52 CONTINUE	0136
000137	NHC(NL)=NNH	0137
000138	NNH=0.	0138
000139	50 CONTINUE	0139
000140	WRITE(6,116)	0140
000141	L1=1	0141
000142	LL=NN1(I1)	0142
000143	DO 54 J=1,NN	0143
000144	WRITE(6,107) (NAME(I,L),L=1,6)	0144
000145	IF (LL .NE. 1) GO TO 54	0145
000146	WRITE(6,109) NHC(I)	0146
000147	L1=L1+1	0147
000148	LL=NN1(L1)	0148
000149	54 CONTINUE	0149
000150	CALL EL111E)	0150
000151	GO TO 2	0151
000152	100 FORMAT(6A6)	0152
000153	102 FORMAT(6E10.3,11)	0153
000154	104 FORMAT(7E10.2)	0154
000155	105 FORMAT(2X,6A6,2E16.8,110)	0155
000156	107 FORMAT(2X,6A6)	0156
000157	109 FORMAT(1H+,3BX,E16.8)	0157
000158	114 FORMAT(1H0,'SLICE',15,2X,'MASS =',E16.8,2X,'SHW =',E16.8,	0158
000159	12X,'LOO CTHT =',15,1X,6A6,/))	0159
000160	116 FORMAT(1H1)	0160
000161	119 FORMAT(15)	0161
000162	120 FORMAT(1H0,17X,'NAME',21X,'MAS(1)',10X,'NR(1)',6X,'SLICE',/)	0162
000163	122 FORMAT(6X,'0',7X,'TAU',7X,'F',5X,'DA CRIT',7X,'ETA',6X,'AVC',7X,	0163
000164	1'R',/)	0164
000165	124 FORMAT(2X,7F9.3)	0165
000166	126 FORMAT(1H1,17X,'NAME',21X,'0G(1)',11X,'C(1)',/)	0166
000167	128 FORMAT(2X,6A6,4X,F9.3,4X,E16.8)	0167
000168	END	0168

✓ ELT ELIST,1,711020, 37616

```
000001      SUBROUTINE ELIST(D,L,I,NAME)      0001
000002      DIMENSION C(200),KI(200)          0002
000003      DIMENSION NAME(200,10),NN(200,10)  0003
000004      REAL NAME,NN                        0004
000005      L=L+1                                0005
000006      C(L)=D                               0006
000007      DO 12 J=1,8                          0007
000008      NN(L,J)=NAME(I,J)                    0008
000009      12 CONTINUE                          0009
000010      RETURN                                0010
000011      ENTRY EL1(L)                          0011
000012      WRITE(6,100)                          0012
000013      IF (L .EQ. 0) RETURN                  0013
000014      DO 10 I=1,L                            0014
000015      WRITE(6,102) (NN(I,L1),L1=1,6),C(I)  0015
000016      10 CONTINUE                          0016
000017      100 FORMAT(1H1,55X,'ERROR LIST',//10X,'NAME',22X,'C(I)',//)  0017
000018      102 FORMAT(2X,6A6,E16.8)              0018
000019      RETURN                                0019
000020      ENO                                    0020
```

✓ ELT LIST, I, 711020, 37610

```
000001          SUBROUTINE LIST                      0001
000002          DIMENSION NAME(200,10),HD(200),MAC(200),RO(200),VM(200),MW(200),  0002
000003          IP(200),KODE(200),EM(200)                0003
000004          DIMENSION A(200),C(200)                 0004
000005          REAL NAME,HD,MW,MAC,MR                   0005
000006          COMMON NAME,HD,MAC,RO,VM,MW,P,KODE,EM,MW 0006
000007          I,A,C,QQ                                   0007
000008          WRITE(6,100)                              0008
000009          WRITE(6,106) ((NAME(I,J),J=1,6),A(I),QQ,C(I),HD(I),MAC(I),RO(I),  0009
000010          VM(I),MW(I),P(I),KODE(I),I=1,MW)         0010
000011          100 FORMAT(1HD,11X,'NAME',26X,'A',8X,'Q',6X,'C(I)',5X,'HD(I)',3X,'MAC(  0011
000012          I)',4X,'RO(I)',4X,'VM(I)',4X,'MW(I)',4X,'P(I)',7X,'KODE',/I  0012
000013          106 FORMAT(2X,6A6,F9.3,2X,F5.1,2X,7E9.3,2X,15)  0013
000014          END                                        0014
```

ELT LU,1,711020, 37620

```
000001      SUBROUTINE LU(Q,A,KODE)      0001
000002      DIMENSION TA(2,50),TQ(2,50)  0002
000003      IF (L .NE. 0) GO TO 200        0003
000004      L=0                             0004
000005      2 L=L+1                          0005
000006      READ(5,150,END=200) TA(1,L),TQ(1,L),TA(2,L),TQ(2,L) 0006
000007      150 FORMAT(4E10.2)              0007
000008      GO TO 2                          0008
000009      200 DO 10 J=1,L                  0009
000010      1=J                             0010
000011      IF (TA(KODE,1) .GE. A) GO TO 12 0011
000012      10 CONTINUE                    0012
000013      WRITE(6,100) A                  0013
000014      RETURN                          0014
000015      12 IF (1 .EQ. 1) GO TO 14        0015
000016      C INTERPOLATE FOR Q = LINEAR F(A) 0016
000017      Q=TQ(KODE,1-1)*(A-TA(KODE,1-1))+TQ(KODE,1)-TQ(KODE,1-1)) 0017
000018      D      /(TA(KODE,1)-TA(KODE,1-1)) 0018
000019      RETURN                          0019
000020      14 Q=TQ(KODE,1)                  0020
000021      RETURN                          0021
000022      100 FORMAT(1H0,'VALUE A',E16.8,' IS OUT OF RANGE') 0022
000023      END                             0023
```

✓ ELT RORDR,1,711020, 37820

```
000001      SUBROUTINE RORDR(A,NDEX)      0001
000002      DIMENSION A1(200),      A3(200),A4(200),A5(200),A6(200),A7(200),      0002
000003      I A8(200),A9(200),A10(200)      0003
000004      DIMENSION A2(200,10)      0004
000005      DIMENSION NAME(200,10),MD(200),MAC(200),RO(200),VM(200),MW(200),      0005
000006      IP(200),KODE(200),EM(200)      0006
000007      REAL NAME,MAC,MD,MW,MM      0007
000008      COMMON NAME,MD,MAC,RO,VM,MW,P,KODE,EM,MM      0008
000009      DO 10 I=1,MM      0009
000010      L=NDEX(I)      0010
000011      A1(I)=A(L)      0011
000012      DO 12 J=1,6      0012
000013      A2(I,J)=NAME(L,J)      0013
000014      12 CONTINUE      0014
000015      A3(I)=MD(L)      0015
000016      A4(I)=MAC(L)      0016
000017      A5(I)=RO(L)      0017
000018      A6(I)=VM(L)      0018
000019      A7(I)=MW(L)      0019
000020      A8(I)=P(L)      0020
000021      A9(I)=KODE(L)      0021
000022      A10(I)=EM(L)      0022
000023      10 CONTINUE      0023
000024      CALL MOVER(A1,1,A,1,MM)      0024
000025      CALL MOVER(A2,10,NAME,10,MM)      0025
000026      CALL MOVER(A3,1,MD,1,MM)      0026
000027      CALL MOVER(A4,1,MAC,1,MM)      0027
000028      CALL MOVER(A5,1,RO,1,MM)      0028
000029      CALL MOVER(A6,1,VM,1,MM)      0029
000030      CALL MOVER(A7,1,MW,1,MM)      0030
000031      CALL MOVER(A8,1,P,1,MM)      0031
000032      CALL MOVER(A9,1,KODE,MM)      0032
000033      CALL MOVER(A10,1,EM,MM)      0033
000034      RETURN      0034
000035      END      0035
```

✓ ELT DATA/IN.1.700017. 67400

000001	ACETONE							001
000002	1.022 720.	.75	77.	50.00	.714	E01		0
000003	ACETALDEHYDE							002
000004	0.251 30.	.70	57.	44.05	.213	E71		002
000005	ACETIC ACID							003
000006	0.025 2.5	.94	63.	60.05	.512	E91		003
000007	ACETYLENE							004
000008	0.250 6400.	.62	42.	26.04	.523	E02		004
000009	ACETONITRILE							005
000010	0.025 7.	.72	51.	41.05	.190	E01		005
000011	ACROLEIN							006
000012	0.025 0.25	.80	66.	56.00	.321	E001		006
000013	ALLYL ALCOHOL							007
000014	0.025 0.50	.76	74.	50.00	.033	E051		007
000015	ISO-AMYL ACETATE							008
000016	0.025 53.	.70	162.	130.10	.814	E071		008
000017	AMYL ALCOHOL							009
000018	0.025 36.	1.40	124.	80.15	.210	E051		009
000019	BENZENE							010
000020	0.250 3.2	.07	96.	70.11	.390	E062		010
000021	N-BUTANE							011
000022	0.250 100.	.60	96.	58.11	.579	E072		011
000023	ISO-BUTANE							012
000024	0.025 100.	.60	104.	50.11	.003	E062		012
000025	BUTENE-1							013
000026	0.250 100.	.62	90.	56.10	.671	E072		013
000027	CIS-BUTENE-2							014
000028	0.025 100.	.63	89.	56.11	.511	E072		014
000029	TRANS-BUTENE-2							015
000030	0.250 100.	.63	89.	56.11	.529	E072		015
000031	1,3 BUTADIENE							016
000032	0.250 220.	.65	81.	54.09	.595	E072		016
000033	ISO-BUTYLENE							017
000034	0.025 100.	.62	89.	56.10	.599	E082		017
000035	N-BUTYL ALCOHOL							018
000036	0.262 30.	.72	102.	74.12	.290	E051		018
000037	ISO-BUTYL ALCOHOL							019
000038	0.025 30.	.81	102.	74.12	.476	E051		019
000039	SEC-BUTYL ALCOHOL							020
000040	0.025 30.	.81	105.	74.12	.577	E061		020
000041	BUTYRIC ACID							021
000042	0.025 14.	.82	100.	80.10	.494	E001		021
000043	CAREGN DISULPHIDE							022
000044	0.025 6.	1.23	62.	76.13	.902	E062		022
000045	CARBON TETRACHLORIDE							023
000046	0.25 6.5	1.60	101.	153.84	.865	E062		023
000047	CARBONYL SULPHIDE							024
000048	0.025 2.5	1.19	40.	60.07	.677	E071		024
000049	CHLORINE							025
000050	0.025 0.3	1.50	45.	70.94	.228	E001		025
000051	CHLOROACETONE							026
000052	0.025 110.	1.15	77.	92.53	.671	E071		026
000053	CHLOROBENZENE							027
000054	0.025 35.	.70	115.	112.56	.117	E052		027

000055	CHLOROFUOROMETHANE							020
000056	0.025 24.	1.11	52.	60.40	.553	E002		020
000057	CHLOROFORM							020
000058	0.250 24.	1.40	83.	119.30	.120	E072		020
000059	CHLOROPROPANE							030
000060	0.025 24.	.70	92.	70.54	.140	E062		030
000061	CHRYLIC ACID							031
000062	0.010 15.5	.753	107.	144.21	.407	E021		031
000063	CUMENE							032
000064	0.020 25.	.700	102.	120.10	.400	E072		032
000065	CYCLOHEXANE							033
000066	0.25 100.	.72	117.	84.16	.445	E062		033
000067	CYCLOHEXANOL							034
000068	0.025 20.	.05	110.	100.20	.724	E042		034
000069	CYCLOPENTANE							035
000070	0.025 100.	.75	100.	70.13	.110	E072		035
000071	CYCLOPROPANE							036
000072	0.025 100.	.72	60.	42.00	.565	E102		036
000073	CYANAMIDE							037
000074	0.025 45.	.07	40.	42.04	.502	E001		037
000075	DECALIN							038
000076	0.025 5.	.764	105.	130.25	.226	E032		038
000077	1,1DIMETHYL CYCLOHEXANE							038
000078	0.025 120.	.60	102.	112.20	.797	E002		039
000079	TRANS 1,2 DIMETHYL CYCLOHEXANE							040
000080	0.025 120.	.60	102.	112.20	.564	E002		040
000081	2,2 DIMETHYL BUTANE							041
000082	0.025 93.	.62	130.	85.17	.140	E052		041
000083	DIMETHYL SULPHIDE							042
000084	0.025 15.	.04	77.	62.13	.200	E001		042
000085	1,1 DICHLOROETHANE							043
000086	0.250 40.	1.12	00.	90.97	.119	E072		043
000087	D1 ISOBUTYL KETONE							044
000088	0.025 20.	.704	200.	142.24	.290	E072		044
000089	1,4 DIOXANE							045
000090	0.250 30.	.93	95.	80.10	.175	E061		045
000091	DIMETHYL FURANE							046
000092	0.025 3.0	.04	110.	95.12	.354	E002		046
000093	DIMETHYL HYDRAZINE							047
000094	0.025 0.1	.69	05.	59.09	.506	E061		047
000095	ETHANE							048
000096	0.250 100.	.53	52.	30.07	.320	E002		048
000097	ETHYL ALCOHOL							049
000098	0.200 100.	.74	62.	46.07	.145	E061		049
000099	ETHYL ACETATE							050
000100	0.250 140.	.03	100.	80.10	.433	E061		050
000101	ETHYL ACETYLENE							051
000102	0.025 100.	.66	01.	54.00	.612	E072		051
000103	ETHYL BENZENE							052
000104	0.025 44.	.76	140.	100.10	.540	E052		052
000105	ETHYLENE DICHLORIDE							053
000106	0.025 40.	1.20	09.	97.00	.434	E072		053
000107	ETHYL ETHER							054
000108	0.250 120.	.66	105.	74.12	.315	E001		054
000109	ETHYL ISOBUTYL ETHER							055
000110	0.250 200.	.75	152.	102.17	.431	E091		055
000111	ETHYL FORMATE							056
000112	0.250 30.	.07	05.	74.00	.990	E061		056

000113	ETHYLENE							057
000114	0.250	100.	.57	40.	20.05	.846	E072	057
000115	ETHYLENE GLYCOL							050
000116	0.025	114.	1.60	65.	106.06	.271	E031	050
000117	TRANS 1 METHYL 3 ETHYL CYCLOHEXANE							050
000118	0.025	117.	.71	105.	126.20	.405	E002	050
000119	ETHYL SULPHIDE							050
000120	0.025	97.	.74	122.	90.10	.396	E061	050
000121	ETHYL MERCAPTAN							061
000122	0.010	2.5	.02	77.	62.10	.100	E071	061
000123	FREON 11							062
000124	0.250	5600.	1.50	80.	130.00	.507	E072	062
000125	FREON 12							063
000126	0.250	500.	1.50	75.	120.90	.204	E002	063
000127	FREON 21							064
000128	0.025	420.	1.41	70.	102.90	.655	E072	064
000129	FREON 22							065
000130	0.025	350.	1.41	61.	86.40	.320	E002	065
000131	FREON 23							066
000132	0.025	12.	1.30	50.	70.00	.127	E092	066
000133	FREON 113							067
000134	0.025	142.	1.56	120.	107.4	.120	E102	067
000135	FREON 114							068
000136	0.250	7000.	1.47	112.	170.90	.131	E002	068
000137	FREON 114 UNSYMETRICAL							069
000138	0.025	7000.	1.47	100.	170.90	.170	E002	069
000139	FREON 125							070
000140	0.025	25.	1.50	77.	120.00	.524	E002	070
000141	FURAN							072
000142	0.025	3.0	.93	05.	60.07	.307	E092	072
000143	FURFURAL							073
000144	0.025	2.0	1.00	95.	96.00	.601	E041	073
000145	HEPTANE							075
000146	.025	200.	.62	162.	100.20	.196	E092	075
000147	HEXENE-1							076
000148	.250	100.	.63	132.	84.16	.052	E062	076
000149	N-HEXANE							077
000150	.250	100.	.62	140.	86.17	.719	E052	077
000151	HEXAHETHYLCYCLOTRISIMEXANE							078
000152	.025	240.	1.16	192.	223.50	.599	E052	078
000153	ISOPRENE							080
000154	.025	140.	.60	104.	60.11	.211	E062	080
000155	METHYLENE CHLORIDE							081
000156	.250	21.	1.30	65.	84.94	.109	E061	081
000157	METHYL ACETATE							082
000158	.250	61.	.80	85.	74.00	.414	E062	082
000159	METHYL BUTYRATE							083
000160	.025	30.	.81	133.	102.13	.169	E062	083
000161	METHYL CHLORIDE							084
000162	.025	21.	1.00	47.	50.49	.112	E071	084
000163	2 METHYL 1 BUTENE							085
000164	.025	1430.	0.66	111.	70.13	.330	E072	085
000165	METHYL CHLOROFORM							086
000166	.25	100.	1.35	100.	133.00	.074	E062	086
000167	METHYL FURANE							087
000168	.025	3.	.87	109.	82.10	.962	E052	087
000169	METHYL ETHYL KETONE							088
000170	.25	59.	.81	97.	72.10	.370	E062	088

000171	METHYL ISOBUTYL KETONE						080
000172	.025 41. .72	155.	100.16	.293	E072		080
000173	METHYL ISOPROPYL KETONE						080
000174	.25 70. .73	118.	86.13	.291	E082		080
000175	METHYL CYCLO HEXANE						081
000176	.025 200. .69	140.	90.10	.236	E062		081
000177	METHYL ACETYLENE						082
000178	.025 165. .67	59.	40.06	.950	E002		082
000179	METHYL ALCOHOL						083
000180	.267 26. .75	42.	32.00	.212	E062		083
000181	3 METHYL PENTANE						084
000182	.025 295. .61	141.	66.17	.900	E052		084
000183	METHYL METHACRYLATE						085
000184	.025 41. .94	122.	100.11	.190	E062		085
000185	MESITYLENE						086
000186	.025 7.5 .730	163.	120.19	.202	E062		086
000187	MONO METHYL HYDRAZINE						087
000188	.025 .035 .77	59.	46.07	.111	E061		087
000189	METHYL MERCAPTAN						088
000190	.010 2. .87	55.	40.10	.343	E071		088
000191	NAPHTHALENE						088
000192	.025 5. .071	140.	120.16	.592	E042		088
000193	NITROGEN TETROXIDE						101
000194	.025 1.0 1.44	64.	92.02	.456	E071		101
000195	OCTANE						103
000196	.025 255. .613	185.	114.23	.982	E052		103
000197	PROPYLENE						104
000198	.250 180. .630	67.	42.00	.186	E082		104
000199	N-PENTANE						105
000200	.250 295. .626	110.	72.15	.194	E062		105
000201	PENTENE-1						106
000202	.025 130. .68	111.	70.13	.236	E072		106
000203	PENTENE-2						107
000204	.025 180. .66	111.	70.13	.184	E072		107
000205	PROPANE						108
000206	.250 180. .59	74.	44.10	.150	E082		108
000207	N-PROPYL ACETATE						109
000208	.025 64. .79	129.	102.10	.300	E052		109
000209	N PROPYL ALCOHOL						110
000210	.250 75. .60	83.	60.09	.613	E051		110
000211	ISOPROPYL ALCOHOL						111
000212	.250 40. .70	83.	60.09	.775	E071		111
000213	N-PROPYL BENZENE						112
000214	.025 44. .743	163.	120.10	.430	E072		112
000215	PROPIONIC ACID						113
000216	.025 15. .99	90.	74.08	.150	E051		113
000217	PROPYL MERCAPTAN						114
000218	.010 82. .84	100.	76.15	.637	E052		114
000219	PROPYLENE ALDEHYDE						115
000220	.025 10. .66	88.	70.09	.470	E071		115
000221	PYRUVIC ACID						116
000222	2.51 0.9 1.06	87.	80.06	.471	E051		116
000223	PHENOL						117
000224	.025 1.0 .92	102.	94.11	.504	E041		117
000225	SULFUR DIOXIDE						119
000226	.025 .0 1.46	44.	64.07	.845	E071		119
000227	STYRENE						120
000228	.025 42. .79	137.	104.14	.976	E072		120

000229	TETRACHLOROETHYLENE						121
000230	.025 67.	1.62	116.	165.00	.159	E062	121
000231	TETRAFLUOROETHYLENE						122
000232	.025 205.	1.52	64.	100.02	.265	E062	122
000233	TETRAHYDROFURANE						123
000234	.025 59.	.89	100.	72.10	.225	E102	123
000235	TOLUENE						124
000236	.250 75.	.70	110.	92.00	.143	E062	124
000237	TRICHLOROETHYLENE						125
000238	.250 52.	1.46	70.	131.40	.525	E062	125
000239	1,2,4 TRIMETHYL BENZENE						126
000240	.025 49.	.749	163.	120.19	.293	E072	126
000241	1,1,3 TRIMETHYL CYCLOHEXANE						127
000242	.025 140.	.68	185.	126.20	.103	E062	127
000243	VALERALDEHYDE						128
000244	.010 70.	.73	110.	86.13	.454	E001	128
000245	VALERIC ACID						129
000246	.018 110.	.786	130.	102.00	.662	E031	129
000247	VINYL CHLORIDE						130
000248	.250 130.	1.00	62.	62.50	.108	E001	130
000249	VINYLDENE CHLORIDE						131
000250	.025 20.	1.21	90.	97.00	.644	E071	131
000251	O-XYLENE						132
000252	.250 44.	.77	130.	106.20	.371	E052	132
000253	M-XYLENE						133
000254	.250 44.	.76	140.	106.20	.648	E052	133

NATIONAL AERONAUTICS AND SPACE ADMINISTRATION
WASHINGTON, D.C. 20546

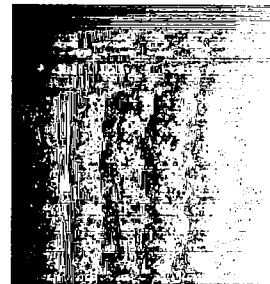
OFFICIAL BUSINESS
PENALTY FOR PRIVATE USE \$300

FIRST CLASS MAIL

POSTAGE AND FEES PAID
NATIONAL AERONAUTICS AND
SPACE ADMINISTRATION



004 001 C1 U 05 720428 S00903DS
DEPT OF THE AIR FORCE
AF WEAPONS LAB (AFSC)
TECH LIBRARY/WLOL/
ATTN: E LOU BOWMAN, CHIEF
KIRTLAND AFB NM 87117



POSTMASTER: If Undeliverable (Section 158
Postal Manual) Do Not Return

"The aeronautical and space activities of the United States shall be conducted so as to contribute . . . to the expansion of human knowledge of phenomena in the atmosphere and space. The Administration shall provide for the widest practicable and appropriate dissemination of information concerning its activities and the results thereof."

— NATIONAL AERONAUTICS AND SPACE ACT OF 1958

NASA SCIENTIFIC AND TECHNICAL PUBLICATIONS

TECHNICAL REPORTS: Scientific and technical information considered important, complete, and a lasting contribution to existing knowledge.

TECHNICAL NOTES: Information less broad in scope but nevertheless of importance as a contribution to existing knowledge.

TECHNICAL MEMORANDUMS: Information receiving limited distribution because of preliminary data, security classification, or other reasons.

CONTRACTOR REPORTS: Scientific and technical information generated under a NASA contract or grant and considered an important contribution to existing knowledge.

TECHNICAL TRANSLATIONS: Information published in a foreign language considered to merit NASA distribution in English.

SPECIAL PUBLICATIONS: Information derived from or of value to NASA activities. Publications include conference proceedings, monographs, data compilations, handbooks, sourcebooks, and special bibliographies.

TECHNOLOGY UTILIZATION PUBLICATIONS: Information on technology used by NASA that may be of particular interest in commercial and other non-aerospace applications. Publications include Tech Briefs, Technology Utilization Reports and Technology Surveys.

Details on the availability of these publications may be obtained from:

SCIENTIFIC AND TECHNICAL INFORMATION OFFICE

NATIONAL AERONAUTICS AND SPACE ADMINISTRATION

Washington, D.C. 20546